

**Removal of microplastics during drinking water treatment:  
Linking theory to practice to advance risk management**

by

Alice Stephanie Gomes

A thesis

presented to the University of Waterloo

in fulfillment of the

thesis requirement for the degree of

Master of Applied Science

in

Civil Engineering (Water)

Waterloo, Ontario, Canada, 2024

© Alice Stephanie Gomes 2024

## **Author's Declaration**

I hereby declare that I am the sole author of this thesis. This is a true copy of the thesis, including any required final revisions, as accepted by my examiners.

I understand that my thesis may be made electronically available to the public.

## Abstract

Microplastics (MPs) have emerged in the past decade as widespread contaminants that are harmful to human and ecosystem health. While their removal from water may be similar to those of other particulate contaminants, its characterization is complicated because MPs can undergo weathering, photolysis, and microbial degradation in the natural environment, resulting in the presence of functional groups (e.g., carbonyl, hydroxyl) on their surfaces, which may affect their removal during drinking water treatment. Given that studies using seeded polystyrene microspheres/MPs as surrogates for oocysts have shown good (but sometimes variable) removals through conventional drinking water treatment composed of coagulation, flocculation and sedimentation (CFS) followed by filtration, MPs are likely to be well removed in optimized conventional drinking water treatment plants. While many studies have focused on the removal of larger (i.e., >50  $\mu\text{m}$  sized microplastics), investigations of the removal of smaller sized (<10  $\mu\text{m}$ ) microplastics by drinking water treatment processes have been limited largely to case studies in which foundational mechanisms necessary for maximizing treatment performance have only been superficially investigated, if at all. To address this gap, the study focused on whether MPs removal by conventional chemical pretreatment (i.e., coagulation, flocculation, and sedimentation) with alum aligns with the removal of other particles, including *Cryptosporidium* oocysts, for which particle destabilization is essential for removal. The study aimed to advance knowledge through three main objectives: (1) characterize MPs removal by CFS with different particle destabilization mechanisms and compare it to other important particulate contaminants (i.e., *Cryptosporidium* spp. oocysts), (2) evaluate the effect of particle size on MPs removal by CFS, and (3) assess the influence of weathering on MPs removal by CFS.

To evaluate MPs removal by chemical pretreatment reliant on (1) adsorption and charge neutralization and (2) enmeshment in precipitate (i.e., sweep flocculation) particle destabilization mechanisms, bench-scale investigations of alum-based CFS (i.e., jar tests) were conducted with synthetic water using pristine and weathered PS microplastics of 1, 5 and 10  $\mu\text{m}$  diameter. Several synthetic raw water matrices were explored to identify scenarios in which both particle destabilization mechanisms were clearly discerned. The final synthetic raw water was composed of deionized water spiked with sodium carbonate and kaolin (70 NTU) at pH 7.0. To demonstrate that MPs removal by CFS aligns with coagulation theory, sixteen alum doses between 0–38.8 mg/L were used to evaluate MPs removal by CFS. Turbidity reduction was also evaluated, and zeta potential was analyzed to identify maximal particle destabilization. MPs removal increased with particle size, aligning with gravitational settling theory. MPs removal during CFS with optimized particle destabilization was generally consistent with reported removals of other particles, including *Cryptosporidium* spp. oocysts during optimized chemical pretreatment, thereby suggesting that similar approaches for risk management may be relevant to MPs. Notably, differences in pristine and weathered MPs removal by CFS were not significant under the conditions investigated, thereby suggesting that weathering does not affect MPs removal when particle destabilization by coagulant addition is optimized. This study bridges the gap between the theories of conventional drinking water treatment and concerns regarding the potential passage of MPs through drinking water treatment plants, demonstrating that MPs can be removed in the same manner as other colloidal particles using conventional chemical pretreatment and—by well-recognized theory-based extension—physico-chemical filtration.

## Acknowledgements

The completion of this thesis would not have been possible without the support and love of several individuals.

First and foremost, I would like to express my deepest gratitude to my supervisors, Dr. Monica B. Emelko and Dr. William B. Anderson, for granting me the opportunity to pursue my Master's under their guidance. Your unwavering support and inspiration have been invaluable throughout this journey. I deeply appreciate the countless lessons I have learned from you, particularly in presentation, writing, professionalism, and the importance of maintaining a positive outlook. I am sincerely thankful for your assistance in streamlining my thoughts and for always being available whenever I needed your guidance, which helped bring this piece together.

I would like to extend my heartfelt gratitude to Dr. Fariba Amiri for providing extensive support with the experimental design and to Dr. Phil Schmidt for offering valuable feedback on writing and result analysis. A special thanks to Omar for being my mentor, guiding me through the challenging path of microplastics research, and assisting with the figures on R software.

Kalani, I am deeply grateful for your willingness to proofread my work at any time of day and for supporting me in every aspect of this journey. Dafne, thank you for always making time to listen to my presentations, for offering statistical insights, proofreading and for assisting me with the paired T-test. Your support has been invaluable whenever I sought guidance, and I cannot thank you both enough for everything. Thanks to Steven for checking my calculations, Tyler for helping with my experiments, and Dana and Elanor for making everything easier for the group, from handling finances to managing meetings.

Thanks to Soosan, Elyse, Carter, Lauren, Kelvin, Celine, Emma and Taylor. Whether it was lending a hand with last-minute tasks, offering words of advice, or simply being there to share a laugh during stressful times, your support has meant so much.

Thank you, Mirza, for tirelessly proofreading until the last minute and encouraging me to become the best version of myself. I am grateful to Ibtida, Raisa apu, and Farah for making my transition to Waterloo smoother. Thank you to my supportive friends from NSU—Fahad, Partha, Sakib, Siam, and Sumaiya—who have constantly motivated me. They stood by me through all the behind-the-scenes challenges that led to this achievement.

## **Dedication**

For my sister, Priscilla Judith Gomes, who believed in me and supported me with unwavering love throughout this journey; my father, Dr. Noel Charles Gomes, and my mother, Merelin Gomes, for always encouraging me to be a better version of myself and teaching me the value of life. Lastly, for my late grandfather, Peter A. Gomes, who is my role model and biggest inspiration, and for my late grandmother, Purnima Pramanik, whom I lost during my writing. She was my all-time cheerleader, and I wish she was here to see me reach the finish line.

## Table of Contents

Author’s Declaration .....	ii
Abstract .....	iii
Acknowledgements.....	iv
Dedication .....	v
List of Figures .....	ix
List of Tables .....	xi
List of Abbreviations .....	xii
Chapter 1 Introduction .....	1
1.1 Research objectives .....	3
1.2 Research approach.....	3
1.3 Thesis organization .....	5
Chapter 2 Literature review .....	6
2.1 Particles in water .....	6
2.1.1 Particulate contaminants.....	6
2.1.2 Regulatory Approaches.....	7
2.1.3 Surface charge of particles in water .....	8
2.2 Emergence of MPs as particulate contaminants of health concern .....	11
2.2.1 Prevalence of microplastics in freshwater.....	11
2.2.2 Health implications .....	12
2.2.3 Physical and chemical properties of MPs .....	14
2.2.4 Weathering of microplastics .....	16
2.3 Particle removal during drinking water treatment.....	17
2.3.1 Water treatment overview .....	17
2.3.2 Particle destabilization by coagulation .....	18

2.3.3 Flocculation and sedimentation.....	21
2.4 Particle destabilization in water treatment practice .....	23
2.5 Observations of particle removal during drinking water treatment .....	26
2.5.1 Inorganic particles and protozoan parasites removal by CFS.....	26
2.5.2 MPs removal by CFS.....	27
2.6 MPs Risk management & regulatory considerations.....	40
2.7 Increased MPs threats to water in a changing climate.....	42
Chapter 3 Materials and methods .....	44
3.1 General approach.....	44
3.2 Experimental design.....	45
3.3 Preparation of materials .....	47
3.3.1 Microplastics (MPs).....	47
3.3.2 Kaolin suspension.....	48
3.3.3 Synthetic water .....	48
3.3.4 Coagulant and other chemicals.....	48
3.4 Experimental Methods.....	49
3.4.1 Jar test procedure .....	49
3.4.2 pH.....	50
3.4.3 Turbidity measurement .....	50
3.4.4 Zeta potential analysis .....	50
3.4.5 MPs Enumeration.....	51
3.5 Data handling and analysis .....	52
Chapter 4 Results and discussion.....	55
4.1 Synthetic raw/untreated water matrix selection .....	55
4.2 Turbidity reduction by CFS.....	58

4.3 MPs removal by bench-scale CFS.....	66
4.3.1 Evaluating consistency in raw water MPs concentrations.....	66
4.3.2 Effect of weathering on MPs removal by CFS.....	67
4.3.3 Effect of MPs size on removal.....	68
Chapter 5 Conclusions and implications.....	70
5.1 Conclusions.....	70
5.2 Implications.....	71
References.....	81
Appendix A : Test runs for the jar test conditions.....	110
Appendix B Detailed jar test data.....	119

## List of Figures

Figure 1.1 Graphical overview of this study focused on demonstrating that both pristine and weathered microplastics are destabilized similarly to other like-sized and -shaped particles (i.e., by adsorption and particle destabilization, and enmeshment in precipitate mechanisms) and therefore removal similarly during conventional chemical pretreatment (i.e., CFS).....	4
Figure 2.1 Size spectrum for waterborne particles. ....	7
Figure 2.2 Difference in electric potential as a function of distance from the charged surface of a particle/microplastics suspended in a dispersion medium such as water. ....	10
Figure 2.3 Charge neutralization and charge reversal by metal salt hydrolysis species for particles in a suspension. Reproduced from Duan & Gregory (2003) with permission.....	19
Figure 2.4 Particle destabilization by (A) adsorption and charge neutralization and (B) sweep flocculation during coagulation using metal salts. ....	20
Figure 2.5 Solubility diagram for Al (III) mononuclear species at 25°C. Metal species are assumed to be in equilibrium along with the amorphous precipitated solid phase. ....	21
Figure 2.6 Differential settling of particles simplified as a function of size (adapted from Crittenden et al., 2012). ....	22
Figure 2.7 Schematic coagulation curves at constant pH for four colloid concentrations ( $S_1 < S_2 < S_3 < S_4$ ) showing zones of destabilization and restabilization. ....	24
Figure 3.1 Experimental approach used to represent (A) conventional chemical pretreatment at (B) bench-scale to investigate microplastics removal by chemical pretreatment. ....	44
Figure 3.2 Research objectives and the associated experimental tasks.....	45
Figure 3.3 (A) Carboxylated [weathered] BB polystyrene and (B) Plain [pristine] YG 1 $\mu\text{m}$ MPs (C) enumerated using epifluorescence microscopy at 20x magnification. ....	51
Figure 4.1 Turbidity and zeta potential after alum addition for 5 $\mu\text{m}$ MPs at pH 7 with (A) ionic strength of 0.1 M and initial turbidity of 45 NTU and (B) ionic strength of 0.25 M and initial turbidity of 71 NTU. ....	57
Figure 4.2 Final study matrix without MPs at an ionic strength of 0.1 M and turbidity of 70 NTU at pH 7, clearly identifying both particle destabilization zones: (adsorption and charge neutralization (“Zone 2” from Stumm & O’Melia, 1968) and sweep flocculation (“Zone 4” from Stumm & O’Melia, 1968). ....	58
Figure 4.3 Combined residual turbidity (n = 6 per MPs size) after alum addition for 1, 5 and 10 $\mu\text{m}$ pristine (n = 3 for each size) and weathered (n = 3 for each size) MPs suspended in the study matrix (mean + standard deviation).....	59

Figure 4.4 Residual turbidity and MPs concentration after alum addition for 1, 5 and 10  $\mu\text{m}$  (A) pristine and (B) weathered microplastics suspended together in the study matrix at an ionic strength of 0.1 M and turbidity of 70 NTU at pH 7. ....62

Figure 4.5 Residual turbidity and zeta potential after alum addition for 1, 5 and 10  $\mu\text{m}$  pristine and weathered microplastics suspended together in the synthetic water with an ionic strength of 0.1 M and turbidity of 70 NTU at pH 7. Data points are connected by lines to assist with visualization. ....64

Figure 4.6 Removal of 1, 5 and 10  $\mu\text{m}$  pristine vs. weathered MPs by chemical pretreatment (i.e., CFS) at bench-scale (mean + standard deviation of triplicate analyses). ....66

## List of Tables

Table 2.1 Zeta potential values for some MPs in water. Reproduced from Chowdhury (2022). .....	14
Table 2.2 Removal of colloidal particles by conventional coagulation/flocculation/sedimentation (CFS). .....	27
Table 2.3 Bench-scale studies on microplastics removal from water by conventional coagulation/flocculation/sedimentation.....	29
Table 3.1 Experimental design components and rationale for their choice.....	46
Table 3.2 Stock concentrations and volumes of different MPs sizes used during experiments. ....	48
Table 3.3 Alum dose and volume of alum stock solution added to each jar (mg/L and $\mu\text{M}$ ). .....	50
Table 3.4 Sample volume filtered at selected alum doses for the different sizes of MPs to ensure an adequate number of MPs were enumerated. ....	52
Table 3.5 Summary of count data used at selected alum doses for two-tailed paired t-test analyses for three sizes of pristine and weathered MPs and their rationale.....	53
Table 3.6 Summary of turbidity data used at selected alum doses for two-tailed paired t-test analyses for three sizes of MPs and their rationale. ....	54

## List of Abbreviations

Abbreviation	Description
ACH	Aluminum chlorohydrate
$\text{Al}_2(\text{SO}_4)_3 \cdot 18\text{H}_2\text{O}$	Hydrated aluminum sulfate
$\text{Al}_2(\text{SO}_4)_3$	Aluminum sulfate
BB	Bright blue microplastics
CFS	Coagulation-flocculation-sedimentation
$\text{CaCO}_3$	Calcium carbonate
DI	Deionized water
DWTP	Drinking water treatment plant
$\text{FeCl}_3$	Ferric chloride
$\text{Fe}_2(\text{SO}_4)_3 \cdot 9\text{H}_2\text{O}$	Hydrated iron sulfate
HDPE	High density polyethylene
IS	Ionic strength
LDPE	Low density polyethylene
MPs	Microplastic/Microplastics
m	Meters
mg	Milligrams
min	Minutes
mL	Milliliters
mm	Millimeters
$\mu\text{M}$	Micromolar
mV	Millivolts
nm	Nanometers

NTU	Nephelometric turbidity units
Na <sub>2</sub> CO <sub>3</sub>	Sodium carbonate
PACl	Polyaluminum chloride
PAM	Polyacrylamide
PE	Polyethylene
PET	Polyethylene terephthalate
PEST	Polyester fibers
PP	Polypropylene
PS	Polystyrene
PVC	Polyvinylchloride
PZC	Point of zero charge
rpm	Revolutions per minute
U.S. EPA	United States Environmental Protection Agency
UV	Ultraviolet
WHO	World Health Organization
YG	Yellow green microplastics
ZP	Zeta potential

## Chapter 1 Introduction

Drinking water treatment plays a critical role in protecting public health because it mitigates exposure to microbial and chemical contaminants, including those that are established and emerging. Emerging contaminants of potential health concern include pharmaceuticals, personal care products, industrial and household chemicals, pesticides, manufactured nanomaterials, and their transformation products. Over the past several decades, regulatory agencies have imposed increasingly stringent industrial and municipal wastewater discharge requirements (Government of Alberta, 2012) and treated drinking water criteria (U.S. EPA, 2018; WHO, 2022; Health Canada, 2024) to limit threats to aquatic organisms and drinking water source from both existing and emerging contaminants, and thus protect public health through the provision of safe drinking water.

Plastic products are widely used, ranging from single-use items such as packaging and bottles to enduring goods such as electronic devices, furniture, and automobiles (Munyaneza et al., 2022; Ahmad et al., 2023). In addition, the COVID-19 pandemic has exerted significant pressure on the preexisting plastic waste management infrastructure due to overconsumption, extensive production, and inadequate disposal practices pertaining to personal protective equipment (Jiang et al., 2023; Khan et al., 2023). People prefer to use plastic items in their daily lives due to their physiochemical characteristics, which include low cost, durability, reliability, transparency, lightweight, and ease of manufacture and availability. Following their use, plastic products can be altered due to various physical and mechanical environmental processes, culminating in the formation of microplastics (MPs) (Khan et al., 2023; Lu et al., 2023). As a result of these weathering processes, different functional groups such as carbonyl, carboxyl, or hydroxyl groups appear on MPs surfaces, modifying active sites on the MPs compared to MPs with smooth surfaces. These “tiny” plastic particles first came to the broader attention of scientists in the 1970s after being identified as a large component of ocean floor debris; since categorization as “microplastics,” interest in their human and environmental health significance has skyrocketed (Thompson et al., 2004).

The observance of MPs in the environment is increasingly documented, fueling concerns about their ubiquity, treatment, and potential impact on ecosystems and human health. MPs range in size from 1  $\mu\text{m}$  to 5 mm and come in various shapes and compositions. The properties of MPs such as their size range, surface charge and chemical affinities (e.g., polarity and hydrophobicity) are comparable to those of other particles whose removal is targeted during drinking water treatment. MPs can be regular or irregular in shape, and their densities range from below to above that of water (1  $\text{g}/\text{cm}^3$ ). They originate

from the breakdown of larger plastic debris or are manufactured at small sizes for specific applications. The presence of MPs in aquatic and terrestrial ecosystems constitutes a substantial danger to these ecosystems' health and long-term sustainability. Because of the large surface area, persistence, and mobility of MPs in aquatic environments, this hazard extends to human food security and public health (Zhang et al., 2022; Khan et al., 2023).

Research has already begun to quantify the impact of MPs on various forms of wildlife (Leslie, 2014; Almroth et al., 2015; Imhof et al., 2016; Cesa et al., 2017) and identified MPs as vectors of toxic substances—such as phthalates, Bisphenol A, Polybrominated Diphenyl Ethers, and heavy metals—through the adsorption of toxins from the environment and subsequent ingestion (Cesa et al., 2017). Fine MPs can be transported through mammalian gastrointestinal tracts to lymph and circulatory systems, placentas to fetuses, and absorbed in the lungs, triggering immune responses (Leslie, 2014). The risks associated with plastic particles smaller than a few microns in size are considered more significant than that of larger particles due to the higher surface area and rate of uptake into cells for the smaller particles and the general uncertainty regarding their concentration in the environment (Triebkorn, et al., 2019). As such there is a need to understand the drivers of MPs removal during drinking water treatment, especially in the smaller 1 to 50  $\mu\text{m}$  size range (Imhof et al., 2016).

Given growing global evidence of MPs health effects and contamination in both source and treated drinking waters, it is important to assess their removal by established treatment processes and mechanisms. Particle removal during conventional drinking water treatment is typically achieved by coagulation, flocculation, sedimentation, and filtration processes. This is typically followed by disinfection (e.g., chlorination), which is particularly effective in inactivating bioparticles/microorganisms (Crittenden et al., 2012). Chemical coagulants are added to water to destabilize and subsequently aggregate particles during flocculation. Flocs are then removed from water in clarifiers, which often rely on gravitational settling. Physico-chemical filtration is a subsequent “polishing” step in which smaller colloidal particles that remain in suspension are removed. Drinking water treatment processes are designed to effectively remove a wide range of organic and inorganic particles from water, particularly when particle destabilization by coagulant addition is maximized—regardless of surface modifications or presence of surface functional groups. Thus, while MPs may present unique health threats if ingested in sufficient quantities, they may not pose unique treatment challenges because they are nonetheless particles and conventional water treatment processes are designed to remove a wide range of particle types from diverse raw water matrices. This expectation is supported by several investigations of pathogen removal

during drinking water treatment in which predominantly polystyrene microspheres (i.e., MPs) have been used as indicators of *Cryptosporidium* spp. oocyst (i.e., bioparticle) removal during drinking water treatment (Emelko, 2003; Emelko & Huck, 2004; Brown & Emelko, 2009; Wang et al., 2017).

### **1.1 Research objectives**

As MPs are an emerging concern in drinking water treatment, there are no specific guidelines or regulations that specify a target for their removal or a maximum acceptable concentration (i.e., MAC) for their presence in treated drinking water. Considering their increased identification in aquatic environments and the potential impacts of smaller sized MPs on both ecosystem and human health, it is essential to understand the effectiveness of conventional drinking water treatment processes in removing them. Accordingly, the primary goal of this research was to investigate if the removal of MPs by conventional chemical pretreatment (i.e., coagulation, flocculation, and sedimentation) with common coagulants is substantially different from that of other particles (including similarly sized protozoan parasites). The specific objectives of this study were to:

1. Characterize MPs removal by coagulation-flocculation-sedimentation (CFS) with different particle destabilization mechanisms and compare it to other important particulate contaminants (i.e., *Cryptosporidium* spp. oocysts),
2. Evaluate the effect of particle size on MPs removal by CFS, and
3. Assess the influence of weathering on MPs removal by CFS.

### **1.2 Research approach**

To draw a parallel between the removal of MPs and colloidal particles of similar sizes, a thorough literature review was conducted. The available MPs research was reviewed; especially the limited number of studies that have focused on MPs treatment. Studies focused on conventional chemical pretreatment (i.e., CFS) of colloidal particles were compared to those focused on MPs treatment. Investigations of *Cryptosporidium* spp. oocysts and microspheres were included in the review. Zeta potential—which provides an indication of surface charge and particle destabilization—was included where possible, to confirm that MPs have surface charges similar to those of other waterborne colloidal particles (e.g., *Cryptosporidium* spp. oocysts).

As shown in Figure 1.1, to address Objective #1 and evaluate MPs removal by chemical pretreatment reliant on (1) adsorption and charge neutralization and (2) enmeshment in precipitate (i.e.,

sweep flocculation) particle destabilization mechanisms, bench-scale investigations of alum-based CFS (i.e., jar tests) were conducted with synthetic water containing pristine and weathered PS microplastics (plain YG and carboxylated BB polystyrene) of 1, 5 and 10  $\mu\text{m}$  diameter. Several synthetic raw water matrices were explored to identify scenarios in which both particle destabilization mechanisms could be clearly discerned. The final synthetic raw water was composed of deionized water spiked with sodium carbonate and kaolin (70 NTU) at pH 7.0. To demonstrate that MPs removal by CFS aligns with coagulation theory, sixteen alum doses between 0–38.8 mg/L were used to evaluate MPs removal by CFS. MPs removal, residual turbidity, and zeta potential were evaluated at several alum doses.

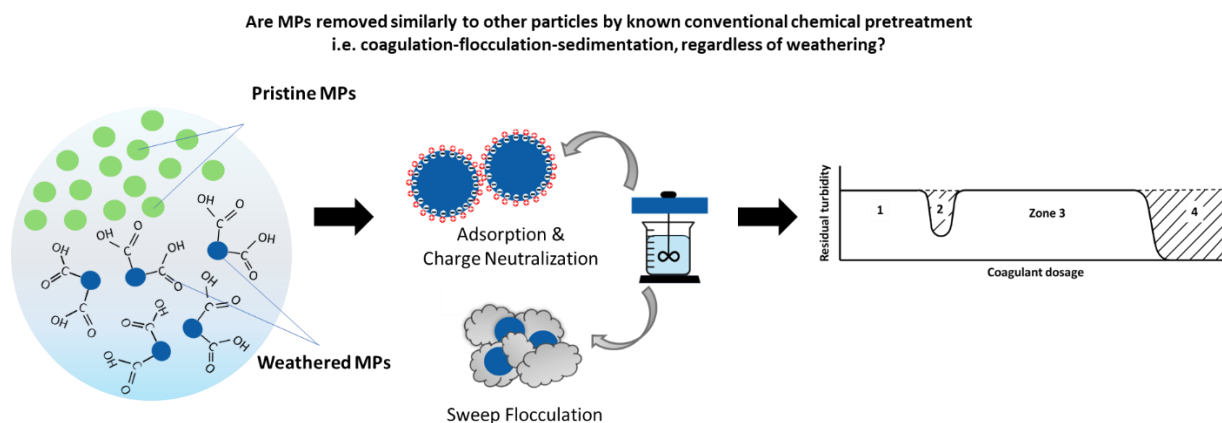


Figure 1.1 Graphical overview of this study focused on demonstrating that both pristine and weathered microplastics are destabilized similarly to other like-sized and -shaped particles (i.e., by adsorption and particle destabilization, and enmeshment in precipitate mechanisms) and therefore removal similarly during conventional chemical pretreatment (i.e., CFS). The conceptual representation of residual turbidity during chemical pretreatment is presented with permission, as described by Stumm & O’Melia (1968).

Objectives #2 and #3 were also investigated at bench-scale. Objective #2 involved conducting jar tests and enumerating MPs removal by CFS. Given that treatment of 1, 5, and 10  $\mu\text{m}$  spherical MPs of the same composition was evaluated, greater removal of larger MPs was anticipated because their greater size and mass would contribute to relatively enhanced aggregation and settling during flocculation and sedimentation (Crittenden et al., 2012). By comparing the removal efficiencies of different MPs sizes, the study aimed to confirm these theoretical expectations.

Objective #3 focused on assessing the influence of weathering on MPs removal by conventional CFS. This involved comparing the removal efficiencies of pristine MPs with those of weathered MPs, which have been used as surrogates to represent weathered MPs in treatment evaluations (Emelko, 2003;

Emelko & Huck, 2004; Brown & Emelko, 2009; Wang et al., 2017; Liu et al., 2019a). By analyzing the differences in removal performance between the pristine and weathered MPs, the study aimed to determine if surface modifications or the presence of certain functional groups affects destabilization and subsequent removal of MPs during the treatment process.

### **1.3 Thesis organization**

Chapter 1 provides a brief introduction and rationale for the research; it includes an overall goal and detailed research objectives.

Chapter 2 includes a detailed review of the literature regarding particles including MPs in water, focusing on their removal through coagulation, flocculation, and sedimentation (CFS). The chapter further examines the importance of surface charge, zeta potential, and solution chemistry during treatment, which are responsible for destabilizing and removing MPs and particles. Key knowledge gaps are also identified.

Chapter 3 details the research approach including the rationale and associated materials and methods.

Chapter 4 presents the research results and a discussion of these results, connecting observations to theory and the literature review.

Finally, Chapter 5 summarizes the conclusions and implications of the research.

## Chapter 2 Literature review

### 2.1 Particles in water

#### 2.1.1 Particulate contaminants

All natural waters—even those with highest quality—require treatment; at a minimum, disinfection to protect public health from waterborne pathogens, which can be considered bioparticles (Emelko et al., 2019). In addition to these organic particles (e.g., viruses, bacteria, protozoa, algae), drinking water sources contain a variety of inorganic particles (e.g., clays, aluminum and iron oxides, hydroxides, asbestos, silica) that are typically described by measurements of suspended solids concentrations or turbidity. The presence of particles in water can have significant health implications, which is why they need to be removed during drinking water treatment. Particles in water include pathogenic microorganisms and chemical contaminants. Pathogenic microorganisms like *Escherichia coli*, *Giardia* spp., *Cryptosporidium* spp., and viruses can cause waterborne diseases such as diarrhea, cholera, dysentery, and gastroenteritis—in some cases, they can survive and proliferate in water systems if not removed properly, leading to widespread health risks (Health Canada, 2016; 2022). Particles also can contain or adsorb toxic chemicals, including pesticides, heavy metals (e.g., arsenic, mercury, lead), and industrial pollutants. These chemicals can have long-term health effects such as cancer, neurological damage, and developmental issues, especially in children (Government of Canada, 2022). Organic particles in water can react with disinfectants like chlorine to form disinfection byproducts (DBPs) such as trihalomethanes (THMs) and haloacetic acids (HAAs). These byproducts have been linked to cancer and other health issues (Feder et al., 2009; Pandian et al., 2022). Particles in water also can shield microorganisms from disinfectants such as chlorine, thereby reducing the effectiveness of water treatment and increasing risks from waterborne disease (Batch et al., 2004; Passantino et al., 2004). In addition to these health concerns, particles can also reduce the aesthetic quality of water because they can make it look cloudy or murky or affect the taste and smell (i.e., high turbidity), making people hesitant to drink it (Crittenden et al., 2012). Traditionally, particles have been categorized into colloidal and suspended categories based on size, with colloidal particles having at least one dimension ranging from nanometers ( $10^{-9}$  m) to micrometers ( $10^{-6}$  m), as illustrated in Figure 2.1 (Tchobanoglous et al., 2014). Notably, these ranges are not absolute and larger nanoplastics are sometimes referred to as MPs.

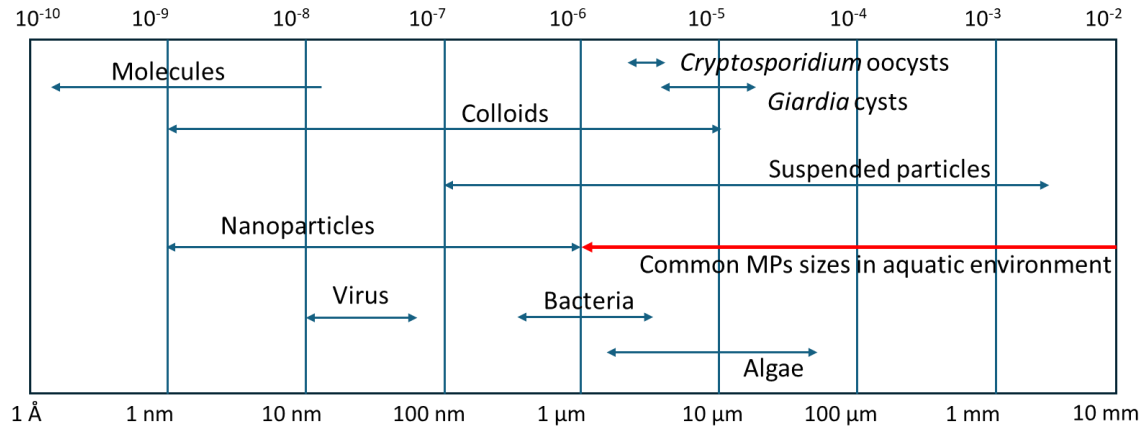


Figure 2.1 Size spectrum for waterborne particles. Modified from Tchobanoglous et al., (2014). For plastics, these ranges are not absolute and larger nanoplastics are sometimes referred to as MPs.

### 2.1.2 Regulatory Approaches

The primary objective of drinking water treatment is to protect public health by producing water with contaminant concentrations below established standards, minimizing health risks to consumers (Hrudey, 2004; Li & Wu, 2019). Regulatory guidelines are generally designed to reflect health risks posed by various microbial (e.g., bacteria, viruses, protozoa), chemical (e.g., heavy metals, pesticides) and radiological contaminants that may be present in untreated water. Among these, microbiological contaminants are prioritized because of the acute risks that they pose to public health.

Maximum Concentration Limits (MCLs) or Maximum Acceptable Concentrations (MACs) are established for many waterborne contaminants of human health significance. Risks associated with suspended solids and the contaminants they carry (e.g., metals) have been managed by treated and distributed water thresholds for turbidity (e.g., U.S. National Interim Primary Drinking Water Regulations (U.S. EPA, 1974). Since the late 1980s, due to the challenges associated with routine monitoring and analysis of parasitic protozoa (i.e., *Giardia* spp. and *Cryptosporidium* spp.), “Treatment Technique” based approaches have been developed in many jurisdictions. They involve provision of treatment credits that are allocated based on evidence of “well-operated” treatment performance such as achieving specific turbidity targets for effluent water (U.S. EPA, 1989; 1998; 2002; 2006; Health Canada, 2019). In North America, regulations focus on minimizing infection risks by mandating that water system operators use granular media filtration (or comparable technologies) and disinfect both surface water and groundwater directly influenced by surface water (U.S. EPA, 1989; 1998; 2002; 2006; O. Reg. 170/03, 2003). Although *Giardia* is the most reported enteric protozoan globally (Adam et al., 2016), *Cryptosporidium* is also

ubiquitous in the environment, especially in surface water. As protozoa and particularly *Cryptosporidium* spp. are difficult to inactivate with traditional oxidant-based disinfection methods like chlorination and ozonation (Korich et al., 1990; Li et al., 2001), the suite of U.S Surface Water Treatment Rules (U.S. EPA, 1989; 1998; 2002; 2006) and their international equivalents (O. Reg. 170/03, 2003) are designed to also remove them to reduce the risk of waterborne diseases caused by microbial contaminants—particularly *Giardia* spp., and *Cryptosporidium* spp.—in public water systems that rely on surface water or groundwater “under the direct influence of surface water”. Currently, water systems must achieve a 99.9% (3-log) removal and/or inactivation of *Giardia* and *Cryptosporidium* and a 99.99% (4-log) removal and/or inactivation of viruses through filtration (or equivalent technology) and disinfection. Turbidity must not exceed 1 NTU at any time and 95% of samples collected each month must have turbidity levels that do not exceed 0.3 NTU for systems using conventional or direct filtration.

### **2.1.3 Surface charge of particles in water**

Particles have charge for a variety of reasons, which include isomorphous replacement, preferential adsorption of ions, and ionization of surface sites. For isomorphous replacement, a lower valence metal atom can replace the higher valence metal atom in metal oxide minerals imparting a negative charge to the crystal material (Crittenden et al., 2012). In preferential adsorption, charged hydrophobic species can be adsorbed onto particles, thereby modifying surface properties and imparting the negative charge and steric stability of particles (Ongerth & Pecoraro, 1996; Crittenden et al., 2012). Lastly, the ionization of metal oxide or hydroxide at the particle surface with increasing pH can impart a negative charge on particles. For example, as the pH increases above pH 2, the silica surface develops a net negative charge primarily due to deprotonation of the silanol group (Stumm 1992; Elimelech et al., 1995; Stumm & Morgan 1996; Crittenden et al., 2012).

Particles suspended in natural water are mostly negatively charged at near-neutral pH due to the presence of natural organic matter (NOM). NOM is composed of a variety of organic molecules, including humic and fulvic acids, which typically carry functional groups like carboxylic and phenolic groups. These functional groups dissociate in water, releasing protons and leaving behind negatively charged sites on the NOM molecules. When NOM, which is negatively charged, adsorbs onto the surface of particles in natural water, the net surface charge of the particles typically becomes negative (Beckett & Le, 1990; Sillanpää, 2014). This negative charge increases the electrostatic repulsion between particles, helping to stabilize them in suspension and preventing aggregation. As a result, particles are more likely to remain dispersed and contribute to the turbidity and color of the water. Since most particles in natural waters

carry a negative surface charge, they remain largely dispersed without extensively aggregating or attaching to other negatively charged surfaces or particles. When these surface charges are neutralized, aggregation and subsequent settling may be facilitated (Edzwald, 1993). This can occur naturally in rivers and lakes (e.g., Stone et al., 2011; Stone et al., 2021; Maltauro et al., 2023) and in engineered treatment processes such as CFS, which is discussed further in Section 2.3.

In natural waters, negatively charged particles accumulate positively charged counter ions near their surface to satisfy electroneutrality. As described by Crittenden et al. (2012) this layer of cations bound to the particle surface by electrostatic and adsorption forces is known as the Stern layer. Beyond this is the Diffuse layer, in which both cations and anions that are loosely attracted is present, but the concentration of counterions charged opposite to the charge of the particle surface is high and decreases over distance from the particle surface until the bulk solution where electric potential is zero and electroneutrality is satisfied. Collectively, the Stern and the Diffuse layers are known as the electric double layer. As particles move through a fluid, the counterions in the double layer move with the particle, which gives rise to a shear plane. As shown in Figure 2.2, the distance from the Stern layer to the edge of the diffuse layer is known as the plane of shear, also known as the slipping plane. Using electrophoresis, which is the movement induced when a charged particle is subjected to an electric field between two electrodes, the electrical potential between the plane of shear and the bulk solution is measured, and this is known as zeta potential (Crittenden et al., 2012).

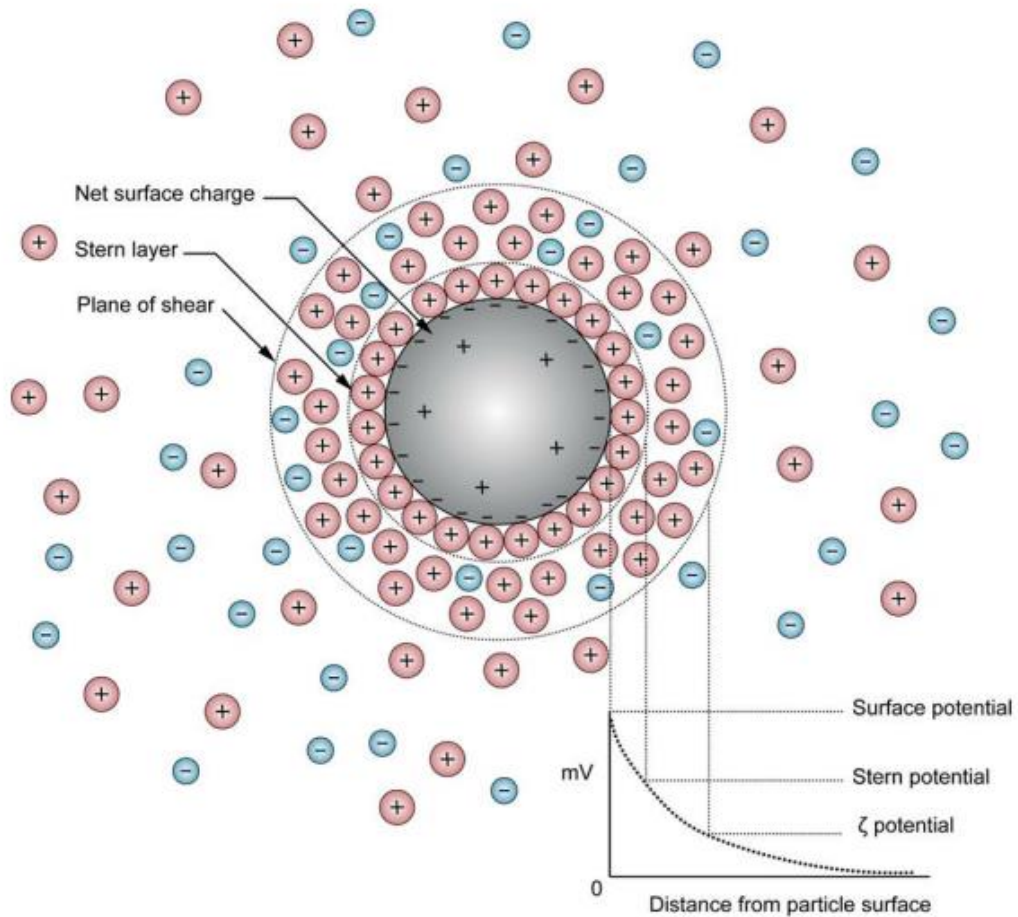


Figure 2.2 Difference in electric potential as a function of distance from the charged surface of a particle/microplastics suspended in a dispersion medium such as water. Zeta potential ( $\zeta$ ) is the difference in electric potential at the plane of shear around the suspended particle and the bulk liquid (Ballantyne, et al. 2024 Reprinted with permission. © The Water Research Foundation).

Zeta potential ( $\zeta$ ) indicates the extent of electrostatic repulsion between charged particles in a suspension and is measured in millivolts (mV). It is important to note that zeta potential is not a direct measurement of the surface charge on the particles. It is an indirect measurement calculated based on the measurement of electrophoretic mobility (Lowry et al., 2016). The zeta potential of most surface waters ranges from -15 to -30 mV, and most particles in natural water have negative zeta potentials, typically ranging from -5 to -50 mV (Rice et al., 1996; Dai & Hozalski, 2003).

## **2.2 Emergence of MPs as particulate contaminants of health concern**

In the past decade, MPs have emerged as particulate contaminants of human and ecosystem health significance. The term “microplastic” was first introduced in a 1968 report by the US Air Force Materials Laboratory, referring to particles formed from the deformation of plastic materials under high stress (Ingram et al., 1968). MPs in aquatic environments were first recognized in 1972 when micro-sized plastic particles were identified in the surface waters of the Sargasso Sea. The term “microplastics” was later coined by Thompson et al. (2004), who defined MPs as plastic particles ranging from 100 nm to 5 mm in size, with particles smaller than 100 nm classified as nanoplastics (Amobonye et al., 2021; Munyaneza et al., 2022).

### **2.2.1 Prevalence of microplastics in freshwater**

The widespread presence of plastics has become a growing environmental concern due to increased production, consumption, and mismanagement. Each year, the world produces approximately 400 million tons of plastic, with half of this amount being used for single-use items such as polyethylene terephthalate (PET), polyethylene (PE), polyvinyl chloride (PVC), polyester fibers (PEST), high-density polyethylene (HDPE), low-density polyethylene (LDPE), polypropylene (PP), polystyrene (PS), and expanded polystyrene (UNEP, 2022). MPs enter aquatic environments through various pathways, and it is essential to consider their sources and impacts. Land-based MPs find their way into surface water through sewage discharges (Parashar & Hait, 2022), commercial and recreational activities such as fishing and watersports (Kooi et al., 2018), wet and dry atmospheric deposition (Allen et al., 2019; Parashar & Hait, 2023), rainwater (Bauer-Civiello et al., 2019), and urban runoff (Han et al., 2022; Wang et al., 2022). Among these, urban runoff is the primary pathway for the transfer of MPs to aquatic environments (Fang et al., 2021; Shruti et al., 2021).

According to a meta-analysis conducted by Chang et al. (2024), MPs have been detected in freshwater ecosystems across at least 36 countries globally. The concentrations of MPs ranged from  $10^{-3}$  to  $10^5$  particles/m<sup>3</sup>, with an average concentration of  $12,465.34 \pm 68,603.87$  particles/m<sup>3</sup> (mean  $\pm$  standard deviation), covering a span of eight orders of magnitude. A few studies have surveyed MPs in raw water intakes from selected DWTPs and as expected their presence has been confirmed (Pivokonsky et al., 2018; Mintenig et al., 2019), with concentrations reaching up to 4,000 MPs/L (Pivokonsky et al., 2018). MPs have also been reported in lakes, rivers, and dams (Dris et al., 2015; Su et al., 2016; Anderson et al., 2017; Leslie et al., 2017; Di & Wang, 2018; Triebkorn et al., 2019), and even in remote environments

(Free et al., 2014; Waller et al., 2017; Green et al., 2018). Another investigation carried out by Oßmann et al. (2018) showed that the number of MPs was measured to be 2649, 4889, and 6292 particles/L in the single use PET plastic bottles, reusable PET plastic bottles and glass bottles, respectively, and most particles (90%) were smaller than 5 µm. In water from glass bottles, PE, PP and PET were also found.

### **2.2.2 Health implications**

The associations between MPs and human health are still evolving and remain unclear, but their presence in drinking water understandably raises public health concerns (Shen et al., 2020). Health effects can be attributed to 1) the MPs particles themselves, 2) additives and adsorbed or absorbed contaminants, and 3) attached microorganisms or biofilm, and microbially altered MPs and associated chemicals (Chowdhury et al., 2024). For example, plastics used in commercial and industrial applications are often treated with additives, known as plasticizers, including flame retardants, stabilizers, antioxidants, and colorants (Campanale et al., 2020). These additives, such as polybrominated diphenyl ethers, phthalates, and bisphenol A, can leach from plastics into drinking water and act as endocrine disruptors, leading to hormonal imbalances and long-term health effects (Khan et al., 2020; Zhang et al., 2022; Chowdhury et al., 2024).

Numerous studies have investigated the direct effects of MPs on aquatic organisms, revealing some health threats (de Sá et al., 2018; Triebkorn et al., 2019). However, many of these studies utilized MPs concentrations significantly higher than those currently detected in nature (Triebkorn et al., 2019). In addition to aquatic organisms, research has begun to explore MPs' interactions with human cells. For example, in vitro experiments by Schirinzi et al. (2017) demonstrated that MPs, primarily 10 µm PS along with 40–250 nm nanoplastics, induced oxidative stress in human cerebral and epithelial cells. Similarly, Triebkorn et al. (2019) found that PS MPs ( $0.25 \pm 0.06$  µm) were taken up by human keratinocytes (the primary type of cell in the outer layer of skin) which might trigger cellular stress and inflammatory responses.

The potential health implications of MPs extend beyond direct effects from the particles themselves. MPs can act as carriers for hydrophobic organic contaminants, which may adsorb onto their surfaces and subsequently be transferred to various organs and tissues at elevated concentrations (Wang et al., 2020a; Chowdhury et al., 2024). This possibility raises concerns about the synergistic effects that could exacerbate the toxicity of both MPs and the adsorbed contaminants. A review by Wright and Kelly (2017) investigated the potential impacts of MPs uptake on human health, particularly through gastrointestinal tract absorption. The ability of MPs to translocate and be absorbed depends on several

factors, including particle size. Larger MPs (>2 µm) tend to remain in the intestinal tract, while smaller MPs may enter the bloodstream but struggle to penetrate deep tissues due to size limitations. These larger particles are typically cleared by the spleen (Bouwmeester et al., 2015). However, as the size of MPs decreases, their potential to enter peripheral tissues and the circulatory system increases, leading to systemic exposure through lymphatic aggregation.

Toxicity assessments from *in vivo* and *in vitro* experiments on human cell lines have shown cytotoxicity, inflammation, and the formation of reactive oxygen species, all considered adverse effects of MPs exposure (Lehner et al., 2019; Schirinzi et al., 2017). While human studies are limited, observations from animal studies suggest that human health impacts are likely, emphasizing the need for caution and further research into MPs ingestion (Thubagere & Reinhard, 2010; Mahler et al., 2012; Schirinzi et al., 2017; Pitt et al., 2018). Importantly, most toxicity studies have focused on PS MPs and nanoplastics, even though other environmentally relevant plastics, including PE, PET, PVC, and PP are also prevalent (Lehner et al., 2019).

The size of MPs and nanoplastics is crucial when considering direct health impacts and toxicity. MPs larger than 1 µm are generally not expected to reach human organs due to their limited ability to cross cellular membranes, although they may cause localized effects such as immune system responses or gut inflammation (Deng et al., 2017; Raifee et al., 2018). In contrast, nanoplastics, especially those smaller than 30 nm, have a greater potential to penetrate cell membranes and accumulate in tissues and organs (Bouwmeester et al., 2015).

In addition to the direct toxicity of MPs particles, their sorptive capacity raises concerns about indirect health implications. MPs can absorb chemicals from the environment, making them potential carriers of chemical contaminants that could be ingested by humans through drinking water (Smith et al., 2018). This is particularly concerning as adsorbed contaminants may transfer from MPs to human tissues, with potentially lethal consequences, as observed in experiments on smaller organisms. For instance, the bioaccumulation of the antibiotic roxithromycin was enhanced in freshwater fish when PS MPs treated with the antibiotic were introduced into the water (Jiang et al., 2018). Increased mortality and reduced antioxidant defenses were observed in fish exposed to PE MPs, which increased the bioavailability of pyrene and its consumption (Oliveira et al., 2013). Analogous human health implications are a growing concern for the drinking water industry, particularly as more information becomes available about the environmental concentrations of waterborne MPs and the toxic contaminants they carry (Bakir et al., 2014).

### 2.2.3 Physical and chemical properties of MPs

Understanding the physical and chemical properties of MPs is important for assessing their behavior, transport, and environmental impact, as well as their removal effectiveness. MPs and other waterborne suspended particles have many similarities (Shen et al., 2020). The physical characteristics of MPs, including their various shapes—such as fragments, fibers, films, pellets, and beads—affect how they move in the environment or interact with organisms and their potential to adsorb other substances. For example, fibers may entangle with other particles or organisms, while beads and pellets might interact differently due to their rounded shapes. Plastics like PE and PP have lower densities (less than 1 g/cm<sup>3</sup>) and tend to float on water surfaces, while heavier plastics like PET and PVC have higher densities (greater than 1 g/cm<sup>3</sup>) and are more likely to sink. Additionally, polymer type influences their chemical stability and degradation rate (Hidalgo-Ruz et al., 2012).

Similar to most particles found in natural systems, MPs are negatively charged and typically hydrophobic, exhibiting low polarity and a strong affinity for nonpolar surfaces (Khan et al., 2023). As shown in Table 2.1, the zeta potential values of MPs demonstrate that the magnitude of negative charge varies with particle size, type, and the water matrix in which they are suspended. The presence of functional groups or ions on the surfaces of MPs causes them to exhibit surface charges (He et al., 2022).

Table 2.1 Zeta potential values for some MPs in water. Reproduced from Chowdhury (2022).

MPs material	Zeta potential (mV)	Conditions	Reference
Carboxylated latex	-50.2 to -7.4	size: 5.0 μm pH: 6.7 DI & distilled water IS: calcium concentration (10 <sup>-6</sup> to 10 <sup>-1</sup> )	Dai & Hozalski, 2003
Fluorescent blue-green carboxylated PS	Uncoagulated: - 41.2 Coagulated: - 0.5	size: 4.675 μm pH: 7.2 fluoridated tap water and low-turbidity raw water ranging from 1.5 to 2.6 NTU	Amburgey et al., 2005
PET HDPE PVC PP	-120 to 20 (Measured at different pH levels in de-ionized water before the addition of black tourmaline powder)	size: 2,540 μm  pH: 3 to 10 DI water	Lameiras et al., 2008

MPs material	Zeta potential (mV)	Conditions	Reference
Unmodified PET, PP, PS HDPE LDPE	-70 to -55	size: ranging from 10 $\mu\text{m}$ to 2 mm pH: 6 to 6.2 electrolyte solution: 0.005 $\text{mol/dm}^3$ KCl and 0.001 $\text{mol/dm}^3$ $\text{KNO}_3$	Kolska et al., 2013
Carboxylated PS	-41.4	size: 4.36 $\mu\text{m}$ pH: 8.2 IS: 4.37 mM	Papineau et al., 2013
Carboxylated yellow- green PS	~-30	size: 4.5 $\mu\text{m}$ pH: 7.5, hardness of 200 mg/L as $\text{CaCO}_3$ , free chlorine of 2 mg/L	Lu & Amburgey, 2016
Unmodified PS Carboxylated PS	-33.9 and -30.7  -19.9 to 17.5	size: 4.5 $\mu\text{m}$ , 10 $\mu\text{m}$ pH: 6 IS: 1 mM KCl	Zhang et al., 2017
PS (surface modified carboxyl group)	-30 to -30.9  -23 to -26.4	size: 0.8 $\mu\text{m}$ , 1.5 $\mu\text{m}$ 0.1 $\mu\text{m}$ , 0.4 $\mu\text{m}$ , 0.6 $\mu\text{m}$ salinity: 3.5, 7.5, 35 PSU	Dong et al., 2018
PS	-80 to -30	size - 0.3 – 0.4 $\mu\text{m}$ pH: 2 to 8 IS: 0.01 to 500 mmol/L NaCl, KCl and $\text{MgCl}_2$	Lu et al., 2018
Unmodified PS	-56.5	size: 4.3 $\mu\text{m}$ pH: 8	Liu et al., 2019a
Glycoprotein modified PS	-36.4	DI water IS: 1 mM NaCl	
Modified PVC (azodicarbonamide modified with 10% by weight of zinc oxide)	14.6	size was not reported distilled water at 25°C, Conductivity: 0.056 $\mu\text{S/cm}$	Cai et al., 2020
Unmodified PVC	-9.59		
PE	-38.8 to -24.4	size: 40 to 48 $\mu\text{m}$ IS: 0.01 to 0.05 Fulvic acid: 0, 5, 10 mg/L	Hou et al., 2020
PE PE with surfactants	-35 to -14 -5 to -9	size - 5 $\mu\text{m}$ pH - 5 to 10	Skaf et al., 2020

DI – deionized; IS – ionic strength; HDPE/LDPE: high/low-density; NPs: nanoplastics; PE: polyethylene; PET: polyethylene terephthalate; PP: polypropylene; PS: polystyrene; PSU: practical salinity units; PVC: polyvinylchloride.

#### 2.2.4 Weathering of microplastics

Environmental exposure can alter MPs. As a result, MPs surface attributes can change over time and undergo chemical reactions that lead to changes in surface functional groups. Weathering processes include physical, chemical, and biological reactions.

Physical weathering involves cracking or fragmentation, while chemical weathering includes photo- or thermal-degradation, and biological reactions encompass microbial degradation, ingestion, or digestion. Mechanical breakdown results from abrasion and disintegration forces due to interactions with sediments, pebbles, waves, and tides in aquatic environments. In terrestrial environments, human activities like soil cultivation and crop rotation contribute to mechanical fragmentation (He et al., 2018). This fragmentation can produce smaller MPs and NPs (<10 nm) through simulated sand or wave action. However, potential disintegration processes, such as freeze-thaw cycles and rainstorm events, are less well studied.

Photodegradation is a form of chemical weathering, where unsaturated structures or additives in polymers absorb UV light, forming polymer radicals. This leads to oxygen addition, hydrogen abstraction, and the eventual cleavage of polymer chains (Feldman, 2002; Gewert et al., 2015; Singh & Sharma, 2008). Thus, it alters MPs' physical and chemical characteristics by forming oxygen-containing functional groups on their surfaces (Barboza et al., 2018; Guo & Wang, 2019). These newly introduced functional groups enhance MPs' ability to adsorb environmental pollutants, including polychlorinated biphenyls, polycyclic aromatic hydrocarbons, and organochlorine pesticides (Kim et al., 2015; Liu et al., 2020). This increased adsorption capability influences the migration, transformation, and bioavailability of these pollutants in the environment (Teuten et al., 2007). Thermal degradation, similar to photodegradation, is initiated by heat instead of UV light (Singh & Sharma, 2008). Although thermal degradation of plastics is a commercial process, it rarely occurs in the natural environment (Mattsson et al., 2015).

Degradation or biodegradation of plastics takes place under different factors that include characteristics of plastics, such as their mobility, crystallinity, molecular weight, the kind of functional groups and additives added to the polymers. Environmental conditions like oxygen levels, water presence, temperature, and biofilms are also important (Tian et al., 2019; Turgay et al., 2019; Chen et al., 2020; Mei et al., 2020; Wang et al., 2020a). During biodegradation of plastic, colonization by the microorganisms on the plastic surface leads to reducing the molecular weight of plastics, converting the polymer to its monomers, followed by their breakdown into carbon dioxide, water, and methane (i.e., mineralization) (Shah et al., 2008; Zheng et al., 2005). Few studies have investigated MPs degradation rates. In one study,

it was found that *Microbispora rosea* can degrade 50% of PBS film after eight days (Tokiwa et al., 2009) while *Aspergillus* sp. degraded 90% of PHB film after six days of cultivation at 50°C (Sanchez et al., 2000; Shah et al., 2008). For the latter, the polyester was degraded and assimilated, yielding 36 mg of cells from a 100 mg sample and 10 mg of yeast extract after 6 days at 50°C (Sanchez et al., 2000).

These physical, chemical, and biological weathering processes generate oxygen-containing groups (C=O, O–H, and C–O), including carboxylic, aldehyde, ketone, and hydroxyl groups, which significantly alter the active sites on MPs compared to their pristine state. As a result, weathered MPs exhibit increased hydrophilicity, polarity, and surface charge, influencing their reactivity and interactions with pollutants (Holmes et al., 2012; Liu et al., 2019b, c). Nonetheless, this change in structure is particularly concerning as MPs possess a large specific surface area (i.e., surface area per unit mass), allowing them to sorb a wide range of organic and inorganic contaminants, including persistent organic pollutants and metals. This sorption occurs through mechanisms such as (1) hydrophobic partitioning interactions, (2) surface adsorption involving electrostatic interactions, non-covalent bonding, hydrogen bonding, and van der Waals forces, and (3) pore filling, where contaminants become trapped within the MPs' pores. Additionally, MPs often serve as substrates for microbial colonization, leading to the formation of biofilms that further modify their buoyancy, reactivity, and transport within the environment (He et al., 2018; Iñiguez et al., 2018).

## **2.3 Particle removal during drinking water treatment**

### **2.3.1 Water treatment overview**

Conventional chemical pretreatment (i.e., coagulation-flocculation-sedimentation) followed by physico-chemical filtration has been used for decades in water treatment, with extensive literature and experience demonstrating its effectiveness in removing both inorganic and organic particles, including *Cryptosporidium* oocysts (Plummer et al., 1995; Abbaszadegan et al., 1997; Oilier et al., 1997; Baudin and Laîné, 1998; Fox et al., 1998; Xagorarakis, 2004; Chuang et al., 2007; Bina et al., 2009; Latour et al., 2013; Petersen et al., 2016). As described by Crittenden et al. (2012), coagulation typically involves the addition of aluminum- or iron-based salts to water, which hydrolyze to form species that adsorb onto colloidal particles or enmesh them in precipitates, destabilizing them and facilitating particle aggregation by tapered mixing during flocculation. During sedimentation, these flocs settle out, leading to removal of particles from the water column. Physico-chemical filtration is a subsequent “polishing” step in which smaller colloidal chemical and microbial contaminants that remain in suspension are removed. Particle

destabilization/coagulation efficiency can be enhanced by optimizing coagulant dose and adjusting pH improving mixing or using composite coagulants that combine metallic and polymeric components (U.S. EPA, 1999). Effective particle destabilization during coagulation is also critical for maximizing particle removal by physico-chemical filtration because it reduces repulsive forces between media grains and particles, promoting adherence through attractive van der Waals forces (Habibian & O'Melia, 1975; Amirtharajah, 1988; Ballantyne et al., 2024).

### **2.3.2 Particle destabilization by coagulation**

Sufficient particle destabilization is essential for effective particle removal by both conventional chemical pretreatment (i.e., CFS) (Habibian & O'Melia, 1975) and physico-chemical filtration (Amirtharajah, 1988; Ballantyne et al., 2024), which is sometimes referred to as rapid sand filtration, granular media filtration, and—most notably—chemically-assisted filtration (Ballantyne et al., 2024). In water treatment, coagulation is the process used to destabilize and remove organic and inorganic particles so that they can be subsequently removed from water during treatment (Letterman & Vanderbrook, 1983; Amirtharajah & O'Melia, 1990). The most commonly used metal salts in coagulation are aluminum sulfate (alum), ferric chloride, and ferric sulfate. Fundamental studies on coagulation chemistry indicate that a range of hydrolyzed Al/Fe species formed upon the addition of alum- or iron-based coagulants are responsible for the removal of suspended particles in water (Jiang, 2001; Saxena et al., 2018).

The mechanisms that are responsible for particle destabilization and aggregation include compression of the 1) double layer, 2) charge neutralization, 3) enmeshment in precipitate, and 4) interparticle bridging (Stumm & O'Melia, 1968; Crittenden et al., 2012; Ballantyne et al., 2024). During double layer compression, the electrostatic repulsive forces generated by charged species on particle surfaces are reduced by increasing the ionic strength through the addition of an indifferent electrolyte. However, this mechanism is not employed in water treatment because the ionic strength needed for such mechanisms is greater than what is acceptable in potable water (Crittenden et al., 2012). Particle surface charge is also neutralized as positively charged hydrolysis species attach to the particles, reducing or neutralizing the net surface charge—a process known as charge neutralization. However, an excess dose of metal salts can cause charge reversal and particle restabilization (Figure 2.3), which leads to more frequent collisions between colloidal particles and greater collision efficiency, which increases system instability and decreases removal efficiency (Zhang et al., 2021; Zhou et al., 2021). With further addition of metal salt, hydroxide precipitation leads to sweep flocculation, in which particles become enmeshed in precipitates that drive surface charge of the formed aggregate (Duan & Gregory, 2003). Adsorption and interparticle

bridging are relevant to polymers only, where multiple sites of their long chain adsorb onto particle surfaces while extending to other surface sites of other particles, thus creating a “bridge” between particle surfaces (Amirtharajah & Mills, 1982; Lartiges et al., 1997; Crittenden et al., 2012; Ballantyne et al., 2024). Therefore, the two primary coagulation mechanisms of commonly used metal salts (i.e., aluminum sulfate/alum and ferric chloride) are adsorption and charge neutralization and enmeshment of particles or sweep flocculation (Amirtharajah & Mills, 1982; Duan & Gregory, 2003; Pernitsky & Edzwald, 2006; Ballantyne et al., 2024).

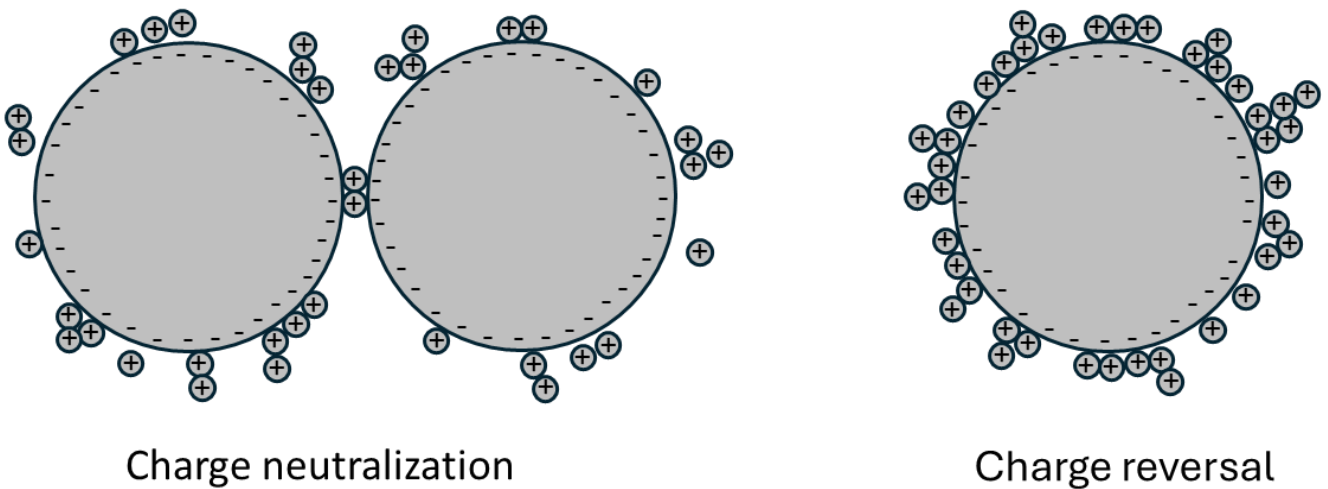
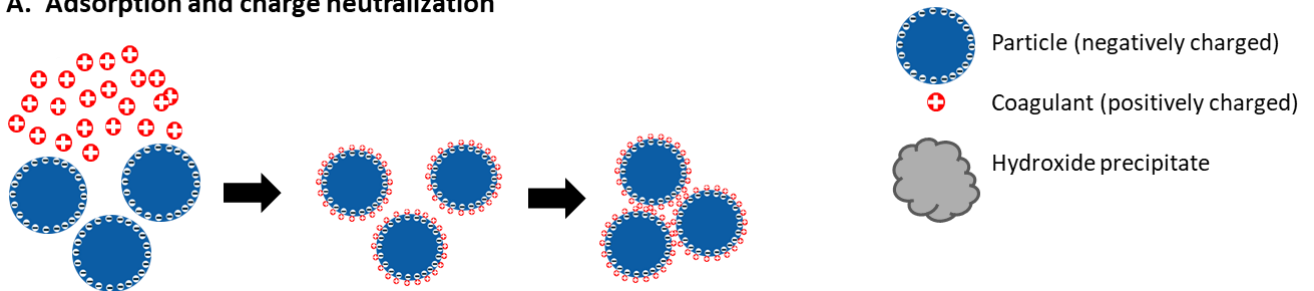


Figure 2.3 Charge neutralization and charge reversal by metal salt hydrolysis species for particles in a suspension. Reproduced from Duan & Gregory (2003) with permission.

Electrophoretic mobility measurements show that the optimum coagulant dose for particle destabilization corresponds with the condition where the zeta potential of the particles is close to zero or a few millivolts around the PZC (Amirtharajah & Mills 1982; Duan & Gregory, 2003; Pernitsky & Edzwald, 2006). Sometimes, the optimum dose range can be quite narrow, necessitating precise dosing control. Generally, the optimum coagulant dose is achieved when the particle surface is only partially covered (less than 50 percent). In the case of aluminum salts as coagulants, charge neutralization occurs at quite low metal concentrations, typically in the order of a few  $\mu\text{M}$  at just below neutral pH (Tadros, 2013). In this situation, it is likely that nucleation of the precipitate occurs on the surface of particles, leading to the growth of an amorphous precipitate with the entrapment of particles in this amorphous structure or a mesh-like surface structure (Crittenden et al., 2012). In this case, metal hydroxide precipitates will form in suspension, they enmesh the colloidal particles and destabilize them (Figure 2.4) (Packham, 1965). This

mechanism predominates in water treatment applications where pH values are generally maintained between pH 6 and 8, and aluminum or iron salts are used at concentrations exceeding saturation with respect to the amorphous metal hydroxide solid that is formed (Tang et al., 2022). For aluminum hydroxide, the PZC is around pH 8, so the metal hydroxide precipitates should be positively charged at lower pH values. For ferric hydroxide, the PZC is somewhat lower around pH 7 (Tadros, 2013).

**A. Adsorption and charge neutralization**



**B. Sweep flocculation**

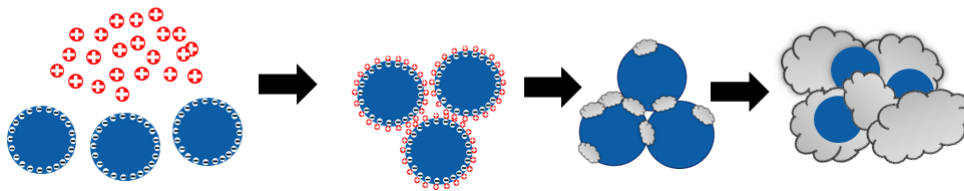


Figure 2.4 Particle destabilization by (A) adsorption and charge neutralization and (B) sweep flocculation during coagulation using metal salts.

Sweep flocculation involves precipitate formation specifically where there is an insufficient number of particles or colloid concentrations available to provide adequate contact opportunities for aggregation within a reasonable time frame (i.e., low turbidity waters). Therefore, the introduction of precipitated particles by metal hydroxides can increase contact opportunities and enhance aggregation and/or attachment to surface media (Stumm & O'Melia, 1968; Bache et al., 1999).

The solubility diagrams developed by Amirtharajah and Mills (1982) and Johnson and Amirtharajah (1983) for aluminum hydroxide (alum) and ferric chloride, respectively, illustrate the dominant mechanisms of particle destabilization with respect to pH and alum dose. Figure 2.5 indicates the solubility diagram for alum. It should be noted that the depicted zones are not fixed; other factors such as temperature and ionic strength also affect solubility and the conditions at which different particle destabilization mechanisms predominate.

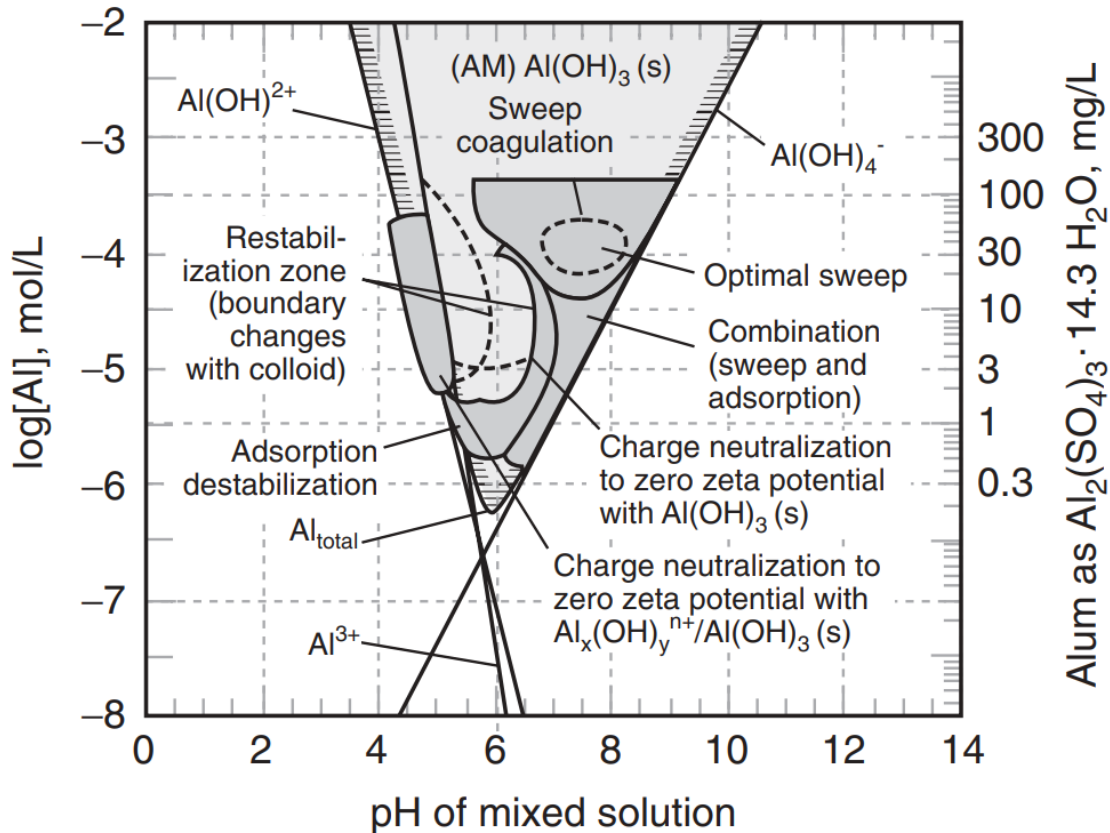


Figure 2.5 Solubility diagram for Al (III) mononuclear species at 25°C. Metal species are assumed to be in equilibrium along with the amorphous precipitated solid phase. Reprinted from Crittenden et al., 2012 with permission.

Particles aggregate and are most efficiently removed from water when they destabilized by coagulation such that the zeta potential is close to zero (PZC) (Bean et al., 1964; Gupta et al., 1975; Ballantyne, et al. 2024). It has been suggested that  $\pm 5$  mV of zero indicates that particle destabilization has been maximized for good water treatment performance in Great Lakes regions such as Toronto, Canada (Ballantyne, et al. 2024). Measured electrophoretic mobility and the corresponding zeta potential are dependent on both particle properties (charge density, size, shape) and matrix effects (pH, ionic strength, NOM concentrations) (Lowry et al., 2016). Therefore, for a given solution of particles, their zeta potential is unique.

### 2.3.3 Flocculation and sedimentation

Flocculation is a process in which small particles—such as clay, protozoan (oo)cysts, MPs—in suspension aggregate to form larger clusters (flocs), making it easier to subsequently separate them from

water than the original particles. This process relies on the collision and attachment of particles in a suspension, resulting in particle aggregates (flocs) that are much larger than the original (primary) particles. For an initially stable suspension, flocculation occurs when there is good (a) destabilization (which is achieved by coagulation) and (b) attachment due to particle collisions.

In a suspension with particles of similar densities, larger particles tend to settle faster than smaller ones primarily due to the influence of gravitational and drag forces. The gravitational force acting on a particle increases with its mass, which is proportional to the cube of the particle's radius. As a result, larger particles experience a stronger downward force compared to smaller particles. While drag force, which opposes the motion of a particle through a fluid, increases with the particle's surface area, the mass increases giving larger particles a higher ratio of gravitational force to drag force, allowing them to settle faster as shown in Figure 2.6. This phenomenon is described by Stokes' law, which states that the settling velocity of particles with similar densities is proportional to the square of their size (O'Melia, 1978; Crittenden et al., 2012).

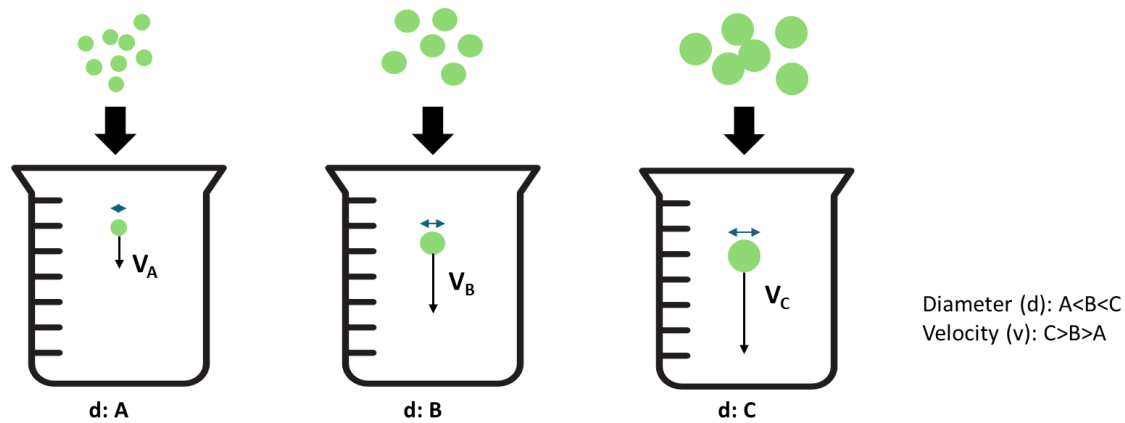


Figure 2.6 Differential settling of particles simplified as a function of size (adapted from Crittenden et al., 2012).

Stokes' law is typically used to describe the settling velocity of discrete, spherical particles in a fluid, where the velocity is influenced by the particle's size, density, and viscosity of the fluid. In the context of flocculation, Stokes' law is often invoked as a conceptual framework to explain the general behavior of particle settling. Although Stokes' law was originally derived for discrete particles, its principles can still provide insights into how aggregated particles might behave. When coagulants are added, it is assumed that the flocs formed settle in the same way as discrete particles, though with different settling characteristic in the suspension medium. The key assumption is that the flocs formed through aggregation

can be treated as larger, quasi-discrete particles with effective sizes and densities different from those of the individual particles (Crittenden et al., 2012).

## **2.4 Particle destabilization in water treatment practice**

As shown in Figure 2.7, Stumm and O'Melia (1968) developed four characteristic curves to reflect particle destabilization by metal salt coagulant addition and its effect on removal of suspended particles (as measured by turbidity) for raw waters with different colloidal particle concentrations ( $S_1 < S_2 < S_3 < S_4$ ). These curves indicate the extent to which both particle destabilization mechanisms—adsorption and charge neutralization (indicated as “Zone 2”) and sweep flocculation (indicated as “Zone 4”)—may be observed. The regions for destabilization and restabilization are described as follows: Zone 1 indicates that insufficient coagulant has been added to the colloidal suspension, so destabilization does not occur. Zone 2 refers to the region where destabilization of colloids has taken place or neutralization of surface charge. Zone 3 denotes the region where restabilization of colloids occurs due to excessive coagulant addition. Zone 4 indicates the region where the coagulant dose is high enough to achieve saturation, leading to the precipitation of metal hydroxide species. The four colloid concentrations (labeled  $S_1$ ,  $S_2$ ,  $S_3$ , and  $S_4$ ) illustrate how increasing coagulant concentration affects particle destabilization.

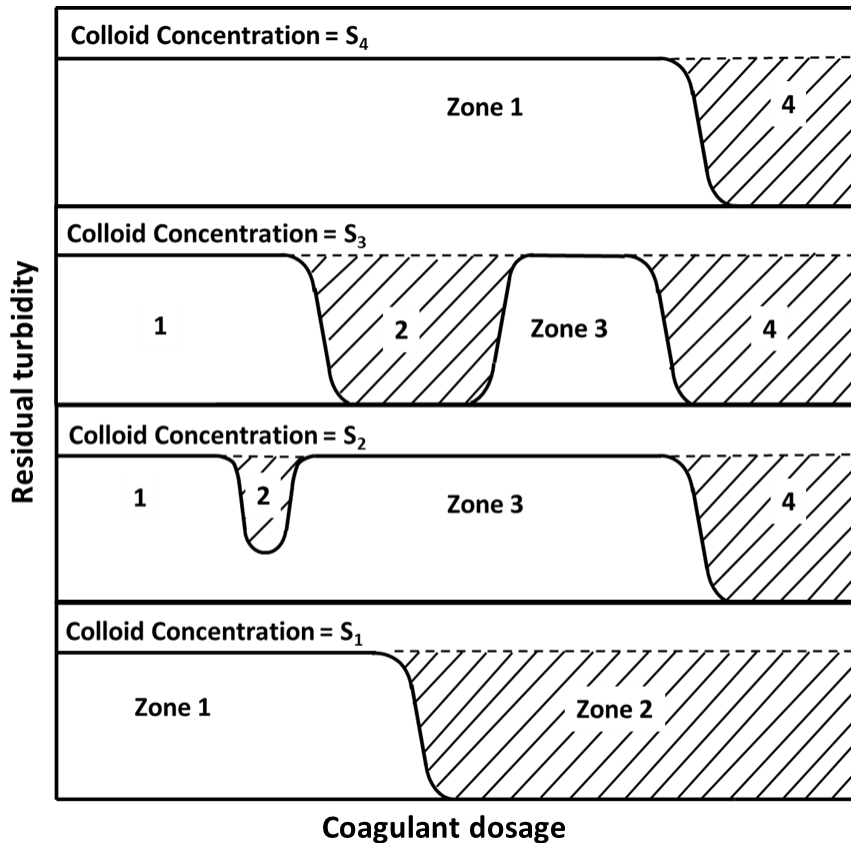


Figure 2.7 Schematic coagulation curves at constant pH for four colloid concentrations ( $S_1 < S_2 < S_3 < S_4$ ) showing zones of destabilization and restabilization. Zone 1: Particles remain stable due to low coagulant dose; Zone 2: Further coagulant addition causes particle destabilization and resulting in charge neutralization or adsorption; Zone 3: Particle restabilization occurs with higher dose causing charge reversal. Zone 4: Precipitation of the metal hydroxide or sweep flocculation occurs with additional coagulant dose. Reproduced from Stumm & O'Melia (1968) with permission.

For the lowest particle concentration,  $S_1$ , particles are removed by sweep flocculation because the concentration is too low for collisions among colloids to flocculate and settle. When a small amount of metal coagulant is introduced, it may be sufficient for destabilization, but the collision rate is too low for significant coagulation within the available time. With a further increase in coagulant concentration, the ratio of coagulant dose to colloid concentration rises, resulting in excessive adsorption, charge reversal, and restabilization of dispersed colloids. Only when a very high concentration of metal salts is applied, leading to the formation of substantial metal hydroxide precipitates does the enmeshment of dispersed particles by the metal hydroxide precipitate result in the destabilization and removal of these

particles. The particle concentration  $S_1$  may be suitable for direct filtration or dissolved air flotation for liquid-solid separation (Stumm & O'Melia, 1968; Crittenden et al., 2012).

At a higher colloid concentration, such as  $S_2$ , the suspension behaves differently from  $S_1$  with increasing coagulant concentration. The suspension is destabilized at low coagulant concentrations, and this destabilization occurs over a relatively narrow range of coagulant dose. Between Zones 1 and 2, the mechanism of destabilization is the adsorption of highly positively charged metal hydrolysis products onto the surfaces of colloids. Some flocculation and settling occur in Zone 2, where adsorption and charge neutralization happen. However, the concentration is too low for effective flocculation, and a high degree of turbidity removal is not possible (Stumm & O'Melia, 1968; Crittenden et al., 2012). If more coagulant is added, the particles stabilize with a positive charge, increasing turbidity, as shown in Zone 3, making substantial colloid removal unlikely. Further increasing the coagulant concentration (Zone 4) causes restabilization of the suspension. The suspension remains restabilized until a high coagulant dose is applied. Once destabilized, significant particle removal is achieved through sweep flocculation but at a lower coagulant concentration than for particle concentration  $S_1$  because the higher particle concentration allows more effective flocculation and settling at a lower coagulant dose.

For high colloid concentrations, such as  $S_3$ , all four coagulation zones are identifiable. In Zone 2, nearly complete removal occurs through charge neutralization, with particles stabilizing at higher coagulant doses. As particle concentration increases, such as in  $S_4$ , the sweep flocculation and charge neutralization zones merge, as the coagulant concentration needed to neutralize the particle charges coincides with the onset of precipitation. This merging indicates that the charge neutralization region exhibits stoichiometry, where Zone 2 begins at successively higher coagulant doses with increasing particle concentrations (Duan, 1997; Crittenden et al., 2012).

Surface precipitation of aluminum hydroxide is suggested to occur in all coagulation zones, as posited by Matijevic (1976). However, it is the solution chemistry, including pH and destabilizing anion concentrations, which dictates whether the adsorbed particles will undergo flocculation. Letterman and Vanderbrook (1983) further proposed that coagulation in Zone 4 is controlled by the solubility of the adsorbed aluminum hydroxide precipitate and surface ionization reactions. Therefore, the influence of solution chemistry, particularly under specific coagulation conditions, must be carefully considered (Gregory, 1973; Gregory, 1976; Bratby, 1980).

## 2.5 Observations of particle removal during drinking water treatment

### 2.5.1 Inorganic particles and protozoan parasites removal by CFS

While treated water monitoring approaches had been traditionally relied upon for regulatory compliance, with the emergence of protozoan pathogens in the 1990's—especially *Cryptosporidium* spp.—it became evident that relying solely on pathogen monitoring to verify the microbiological safety of treated water was ineffective and insufficient (Regli et al., 1991; Haas et al., 1996). This is because treatment systems must achieve several order-of-magnitude reductions for some pathogens to meet health-based risk criteria for treated drinking water, which can result in required treated water pathogen concentrations that are extremely low (e.g., one pathogen in 100,000 liters) and thus, difficult to evaluate with available sampling approaches (Schmidt et al., 2020). As a result, a risk-based, “treatment technique” approach was developed to provide regulatory credits for well-operated treatment.

To quantify treatment efficiency, pathogen and other discrete particle removal is on a log scale (U.S. EPA, 1989; 1998; 2002; 2006; Emelko et al., 2008; 2010; Schmidt et al., 2010; Chik et al., 2018). Both can be collectively referred to as log-reduction, which is synonymous with decimal reduction and decimal elimination (e.g., Teunis et al., 2009; Hijnen & Medema, 2010; Schmidt et al., 2020). Numerous studies of particle removal by CFS have been conducted at bench, pilot, and full-scale. Table 2.1 summarizes several studies illustrating the removal of colloidal particles—including *Cryptosporidium* spp. oocysts, *Giardia* spp. cysts, *E. coli* bacteria, silica, and kaolin—by conventional CFS. Collectively, these studies suggest that 0.15 to 4-log removal of colloidal particles can be achieved by conventional CFS. Filtration processes following CFS are granted 3-log removal credit for 3-6  $\mu\text{m}$  *Cryptosporidium* oocysts and 10-12  $\mu\text{m}$  *Giardia* spp. cysts if they are considered well-operated based on filter effluent turbidity targets (O. Reg. 169/03, 2020; U.S. EPA 2006), although removals ranging from <2- to >5-log have been reported and pilot- and full-scales (LeChevallier et al. 1991; LeChevallier and Norton 1992; West et al. 1994; Kelley et al. 1995; Patania et al. 1995; Nieminski and Ongerth 1995; Ongerth and Pecoraro 1995; States et al. 1997; Baudin and Laine 1998; Dugan et al., 2001; Emelko 2001; Hashimoto et al., 2001; Huck et al., 2001; Emelko 2003; Emelko et al. 2003, 2005; Harrington et al. 2003; Emelko & Huck 2004; Amburgey et al., 2005; Hijnen & Medema 2007; Assavasilavasukul et al., 2008; Ballantyne et al., 2024).

Table 2.2 Removal of colloidal particles by conventional coagulation/flocculation/sedimentation (CFS).

Colloid type	Water matrix	Coagulant	Removal (log <sub>10</sub> )	Reference
<i>C. parvum</i> oocysts	raw water	ferric chloride	0.6 to 0.8	Plummer et al., 1995
<i>C. parvum</i> oocysts	raw water	ferric chloride, polyaluminum chloride, & alum	1.7 to 2.1	Abbaszadegan et al., 1997
<i>C. parvum</i> oocysts	raw water	alum	1-4	Oilier et al., 1997
<i>C. parvum</i> oocysts & <i>Giardia</i> cysts	raw water	alpoclar, polyaluminum chloride & PCBA	0.4 to >2 & 0.15 to >2.8	Baudin and Laîné, 1998
<i>C. parvum</i> oocysts	raw water	alum & ferric chloride	0.7 to 1.5	Fox et al., 1998
Silica	raw water	alum & polyaluminum chloride	0.222 to 0.301 & 0.699	Chuang et al., 2007
Kaolin & <i>E. coli</i>	synthetic water	alum & chitosan	0.59 to 1.74 & 2 to 3	Bina et al., 2009
Silica	raw water	alum, polyaluminum nitrate sulfate-based coagulants; PANS-PA1 and PANS-PA2 and polyaluminum chloride-based coagulants: PACI-HB, PACI-MB	0.569 to 1.52 (over a range of pH)	Latour et al., 2013
<i>C. parvum</i> oocysts	raw water	<i>Moringa oleifera</i>	0.398	Petersen et al., 2016

### 2.5.2 MPs removal by CFS

Although MPs have only emerged as contaminants of human and ecosystem health significance in the last decade or so, their removal by various water treatment processes has already been studied for several decades. “Microspheres” and “microbeads,” are MPs and their removal has been extensively studied in bench-, pilot-, and field-scale experiments as surrogates for protozoan (oo)cysts, including *Cryptosporidium* oocysts and *Giardia* cysts, in evaluating particle removal processes. These MPs, with a negative surface charge similar to oocysts, highlight the significance of surface charge in particle destabilization. Studies utilizing MPs as surrogates for removal of pathogens have shown that adequate

coagulant application can effectively destabilize and remove these particles so that they can be effectively removed by CFS (Table 2.3) and subsequent physico-chemical filtration (Emelko, 2003; Emelko & Huck, 2004; Brown & Emelko, 2009; Wang et al., 2017; Liu et al., 2019a; Wang et al., 2020b) where operational conditions (Darby & Lawler, 1990; Moran et al., 1993; Huck et al., 2002; Emelko & Huck, 2004), as well as media roughness, can affect particle removal, especially at low coagulant doses (Yoon et al., 2006; Jin et al., 2015a,b; 2016; 2017). As MPs are particles with attributes that, in many ways, resemble those of other colloidal particles, such as their size, surface charge, and tendency to adsorb contaminants, it would be expected that they are removed at levels that are similar to those of other similar-sized and -shaped particles (e.g., *Cryptosporidium* spp. oocysts); especially when particle destabilization by coagulation is maximized so that the differences in surface properties between particle types are minimized. Comparison of Tables 2.2 and 2.3 demonstrates general similarities in removals of natural particles (including *Cryptosporidium* oocysts) and MPs in the 1 to 20  $\mu\text{m}$  size range by CFS. These studies have not focused on effects of factors such as weathering, however. As recognition of the health implications of MPs has increased, many studies have focused on the removal of larger (i.e.,  $>50 \mu\text{m}$  sized MPs), but investigations of the removal of smaller sized ( $<10 \mu\text{m}$ ) MPs by drinking water treatment processes have been limited largely to case studies in which foundational mechanisms of particle destabilization that are necessary for maximizing treatment performance have only been superficially investigated, if at all (Table 2.3). Accordingly, widespread concerns are still voiced regarding MPs removal during drinking water treatment—especially in smaller size ranges, and particularly as their surface characteristics change due to weathering and the implications of those changes for chemical pretreatment have also not been systematically investigated.

Table 2.3 Bench-scale studies on microplastics removal from water by conventional coagulation/flocculation/sedimentation.

MPs size ( $\mu\text{m}$ )	MPs type	MPs density ( $\text{g}/\text{cm}^3$ )	Aqueous matrix (as described)	Coagulant	Coagulant dose (as described)	Coagulation believed to be optimized?	Optimization parameter	Zeta potential before coagulation (mV)	Zeta potential after coagulation (mV)	MPs initial concentration	MPs concentration in supernatant	MPs removal (%) <sup>a</sup>	MPs removal ( $\log_{10}$ ) <sup>a,b</sup>	Reference
3	PS	1.05	Raw water from treatment plant  pH: 6.49 turbidity: 26.86 NTU	alum (with a polymer)	Control 10 mg/L 25 mg/L 40 mg/L	NR	NR	NR	NR	$2.56 \times 10^6$ beads/mL	93.9 beads/mL 493.3 beads/mL 204.4 beads/mL	-	2.3 2.4 0.7 1.6	Links, 2015
3	PS	1.05	surface water Lake Erie pH: 7.97 turbidity: $601.5 \pm 35.1$ NTU alkalinity: 95 mg $\text{CaCO}_3/\text{L}$  Grand River pH: 7.9-8.22 turbidity: 6.29 NTU alkalinity: 165-230 mg $\text{CaCO}_3/\text{L}$	alum	10 mg/L 20 mg/L 30 mg/L 40 mg/L 50 mg/L	NR	NR	- 60.1 to -11.6	NR	$223.4 \pm 22.7$ MPs/mL	$241.5 \pm 8.5$ $47.0 \pm 1.4$ $20.4 \pm 0.2$ $10.0 \pm 0.4$ $10.3 \pm 0.3$	96.1	1.41	Xue et al., 2021
4.5	PS	1.05	surface water Happy Valley Reservoir pH: 8.0 turbidity: 4.3 NTU DOC: 4.40 mg/L Color: 10 HU UVA <sub>254 nm</sub> : $0.104 \text{ cm}^{-1}$	alum	0 mg/L 10 mg/L 30 mg/L	NR	NR	NR	NR	NR	NR	NR	0 0.1 0.8	Monis et al., 2017

MPs size ( $\mu\text{m}$ )	MPs type	MPs density ( $\text{g}/\text{cm}^3$ )	Aqueous matrix (as described)	Coagulant	Coagulant dose (as described)	Coagulation believed to be optimized?	Optimization parameter	Zeta potential before coagulation (mV)	Zeta potential after coagulation (mV)	MPs initial concentration	MPs concentration in supernatant	MPs removal (%) <sup>a</sup>	MPs removal ( $\log_{10}$ ) <sup>a,b</sup>	Reference
6	PS	1.05	surface water Lake Erie pH: 7.97 turbidity: 601.5 $\pm$ 35.1 NTU alkalinity: 95 mg $\text{CaCO}_3/\text{L}$  Grand River pH: 7.9-8.22 turbidity: 6.29 NTU alkalinity: 165-230 mg $\text{CaCO}_3/\text{L}$	alum	10 mg/L 20 mg/L 30 mg/L 40 mg/L 50 mg/L	NR	NR	- - 60.1 to -11.6	NR	215.1 $\pm$ 13.4 MPs/mL	224.4 $\pm$ 5.2 82.7 $\pm$ 1.7 29.1 $\pm$ 0.2 23.6 $\pm$ 0.3 19.5 $\pm$ 1.6	85.2	0.83	Xue et al., 2021
15	PE	NR	synthetic surface water turbidity: 5.4 $\pm$ 0.2 NTU  natural surface water pH: 7.8 $\pm$ 0.1 turbidity: 5.5 $\pm$ 0.3 NTU	alum	5-60 mg/L	Yes	jar test data	NR	NR	NR	NR	20	0.097	Alioua & Lapointe, 2023
15	PE	NR	surface water pH: 7.2 $\pm$ 0.1 turbidity: 38 $\pm$ 2 NTU dissolved organic carbon concentration: 7.0 $\pm$ 0.2 mg C/L	alum (with PAM as the coagulant aid)	0.45-3.64 mg/L	No	NR	NR	NR	500 MPs/L	55 $\pm$ 7 MPs/L	89	0.96	Lapointe et al., 2020

MPs size ( $\mu\text{m}$ )	MPs type	MPs density ( $\text{g}/\text{cm}^3$ )	Aqueous matrix (as described)	Coagulant	Coagulant dose (as described)	Coagulation believed to be optimized?	Optimization parameter	Zeta potential before coagulation (mV)	Zeta potential after coagulation (mV)	MPs initial concentration	MPs concentration in supernatant	MPs removal (%) <sup>a</sup>	MPs removal ( $\log_{10}$ ) <sup>a,b</sup>	Reference
25	PS	1.05	surface water Lake Erie pH: 7.97 turbidity: 601.5 $\pm$ 35.1 NTU alkalinity: 95 mg $\text{CaCO}_3/\text{L}$  Grand River pH: 7.9-8.22 turbidity: 6.29 NTU alkalinity: 165-230 mg $\text{CaCO}_3/\text{L}$	alum	10 mg/L 20 mg/L 30 mg/L 40 mg/L 50 mg/L	NR	NR	-60.1 to -11.6	NR	239.2 $\pm$ 20.1 MPs/mL	183.0 $\pm$ 2.0 20.8 $\pm$ 1.0 6.0 $\pm$ 0.0 6.1 $\pm$ 0.7 5.8 $\pm$ 0.2	90.6	1.03	Xue et al., 2021
10–30	PE	0.91	synthetic water DI water pH: 7 $\pm$ 0.5 turbidity: 14.3 $\pm$ 0.5 DOC: 2.4 $\pm$ 0.03	alum	10–50 mg/L	Yes	jar test data	-14.2	NR	208 MPs in 5 mL DI	NR	52% (30 mg/L)	0.32	Shahi et al., 2020
45	PS	1.05	surface water Lake Erie pH: 7.97 turbidity: 601.5 $\pm$ 35.1 NTU alkalinity: 95 mg $\text{CaCO}_3/\text{L}$  Grand River pH: 7.9-8.22 turbidity: 6.29 NTU alkalinity: 165-230 mg $\text{CaCO}_3/\text{L}$	alum	10 mg/L 20 mg/L 30 mg/L 40 mg/L 50 mg/L	NR	NR	-60.1 to -11.6	NR	88.8 $\pm$ 13.2 MPs/mL	82.5 $\pm$ 0.5 51.6 $\pm$ 2.0 39.0 $\pm$ 0.0 26.2 $\pm$ 4.0 10.0 $\pm$ 0.0	63.3-89.9	0.44-1	Xue et al., 2021

MPs size ( $\mu\text{m}$ )	MPs type	MPs density ( $\text{g}/\text{cm}^3$ )	Aqueous matrix (as described)	Coagulant	Coagulant dose (as described)	Coagulation believed to be optimized?	Optimization parameter	Zeta potential before coagulation (mV)	Zeta potential after coagulation (mV)	MPs initial concentration	MPs concentration in supernatant	MPs removal (%) <sup>a</sup>	MPs removal ( $\log_{10}$ ) <sup>a,b</sup>	Reference
40–48	PE	NR	synthetic water DI water pH adjusted between 6.8 to 7.2 using 0.1 N-HCl and NaOH	ferrate	0.9 mg/L 1.8 mg/L 2.7 mg/L 3.6 mg/L	Yes	jar test data	$-3.4 \pm 0.85$	$\sim +7.5 \pm 0.35$ to $+9.5 \pm 0.45$ (after 3.6 mg/L)	10 mg/L	NR	98.4	1.80	Lee et al., 2023
<50	PVC	1.38	HPLC grade water pH: 5 – 8 Alkalinity: 1 mmol/L by 0.1 M $\text{NaHCO}_3^-$	$\text{Fe}_2(\text{SO}_4)_3 \cdot 9 \text{H}_2\text{O}$	20 mg/L 40 mg/L 60 mg/L	Yes	jar test data	NR	NR	1.38 mg/L (TOC); $18 \times 10^6$ particles/L	0.37 to 0.45 mg/L	40-50	0.22-0.30 and 0.70	Prokopov a et al., 2021
<50	PVC	1.38	HPLC grade water pH: 5 – 8 Alkalinity: 1 mmol/L by 0.1 M $\text{NaHCO}_3^-$	$\text{Al}_2(\text{SO}_4)_3 \cdot 18 \text{H}_2\text{O}$	20 mg/L 40 mg/L 60 mg/L	Yes	jar test data	NR	NR	1.38 mg/L (TOC); $18 \times 10^6$ particles/L	0.35 to 0.51 mg/L	80	0.22-0.30 and 0.70	Prokopov a et al., 2021
30–50	PE	0.91	synthetic water DI water pH: $7 \pm 0.5$ turbidity: $14.3 \pm 0.5$ DOC: $2.4 \pm 0.03$	alum	10–50 mg/L	Yes	jar test data	-14.2	NR	208 MPs in 5 mL DI	NR	100 (30 mg/L)	3	Shahi et al., 2020
64	Wheat here d PE	NR	surface water pH: $7.2 \pm 0.1$ turbidity: $38 \pm 2$ NTU dissolved organic carbon concentration: $7.0 \pm 0.2$ mg C/L	alum (with PAM as the coagulant aid)	0.45–3.64 mg/L	Yes	jar test data	NR	NR	500 MPs/L	$80 \pm 11$ MPs/L	89	0.96	Lapointe et al., 2020

MPs size ( $\mu\text{m}$ )	MPs type	MPs density ( $\text{g}/\text{cm}^3$ )	Aqueous matrix (as described)	Coagulant	Coagulant dose (as described)	Coagulation believed to be optimized?	Optimization parameter	Zeta potential before coagulation (mV)	Zeta potential after coagulation (mV)	MPs initial concentration	MPs concentration in supernatant	MPs removal (%) <sup>a</sup>	MPs removal ( $\log_{10}$ ) <sup>a,b</sup>	Reference
64	Weat here d PE	NR	surface water pH: $7.2 \pm 0.1$ turbidity: $38 \pm 2$ NTU dissolved organic carbon concentration: $7.0 \pm 0.2$ mg C/L	ACH	0.91–3.64 mg/L	Yes	jar test data	NR	NR	500 MPs/L	NR	93	1.16	Lapointe et al., 2020
50–70	PE	0.91	synthetic water DI water pH: $7 \pm 0.5$ turbidity: $14.3 \pm 0.5$ DOC: $2.4 \pm 0.03$	alum	10–50 mg/L	Yes	jar test data	-14.2	NR	208 MPs in 5 mL DI	NR	100 (30 mg/L)	3	Shahi et al., 2020
90	PS	1.05	surface water Lake Erie pH: 7.97 turbidity: $601.5 \pm 35.1$ NTU alkalinity: 95 mg $\text{CaCO}_3/\text{L}$  Grand River pH: 7.9–8.22 turbidity: 6.29 NTU alkalinity: 165–230 mg $\text{CaCO}_3/\text{L}$	alum	10 mg/L 20 mg/L 30 mg/L 40 mg/L 50 mg/L	NR	NR	–60.1 to –11.6	NR	$60.6 \pm 25.4$ MPs/mL	$22.6 \pm 2.6$ $22.3 \pm 0.5$ $23.2 \pm 3.4$ $22.8 \pm 0.6$ $12.7 \pm 0.9$	44.5–80.5	0.26–0.71	Xue et al., 2021
<100	PET	1.38	pH: 3, 5, 7 & 9	PACl	20 mg/L 50 mg/L 100 mg/L 200 mg/L	Yes	zeta potential data	-6.2	-1.59	100 mg	NR	35.5	0.19	Zhang et al., 2021

MPs size ( $\mu\text{m}$ )	MPs type	MPs density ( $\text{g}/\text{cm}^3$ )	Aqueous matrix (as described)	Coagulant	Coagulant dose (as described)	Coagulation believed to be optimized?	Optimization parameter	Zeta potential before coagulation (mV)	Zeta potential after coagulation (mV)	MPs initial concentration	MPs concentration in supernatant	MPs removal (%) <sup>a</sup>	MPs removal ( $\log_{10}$ ) <sup>a,b</sup>	Reference
~100	PS	1.04–1.06 $\text{g}/\text{cm}^3$	tap water pH $7.7 \pm 0.1$ turbidity: $0.2 \pm 0.1$ NTU  surface water pH $8.4 \pm 0.1$ (pH was later adjusted using NaOH and HCl to 1, 3, 5, 7, 12 and 13) turbidity: $0.8 \pm 0.3$ NTU	alum	3.4 mg/L	Yes	jar test data	NR	NR	10 mg/L	NR	$98.9 \pm 0.94$	$1.96 \pm 0.004$	Li et al., 2021
70–100	PE	0.91	synthetic water DI water pH: $7 \pm 0.5$ turbidity: $14.3 \pm 0.5$ DOC: $2.4 \pm 0.03$	alum	10–50 mg/L	Yes	jar test data	-14.2	NR	208 MPs in 5 mL DI	NR	100 (30 mg/L)	3	Shahi et al., 2020
140	PE	NR	synthetic surface water turbidity: $5.4 \pm 0.2$ NTU  natural surface water pH: $7.8 \pm 0.1$ turbidity: $5.5 \pm 0.3$ NTU	alum	5–60 mg/L	Yes	jar test data	NR	NR	NR	NR	62	0.42	Alioua & Lapointe, 2023
140	PE	NR	surface water pH: $7.2 \pm 0.1$ turbidity: $38 \pm 2$ NTU dissolved organic carbon concentration: $7.0 \pm 0.2$ mg C/L	alum (with PAM as the coagulant aid)	0.45–3.64 mg/L	No	NR	NR	NR	500 MPs/L	$90 \pm 14$ MPs/L	82	0.75	Lapointe et al., 2020

MPs size ( $\mu\text{m}$ )	MPs type	MPs density ( $\text{g}/\text{cm}^3$ )	Aqueous matrix (as described)	Coagulant	Coagulant dose (as described)	Coagulation believed to be optimized?	Optimization parameter	Zeta potential before coagulation (mV)	Zeta potential after coagulation (mV)	MPs initial concentration	MPs concentration in supernatant	MPs removal (%) <sup>a</sup>	MPs removal ( $\log_{10}$ ) <sup>a,b</sup>	Reference
140	PS	NR	surface water pH: $7.2 \pm 0.1$ turbidity: $38 \pm 2$ NTU dissolved organic carbon concentration: $7.0 \pm 0.2$ mg C/L	alum (with PAM as the coagulant aid; dose 0.05–30 mg/L)	0.45–3.64 mg/L	No	NR	NR	NR	500 MPs/L	NR	84	0.80	Lapointe et al., 2020
300	PET	NR	synthetic water DI water pH adjusted between 6.8 to 7.2 using 0.1 N-HCl and NaOH	ferrate	0.9 mg/L 1.8 mg/L 2.7 mg/L 3.6 mg/L	Yes	jar test data	$-8.4 \pm 1.83$	$+2.1 \pm 0.12$ (after 3.6 mg/L)	10 mg/L	NR	>75	>0.60	Lee et al., 2023
100-400	PET	1.38	pH: 3, 5, 7 & 9	PACl	20 mg/L 50 mg/L 100 mg/L 200 mg/L	Yes	zeta potential data	-6.2	-1.59	100 mg	NR	46.2	0.27	Zhang et al., 2021
400-500	PET	1.38	pH: 3, 5, 7 & 9	PACl	20 mg/L 50 mg/L 100 mg/L 200 mg/L	Yes	zeta potential data	-6.2	-1.59	100 mg	NR	~100	3	Zhang et al., 2021
<500	PS	1.05	synthetic water DI water pH: 5 – 9 ionic strength (value NR) was induced by adding NaCl Na <sub>2</sub> SO <sub>4</sub> Na <sub>2</sub> CO <sub>3</sub> ; turbidity and alkalinity NR)	FeCl <sub>3</sub>	30 mg/L 60 mg/L 90 mg/L 120 mg/L 150 mg/L 180 mg/L	Yes	jar test data	-15.8	-0.49	100, 300, 500, 700, and 1000 mg/L	NR	~77.83%	0.65	Zhou et al., 2021

MPs size ( $\mu\text{m}$ )	MPs type	MPs density ( $\text{g}/\text{cm}^3$ )	Aqueous matrix (as described)	Coagulant	Coagulant dose (as described)	Coagulation believed to be optimized?	Optimization parameter	Zeta potential before coagulation (mV)	Zeta potential after coagulation (mV)	MPs initial concentration	MPs concentration in supernatant	MPs removal (%) <sup>a</sup>	MPs removal ( $\log_{10}$ ) <sup>a,b</sup>	Reference
<500	PS	1.05	synthetic water DI water pH: 5 – 9 ionic strength (value NR) was induced by adding NaCl Na <sub>2</sub> SO <sub>4</sub> Na <sub>2</sub> CO <sub>3</sub> ; turbidity and alkalinity NR)	PACl	30 mg/L 60 mg/L 90 mg/L 120 mg/L 150 mg/L 180 mg/L	Yes	jar test data	-15.8	-3.79	100, 300, 500, 700, and 1000 mg/L	NR	77.83	0.65	Zhou et al., 2021
<500	PE	1.05	synthetic water DI water pH: 5 – 9 ionic strength (value NR) was induced by adding NaCl Na <sub>2</sub> SO <sub>4</sub> Na <sub>2</sub> CO <sub>3</sub> ; turbidity and alkalinity NR)	FeCl <sub>3</sub>	30 mg/L 60 mg/L 90 mg/L 120 mg/L 150 mg/L 180 mg/L	Yes	jar test data	-14.6	-0.57	100, 300, 500, 700, and 1000 mg/L	NR	~29.70	0.15	Zhou et al., 2021
<500	PE	1.05	synthetic water DI water pH: 5 – 9 ionic strength (value NR) was induced by adding NaCl Na <sub>2</sub> SO <sub>4</sub> Na <sub>2</sub> CO <sub>3</sub> ; turbidity and alkalinity NR)	PACl	30 mg/L 60 mg/L 90 mg/L 120 mg/L 150 mg/L 180 mg/L	Yes	jar test data	-14.6	-7.76	100, 300, 500, 700, and 1000 mg/L	NR	29.70	0.15	Zhou et al., 2021

MPs size ( $\mu\text{m}$ )	MPs type	MPs density ( $\text{g}/\text{cm}^3$ )	Aqueous matrix (as described)	Coagulant	Coagulant dose (as described)	Coagulation believed to be optimized?	Optimization parameter	Zeta potential before coagulation (mV)	Zeta potential after coagulation (mV)	MPs initial concentration	MPs concentration in supernatant	MPs removal (%) <sup>a</sup>	MPs removal ( $\log_{10}$ ) <sup>a,b</sup>	Reference
NR	PET	NR	synthetic water ultrapure water pH: 6, 7 & 8 NaCl and NaHCO <sub>3</sub> solutions (5.0 mmol/L) were prepared to control ion strength and alkalinity in coagulation tests	alum	0.01 mmol Al/L 0.03 mmol Al/L 0.05 mmol Al/L 0.10 mmol Al/L 0.15 mmol Al/L 0.20 mmol Al/L	NR	NR	NR	NR	100 mg/L	NR	nearly 100 (as stated)	3.00	Lu et al., 2021
NR	Tetracycline	NR	synthetic water ultrapure water pH: 6, 7 & 8 NaCl and NaHCO <sub>3</sub> solutions (5.0 mmol/L) were prepared to control ion strength and alkalinity in coagulation tests	alum	0.01 mmol Al/L 0.03 mmol Al/L 0.05 mmol Al/L 0.10 mmol Al/L 0.15 mmol Al/L 0.20 mmol Al/L	NR	NR	NR	around 1 (from diagram; over a range of pH)	50 mg/L	NR	41	0.23	Lu et al., 2021
NR	HDPE	NR	synthetic water tap water pH: maintained at 3, 5, 7, 9 and 11 by adding a predetermined dosage of 0.1 mol/L NaOH/HCl	alum (with PAM)	50 mg/L 100 mg/L 150 mg/L 200 mg/L 250 mg/L	Yes	jar test data	NR	NR	NR	NR	84	0.80	Monira et al., 2021

MPs size ( $\mu\text{m}$ )	MPs type	MPs density ( $\text{g}/\text{cm}^3$ )	Aqueous matrix (as described)	Coagulant	Coagulant dose (as described)	Coagulation believed to be optimized?	Optimization parameter	Zeta potential before coagulation (mV)	Zeta potential after coagulation (mV)	MPs initial concentration	MPs concentration in supernatant	MPs removal (%) <sup>a</sup>	MPs removal ( $\log_{10}$ ) <sup>a,b</sup>	Reference
NR	LDPE	NR	synthetic water tap water pH: maintained at 3, 5, 7, 9 and 11 by adding a predetermined dosage of 0.1 mol/L NaOH/HCl	alum (with PAM)	50 mg/L 100 mg/L 150 mg/L 200 mg/L 250 mg/L	Yes	jar test data	NR	NR	NR	NR	92	1.10	Monira et al., 2021
NR	PP	NR	synthetic water tap water pH: maintained at 3, 5, 7, 9 and 11 by adding a predetermined dosage of 0.1 mol/L NaOH/HCl	alum (with PAM)	50 mg/L 100 mg/L 150 mg/L 200 mg/L 250 mg/L	Yes	jar test data	NR	NR	NR	NR	96	1.40	Monira et al., 2021

<sup>a</sup>Where only a single removal value is shown it is the highest of the removals recorded.  
<sup>b</sup>Removals expressed as percentages were converted to  $\log_{10}$ .  
ACH: aluminum chlorohydrate;  $\text{Al}_2(\text{SO}_4)_3 \cdot 18\text{H}_2\text{O}$ : hydrated aluminum sulfate;  $\text{Fe}_2(\text{SO}_4)_3 \cdot 9\text{H}_2\text{O}$ : hydrated iron sulfate;  $\text{FeCl}_3$ : ferric chloride; HDPE/LDPE: high/low density polyethylene; NR: Not reported; PAM: polyacrylamide; PACl: polyaluminum chloride; PET: polyethylene terephthalate; PE: polyethylene; PP: polypropylene; PS: polystyrene; PVC: polyvinylchloride;

The data presented in Table 2.3 suggest that smaller MPs are more difficult to remove by CFS than larger ones (Links, 2015; Monis et al., 2017; Lapointe et al., 2020; Shahi et al., 2020; Li et al., 2021; Monira et al., 2021; Prokopova et al., 2021; Xue et al., 2021; Zhang et al., 2021; Zhou et al., 2021; Alioua & Lapointe, 2023; Lee et al., 2023). This is attributed to their higher surface area-to-volume ratio and associated greater stability in aqueous suspensions (Tang et al., 2014; Wang et al., 2020c), especially for a given concentration of coagulant. Larger MPs are also more likely to attach to flocs, increasing their likelihood of settling (Wang et al., 2020c). As well, this observation aligns with simple settling theory (described above) for discrete particles. In some cases, relatively large MPs (0.5–5 mm), which are less consistent with MPs particle sizes typically found in raw/untreated water supplies, were used.

Notably, several of the studies in Table 2.3 did not report key details, such as the sizes or types of MPs or the extent of particle destabilization, making it difficult to draw a conclusion based solely on the reported removals of MPs. For example, while Lu et al. (2021) investigated PE MPs across a wide pH range and reported “nearly 100% removal” under optimal particle destabilization conditions, other studies did not indicate if particle destabilization was optimized or how it was assessed if considered and believed to be optimized. Critically, in most of the investigations reported to date, the “optimization” of MPs removal by CFS has been evaluated based on the highest MPs removal observed over an ostensibly arbitrary range of coagulant doses, a selected coagulant dose (in absence of performance assessment), or broader performance (e.g., turbidity) rather than mechanisms or of extent of particle destabilization indicated by surface charge via evaluation of zeta potential. It is further worth noting that there are some cases in which zeta potential was reported although the MPs studied exceed the maximum particle size (i.e., typically 10  $\mu\text{m}$ ) for which zeta potential analysis is valid using cited instruments.

It is important to recall that MPs and other discrete particle concentrations are estimates obtained by using imperfect analytical methodologies to obtain counts from samples—the methods especially preclude accurate representation of concentrations expected to result in non-detects; these include low concentrations and those estimated using microbial methods with low or variable analytical recovery (Chik et al., 2018). Measurement errors associated with random sampling and imperfect and/or variable analytical recovery (Emelko et al., 2008; 2010; Schmidt et al., 2010; Chik et al., 2018) are widely recognized (Nahrstedt & Gimbel, 1996; Gronewold et al., 2008; Schmidt & Emelko, 2011; Pouillot et al., 2013) and apply to all discrete detection and enumeration methods (Emelko et al., 2010). Failure to avoid (by targeting counts of at least 10 particles per sample [Emelko et al., 2008]) or account for non-detects and measurement errors can bias concentration estimates and associated risk estimates, sometimes by

orders of magnitude (Pouillot et al., 2013; Schmidt et al., 2013; Chik et al., 2018). Thus, systematic analyses of MPs size and weathering effects on removal by CFS are presently lacking.

## **2.6 MPs Risk management & regulatory considerations**

Discharges of MPs to aquatic systems are not explicitly regulated yet, though numerous agreements, guidelines, and action plans generally address "all wastes." One significant initiative is the Honolulu Strategy, developed in 2011 by the U.S. National Oceanic and Atmospheric Administration (NOAA) and the United Nations Environment Program. This global framework aims to reduce the ecological, human health, and economic impacts of plastics, particularly MPs, in the marine environment (UNEP & NOAA, 2011). At the 4<sup>th</sup> UN Environmental Assembly in 2019, Environment Ministers from 157 countries agreed to reduce single-use plastic products by 2030 (UNEP, 2019).

In response to environmental concerns, the Government of Canada has prioritized regulating the manufacture, use, and sale of MPs in commercial products like microbeads. Microbeads were added to the List of Toxic Substances under the Canadian Environmental Protection Act 1999, and the "Microbeads in Toiletries Regulations" were published in 2017 (Environment Canada, 1999). Following this, in the U.S. nine states—Illinois, Indiana, Maine, Colorado, Wisconsin, Maryland, New Jersey, Connecticut, and California—passed laws from 2015 to 2019 prohibiting the sale and manufacture of microbeads in personal care products. The U.S. federal government also enacted "The Microbeads-Free Waters Act of 2015," which restricts the manufacture of rinse-off cosmetics containing plastic microbeads (H.R. 1321). However, the U.S. EPA has not established specific criteria for plastic waste in drinking water, leaving it to individual states to make these determinations (U.S. EPA, 2021a). The Safe Drinking Water Act (SDWA) is focused on maintaining the safety of drinking water in the U.S. by setting allowable limits for both natural and anthropogenic contaminants. However, plastic polymers are not presently recognized as anthropogenic contaminants under the SDWA (U.S. EPA, 2021b).

Similarly, European Union (EU) member states, including Austria and Belgium, proposed laws regulating microbeads in cosmetic products in 2014, leading to broader restrictions on MPs in products in 2019 (EU, 2015; Environment Canada, 2015). In 2018, the European Commission's Group of Chief Scientific Advisors thoroughly reviewed scientific evidence on microplastics pollution using the EU's Scientific Advice Mechanism (SAM - Research and Innovation - European Commission, 2019). In 2019, the European Chemicals Agency (ECHA) considered a proposal to restrict intentionally added microplastics in products

(European Chemicals Agency, 2019). Consequently, the European Commission's Circular Economy Action Plan established mandatory requirements for the recycling of plastic packaging, among other measures (European Commission, 2020). Provisional approval was granted for the revision of the EU Drinking Water Directive (DWD) to include regular monitoring of microplastics in drinking water and to report these findings to the European Commission. The results from this monitoring will assist in better informing the establishment of future concentration limits for microplastics.

These regulations aimed to reduce the quantity of plastic microbeads entering freshwater and marine ecosystems. Following this trend, California became a pioneer in drinking water regulation by adopting Senate Bill No. 1422 in 2018, which added MPs regulations to the California Safe Drinking Water Act. On March 19, 2020, the California State Water Resources Control Board became the first regulatory agency to define "Microplastics in Drinking Water" (California Water Boards, 2020). The Act mandates the State Water Board to (1) adopt a standard methodology for testing drinking water for MPs, (2) require four years of monitoring—issuing monitoring orders to specific public water systems in two phases, with Phase 1 running from Fall 2023 to Fall 2025 and Phase 2 from Fall 2026 to Fall 2028—with public disclosure of results, (3) consider issuing guidance for interpreting these results, and (4) accredit laboratories for MPs analysis (California Water Boards, 2020).

Despite these advances and growing understanding of MPs toxicology and removal during drinking water treatment, risk management in the provision of drinking water is largely precluded because there are still specific health endpoints (i.e., maximum allowable concentrations [MACs] or maximum contaminant levels [MCLs]) for MPs in drinking water. Thus, at present, health risks from MPs in drinking water are indirectly managed through existing turbidity standards. While turbidity management certainly contributes to MPs risk management, it is likely limited in public health protection impact because MPs are extremely persistent, not rapidly biodegradable, and may remain in the environment for long periods (Browne et al., 2011b). They can also break down into smaller particles, further complicating regulatory efforts (Fahrenfeld et al., 2019; Sait et al., 2021). Unlike the typically regulated dissolved chemicals or pathogenic organisms, MPs encompass a large group of polymers with diverse chemical and physical properties that include high toxicity in some cases (Katare et al., 2021; Casagrande et al., 2024). Additionally, there is a need for standardized procedures for MPs sample collection and analysis. Guidance for minimizing uncertainty in the resulting estimates of MPs concentration and risk analysis is available by adaptation from the pathogen literature and regulatory guidance (Emelko et al., 2008; Pouillot et al., 2013; Schmidt et al., 2013; Chik et al., 2018), as described above in Section 2.5.

A modular, readily expandable framework for managing MPs threats in drinking water was recently developed by Chowdhury et al., (2024). Using available health-based targets for contaminants that can adsorb to MPs, a “Threshold Microplastics Concentration” (TMC) concept and framework was developed “to indicate the total number of microplastic particles per liter of untreated source water or treated water that may constitute exposure to potentially harmful concentrations of chemical contaminants retained on microplastics if ingested” (Chowdhury et al., 2024). It should be noted that exceeding the TMC does not necessarily indicate unacceptable health risk; rather, it indicates that further investigation of water quality and treatment performance may be warranted. This MPs concentration-based risk management approach integrates MPs concentration data, health endpoints, and treatment performance information and can thus be used to identify thresholds at which significant health effects from MPs are not expected in associated with the ingestion of drinking water. Accordingly, the provision of currently unavailable performance data reflecting the range of MPs removal at operational conditions optimized for MPs removal by conventional CFS can enhance risk assessment and treatment optimization strategies for broader management of risks from waterborne MPs.

## **2.7 Increased MPs threats to water in a changing climate**

While the various pathways may not be immediately evident, changing climate exacerbates MPs threats to drinking water because it intensifies their spread, concentration, and persistence in aquatic systems—it may also affect their toxicity. Specifically, rising temperatures accelerate MPs degradation, creating higher concentrations of smaller MPs (Haque & Fan, 2023). Warmer water also speeds up chemical reactions between plastics and pollutants, potentially increasing the toxicity of MPs particles (Sulukan et al., 2022). In areas with water scarcity, reliance on polluted water sources may increase (Postel, 2007), leading to greater human exposure to MPs. Reduced volumes of water in rivers and lakes can also concentrate pollutants (Malmqvist & Rundle, 2002), including MPs, in remaining water supplies. As global mean temperatures increase and weather patterns and ocean currents change, microplastics also will likely be redistributed over wider regions (Welden & Lusher, 2017). They will eventually enter freshwater systems through atmospheric deposition, precipitation, and runoff.

Climate change also leads to more frequent and intense extreme weather events (e.g., storms, heavy rainfall) and climate shocks (e.g., wildfires, droughts) that can increase runoff from terrestrial to aquatic systems, carrying MPs from urban areas, agriculture, and waste disposal sites into rivers, lakes, and oceans. For example, on built landscapes, heavy rainfall can cause the overflow of sewage systems

(Nasrin et al., 2017), which may contain significant levels of MPs (Sun et al., 2019; Zhu et al., 2024). On natural landscapes, droughts, rising sea levels, or vegetation loss may reduce infiltration and associated water purification (Mishra, 2023), thereby increasing potential MPs contamination of both ground and surface water supplies. Wildfires can especially lead to longer term contamination threats because vegetation loss leads to increased amounts of precipitation reaching the land surface (Williams et al., 2019). This results in increased erosion and solids runoff (Silins et al., 2009; Alessio et al., 2021), even at larger watershed scales (Emmerton et al., 2020). As a result, post-fire runoff can contain elevated levels of solids (including MPs) and associated contaminants, including nutrients (Emelko et al., 2011; Silins et al., 2014; Gustine et al., 2021). Longer-term releases of nutrients such as bioavailable phosphorus from suspended solids have been observed in some areas (Stone et al., 2011; Emelko et al., 2016). They can be significant because they promote primary productivity (Silins et al., 2014) and increase macroinvertebrate populations (Martens et al., 2019). Macroinvertebrates can ingest microplastics, potentially leading to MPs bioaccumulation and biomagnification (Miller et al., 2020), as well as reduced efficiency of organic matter breakdown and nutrient cycling (Prata et al., 2023). These effects can be further magnified when they converge with those from anthropogenic landscape disturbances (Watt et al., 2021).

Climate shock-associated changes in water quality can challenge drinking water treatability. While elevated turbidity/suspended solids largely can be treated with conventional technologies (Crittenden et al., 2012), health endpoints have not yet been developed for MPs; thus, it is possible that conventional solids removal processes may need to be augmented, especially to remove high levels of small MPs/nanoplastics. Changes in other aspects of water quality may also make it more difficult to sufficiently remove MPs and other suspended solids. For example, changes in dissolved organic carbon (DOC) concentrations and aromaticity are known drivers of coagulant demand (Sharp et al., 2006; Emelko et al., 2011). If these changes occur rapidly or unexpectedly (e.g., after a wildfire) they may compromise the efficiency of chemical pretreatment (Emelko & Sham, 2014), insufficient coagulant addition may enable MPs passage through treatment processes. Moreover, as reliance on nature-based solutions is increasingly advocated for managing climate threats to water resources (Seddon et al., 2020); it is important to recall that they must be fit-for-purpose (Blackburn et al., 2021) and consider potential consequence of MPs to their overall performance, as biotechnologies are not fully resilient to water quality change (Blackburn et al., 2023) and MPs may further alter biological metabolism and functions.

## Chapter 3 Materials and methods

### 3.1 General approach

MPs removal by conventional chemical pretreatment (i.e., CFS; Figure 3.1A) with alum was studied at bench-scale (Figure 3.1B) to investigate if it generally aligns with the removal of other particles, including particulate contaminants such as *Cryptosporidium* oocysts (i.e., bioparticles). Investigations using a synthetic matrix were conducted to characterize MPs removal by CFS with particle destabilization by (1) adsorption and charge neutralization and (2) sweep flocculation, as illustrated by the curve for colloidal particle concentration (Figure 3.1C). Different sizes of plain and carboxylated MPs were used to respectively represent pristine and weathered MPs and assess the influence of MPs size and surface modification on removal through CFS.

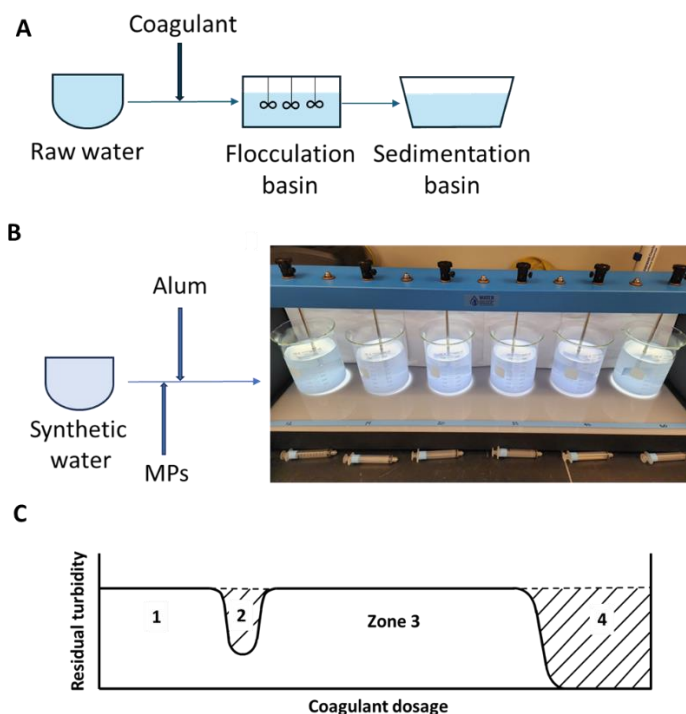


Figure 3.1 Experimental approach used to represent (A) conventional chemical pretreatment at (B) bench-scale to investigate microplastics removal by chemical pretreatment. The (C) residual turbidity profile that was targeted enables investigation of both particle destabilization mechanisms—adsorption and charge neutralization (shown in zone 2) and sweep flocculation (shown in zone 4). Residual turbidity profile reproduced from Stumm & O’Melia (1968) with permission.

### 3.2 Experimental design

A synthetic raw/untreated water was designed to minimize matrix effects. Kaolin was added to ultrapure (MilliQ™) water to increase and control turbidity and sodium carbonate was used to add ionic strength, which varies in potable water, typically ranging from 0.01 to 0.100 M, depending on its source and the treatment it undergoes. Initially, several experiments with varying combinations of turbidity and ionic strength were conducted, as presented in Appendix A, to identify the optimal conditions for observing particle destabilization (i.e., the occurrence of two substantial local minima in turbidity after CFS, as shown in Figure 2.7). Natural water contains a variety of constituents, such as organic carbon, that can counteract the effect of ionic strength on particle destabilization and subsequent aggregation. The final combination was selected based on the shape of the residual turbidity curve, which allowed for the distinction of both particle destabilization zones—(1) adsorption and charge neutralization and (2) sweep flocculation. The expected residual turbidity profile, highlighted in Figure 3.1C, shows a characteristic curve suggested by Stumm and O’Melia (1968), facilitating the investigation of MPs destabilization with these mechanisms. To further confirm destabilization, zeta potential was evaluated; particle destabilization is maximized when zeta potential is within a few millivolts of zero (Amirtharajah & Mills 1982; Duan & Gregory, 2003; Pernitsky & Edzwald, 2006). A schematic in Figure 3.2 details the objectives and the associated experimental tasks.

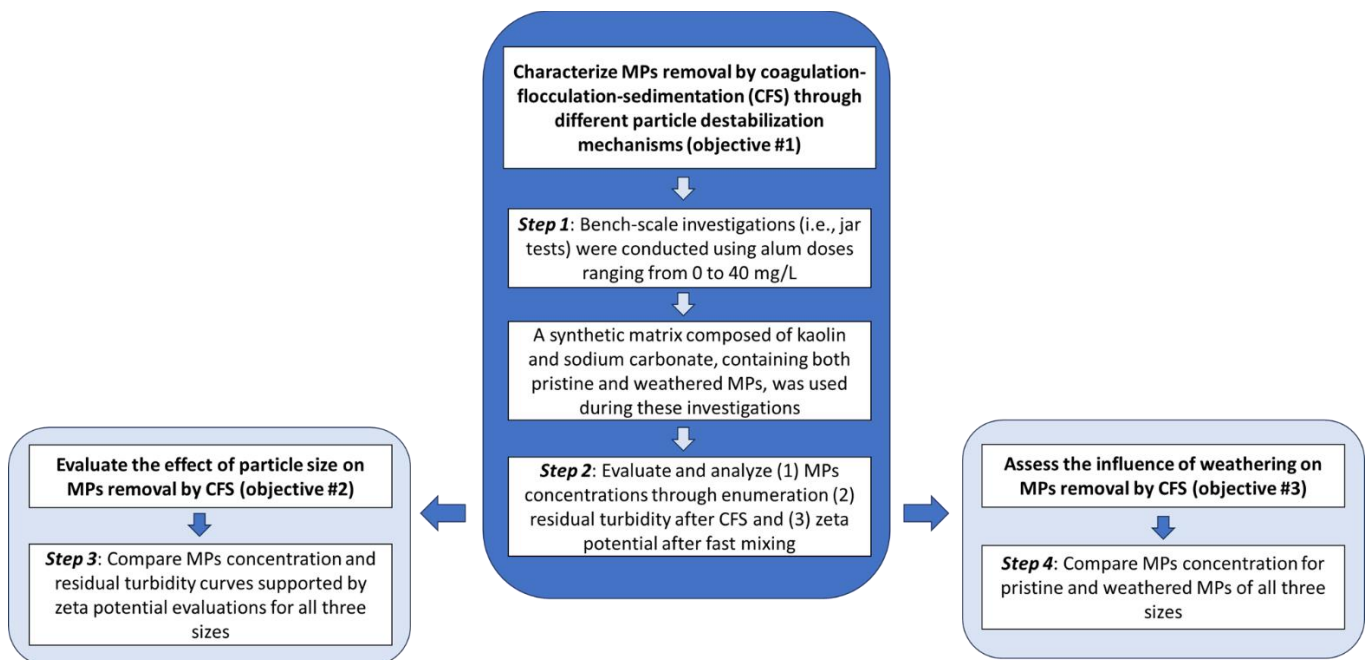


Figure 3.2 Research objectives and the associated experimental tasks.

Bench-scale experiments (i.e., jar tests) were then conducted to assess the impact of coagulant dose on the removal of three different sizes (1, 5, and 10  $\mu\text{m}$ ) of pristine and weathered MPs in synthetic water using alum, as shown in Figure 3.2. These experiments were performed in triplicate, with the two MPs types dosed together in every jar. An initial MPs concentration of  $1 \times 10^5$  particles/mL in each jar was used to evaluate the effect of particle size on MPs removal. While the MPs concentration is high relative to what is observed in the environment, this is necessary to ensure a meaningful assessment of treatment performance—this approach has been used for protozoa as well (Huck et al., 2002; Emelko et al., 2006; Ballantyne et al., 2024). This was based on an assumed 2-log removal of MPs with a target count of 150 MPs per slide, as detailed below in the discussions of MPs enumeration. For each MPs size, the settled water turbidity and zeta potential were measured and plotted as a function of alum dose, detailed in section 3.5. Table 3.1 provides a detailed rationale for the choice of MPs material, type, and size.

Table 3.1 Experimental design components and rationale for their choice.

Experimental design element	Experimental design selection	Rationale for selection
MPs material	Polystyrene (PS)	<ul style="list-style-type: none"> <li>• PS is commonly found in natural water</li> <li>• Widely investigated as pathogen (especially protozoan (oo)cyst surrogate)</li> </ul>
MPs type	Pristine & weathered	<ul style="list-style-type: none"> <li>• It has been suggested that MPs weathering/surface modifications may affect their removal during treatment (relative to pristine MPs)</li> </ul>
MPs size	1, 5, & 10 $\mu\text{m}$	<ul style="list-style-type: none"> <li>• Relatively few studies of smaller sized MPs removal during treatment are available</li> <li>• Smaller MPs pose greater health risk due to absorptive capacity, particularly in gastrointestinal tract (Wright and Kelly, 2017).</li> </ul>

To evaluate the effects of MPs size and weathering on their removal by CFS (Objectives #2 and #3), experimental conditions had to be established to enable evaluation of both adsorption and charge neutralization and enmeshment in precipitate particle destabilization mechanisms. Given that turbidity is influenced by both particle concentration and size, variations in turbidity upon alum addition were expected to indicate changes in MPs concentration within the suspension. Initially, suspended MPs in water carry a negative surface charge, maintaining stability due to mutual electrostatic repulsion, much like other particles. As zeta potential is indicative of surface charge, evaluating particle charge across all alum doses informed destabilization; maximal destabilization occurs within a few millivolts of zero. The alum solubility diagram presented in Figure 2.5 further illustrates that the mechanisms of adsorption,

charge neutralization and enmeshment in precipitate are most effective for lower coagulant doses when pH is in the vicinity of 6 to 7. Aluminum exhibits minimal solubility under these conditions, leading to the precipitation of amorphous aluminum hydroxide at relatively lower coagulant doses (than at other pHs), thereby promoting particle destabilization by enmeshment in precipitate. The limited solubility of aluminum under neutral pH ensures that sufficient hydroxide precipitates are formed to effectively enmesh the destabilized MPs, facilitating their removal during water treatment (Duan & Gregory, 2003). Therefore, maintaining a pH of 7 was important to demonstrate MPs destabilization through both mechanisms.

The characteristic curves ( $S_1$ ,  $S_2$ ,  $S_3$ , and  $S_4$ ) suggested by Stumm and O'Melia (1968) in Figure 2.7 demonstrate different turbidity profiles after coagulation of suspensions containing different colloidal particle concentrations in water. They indicate, delineating four distinct zones of particle destabilization and restabilization upon coagulant addition. The  $S_2$  curve was targeted for development of a synthetic matrix to investigate MPs removal by CFS through known coagulation mechanisms—adsorption and charge neutralization and enmeshment in precipitate. Removal of pristine (yellow green) and weathered (bright blue) MPs were evaluated concurrently.

### **3.3 Preparation of materials**

#### **3.3.1 Microplastics (MPs)**

Polystyrene MPs (surfactant free) of two types (carboxylated YG & plain BB) and three sizes: 1, 5, and 10  $\mu\text{m}$  diameter were used. Pristine 5  $\mu\text{m}$  MPs were purchased from CD Bioparticles, (USA) and the remaining types and sizes were purchased from Polysciences Inc. (USA). The MPs had a density of 1.045  $\text{g}/\text{cm}^3$  which kept them in suspension prior to coagulant addition. For the bench-scale experiments, all MPs stock suspensions were serially diluted to achieve desired concentrations of MPs using Milli-Q™ (Table 3.2). The prepared MPs suspensions were then vortexed for 10 seconds before coagulant addition to ensure even distribution of particles in the suspension.

Table 3.2 Stock concentrations and volumes of different MPs sizes used during experiments.

MPs size (µm)	Stock suspension* (MPs/mL)	Diluted suspension (MPs/mL)	Volume added (µL)
1	$4.55 \times 10^{10}$	$4.55 \times 10^7$	45.5
5	$4.99 \times 10^8$	$4.99 \times 10^7$	49.9
10	$4.55 \times 10^7$	N/A	45.5

\*Concentration provided by manufacturer

### 3.3.2 Kaolin suspension

Kaolin suspension preparation was conducted as per Duan (1997) where initially, a high-concentration kaolin suspension was made as a stock and then diluted to be used as a working suspension for making synthetic water. For preparing the stock suspension, 200 g of dry kaolin (Sigma-Aldrich, USA) was slowly added to 500 mL of Milli-Q™ water and stirred with a glass rod. Then the kaolin suspension was further diluted with Milli-Q™ water to a volume of 1 L, and the pH was adjusted to 7.5 with NaOH. The suspension was allowed to stand in a 1 L graduated cylinder overnight. Then the upper 500 mL was carefully decanted and retained and further diluted to around 800 mL as a working suspension (adjusted pH again to 7.5).

### 3.3.3 Synthetic water

For the synthetic water used in jar tests, 3.2 mL of 0.25 M Na<sub>2</sub>CO<sub>3</sub> solution was added to 800 mL of Milli-Q™ water in a 1000 mL beaker to provide an ionic strength of 0.1 M and thoroughly mixed at 50 rpm for 15–20 minutes. Then, 336 µL of the kaolin working suspension was added to achieve a turbidity of approximately 70 NTU. The pH was measured and adjusted to 7.0 by adding 875 µL of 1 M HNO<sub>3</sub> solution. Synthetic water was used to minimize surface water matrix effects on coagulation and to control parameters such as pH, ionic strength, and turbidity during the experiments.

### 3.3.4 Coagulant and other chemicals

#### a. Aluminum sulfate (alum)

Alum stock solutions of three different concentrations: 0.080 M (2.7 g in 50 mL; 53.3 g/L), 0.032 M (1.1 g in 50 mL; 21.3 g/L) and 0.008 M (0.27 g in 50 mL; 5.3 g/L) were prepared by dissolving aluminum sulfate hydrate (Al<sub>2</sub>O<sub>12</sub>S<sub>3</sub>·18H<sub>2</sub>O) (Fisher Chemicals, Ottawa) in Milli-Q™ water. Three dosing solutions with different concentrations were prepared and used to ensure that the volume of dosing solution added, does not significantly alter the initial volume of the water matrix, allowing for precise dosing with

micro syringes (Thermo Fisher Scientific, Ottawa). The alum solutions were placed on stir plates with magnetic stir bars to ensure thorough mixing and allowed to hydrate for at least an hour before use in experiments. A fresh stock solution was prepared before each set of jar tests to maintain consistency.

#### **b. Sodium carbonate ( $\text{Na}_2\text{CO}_3$ )**

To prepare 0.25 M of  $\text{Na}_2\text{CO}_3$ , 6.625 g of anhydrous  $\text{Na}_2\text{CO}_3$  powder (Sigma-Aldrich, USA) was dissolved in 250 mL Milli-Q™ water in a volumetric flask and gently mixed.

#### **c. Nitric acid ( $\text{HNO}_3$ ) and sodium hydroxide ( $\text{NaOH}$ )**

To prepare 0.1 M of  $\text{NaOH}$ , 1.00 g of  $\text{NaOH}$  pastilles (i.e., beads) were dissolved in 250 mL Milli-Q™ water in a volumetric flask. To prepare 1 M  $\text{HNO}_3$ , approximately 15.9 mL of concentrated (70% wt/wt)  $\text{HNO}_3$  (Sigma-Aldrich, USA) was added to some Milli-Q™ water in a 250 mL volumetric flask and then made up to the mark with Milli-Q™ water. These two solutions were used for pH adjustment.

### **3.4 Experimental Methods**

#### **3.4.1 Jar test procedure**

Alum was added into 800 mL of test water in a 1,000 mL jar at the doses specified in Table 3.3 and rapidly mixed for 30 s at 200 rpm using a Phipps & Bird™ PB 700™ jar tester. Zeta potential was immediately measured following rapid mixing. This was followed by 15 min of slow mixing at 50 rpm and then 20 min of sedimentation after which turbidity was measured. The initial turbidity was measured immediately after adding kaolin to the control jar.

Table 3.3 Alum dose and volume of alum stock solution added to each jar (mg/L and  $\mu\text{M}$ ).

Targeted dose (mg/L)	Targeted dose ( $\mu\text{M}$ )	Stock solution concentration (M)	Volume of alum stock solution added to jar (mL)
0.00	0	0.008	0
0.97	2		0.20
1.46	3		0.30
1.94	4		0.40
2.92	6		0.60
3.89	8		0.80
4.86	10		1.00
5.83	12		0.032
6.81	14	0.35	
7.78	16	0.40	
8.75	18	0.45	
9.72	20	0.080	0.20
14.58	30		0.30
19.45	40		0.40
29.17	60		0.60
38.89	80		0.80

### 3.4.2 pH

pH was measured with a glass-bulb, liquid-junction electrode (Fisher Scientific, Canada). The pH meter was calibrated weekly with pH 4, pH 7 and pH 10 standards.

### 3.4.3 Turbidity measurement

Turbidity was analyzed following Hach Method 10133 (2005) with a 2100N Turbidimeter (Hach, Canada; Matos et al., 2024). The instrument was calibrated daily with 0, 1, 10, 100, and 1,000 NTU primary formazin standards (hydrazine sulfate and hexamethylene tetramine, from Sigma-Aldrich, USA). Samples were collected in 30 mL glass Lab Turbidimeter Sample Cells (Hach, Canada) using 10 mL syringes after 20 minutes of settling.

### 3.4.4 Zeta potential analysis

Zeta potential was evaluated using Zetasizer Nano (Malvern Panalytical, Toronto). Samples for zeta potential measurements were collected using a 10 mL syringe immediately after rapid mixing ( $t = 30$  s). Disposable folded capillary cells (Malvern Panalytical, Toronto) were rinsed with sample three times before inserting in the Zetasizer according to the ISO 13099-1:2012 Standard Method.

### 3.4.5 MPs Enumeration

MPs enumeration was conducted using direct membrane filtration (Emelko et al., 2008) and microscopy (Carl Zeiss Axioskop 2 plus). In brief, water samples were vacuum filtered through 25 mm diameter, 0.4  $\mu\text{m}$  nominal porosity polycarbonate (PC) filter membranes which were mounted using few drops of PBS (i.e., 10x phosphate-buffered saline) on a manifold at -21 inches of Hg (-533 mm Hg) and PS MPs were thereby retained on the membrane filter. The membrane filter was then mounted with “No-Fade” mounting medium (Waterborne, Inc, New Orleans, LA) on a microscope slide, and the retained MPs were then enumerated microscopically as shown in Figure 3.3.

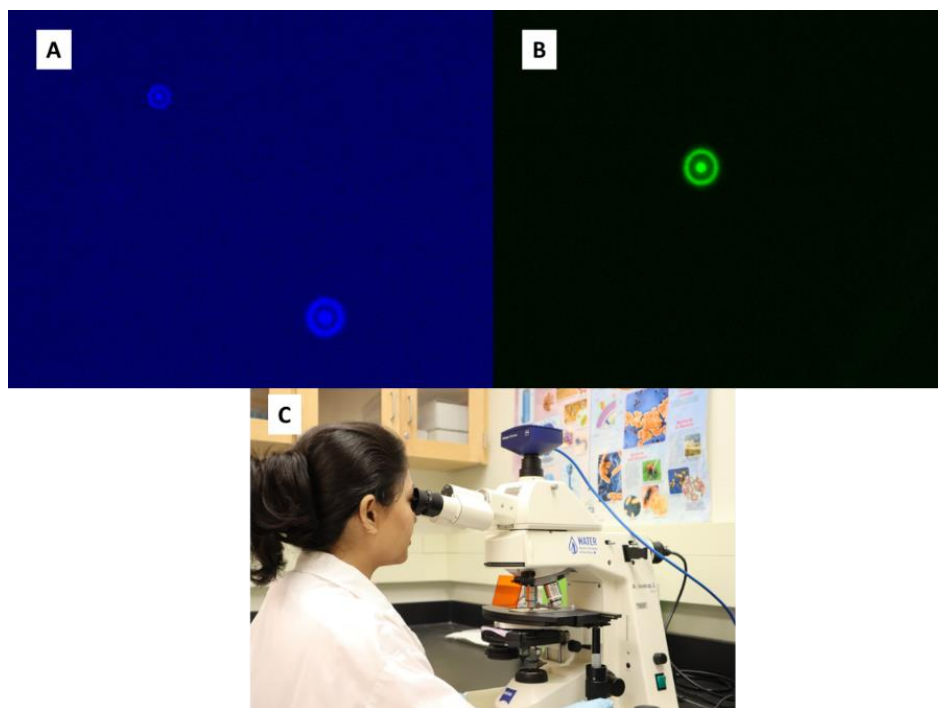


Figure 3.3 (A) Carboxylated [weathered] BB polystyrene and (B) Plain [pristine] YG 1  $\mu\text{m}$  MPs (C) enumerated using epifluorescence microscopy at 20x magnification.

For an initial MPs concentration of  $1 \times 10^5$  particles/mL, sample volumes (as shown in Table 3.4) were chosen to yield between 10 (and preferably 30) to 150 MPs per slide to minimize measurement errors associated with random sampling and imperfect and/or variable analytical recovery (Emelko et al., 2008; 2010; Schmidt et al., 2010; Chik et al., 2018). Specifically, counting fewer than 10 particles increases uncertainty and may not provide a sufficiently representative sample. Conversely, counting more than 150 particles can result in overcrowding on the slide making it difficult to distinguish and accurately count individual particles. All bottles and manifolds were rinsed with a detergent solution (1X phosphate-

buffered saline with Tween 80 [PBST]) before and after use. After filtration, the membranes were mounted on glass slides to facilitate MPs enumeration through microscopy.

Table 3.4 Sample volume filtered at selected alum doses for the different sizes of MPs to ensure an adequate number of MPs were enumerated.

Sample volume (mL)	Doses analyzed for 1 $\mu\text{m}$ MPs (mg/L)	Doses analyzed for 5 $\mu\text{m}$ MPs (mg/L)	Doses analyzed for 10 $\mu\text{m}$ MPs (mg/L)
1	0	0	0
1	1.46	1.94	1.94
1	1.94	2.92	2.92
1	2.92	3.89	3.89
1	3.89	4.86	4.86
1	4.86	5.83	5.83
10	9.72	9.72	9.72
100	29.17	29.17	29.17

### 3.5 Data handling and analysis

Jar test experiments were conducted in triplicate. Eight alum doses were investigated for each of three MPs sizes (1, 5, and 10  $\mu\text{m}$ ). Post-sedimentation turbidity was analyzed after 20 mins of sedimentation. Mean turbidity was plotted as a function of alum dose for each size of MPs to confirm that characteristic curves proposed by Stumm and O’Melia (1968) for particle/solids removal by chemical pretreatment were established so that optimal particle destabilization by (i) adsorption and charge neutralization and (ii) enmeshment in precipitate mechanisms could be clearly and reproducibly identified. In the residual turbidity curves, there are two local minima. Each corresponds to one of the particle destabilization mechanisms. The first local minimum corresponds to particle destabilization by adsorption and charge neutralization and the second corresponds to particle destabilization by enmeshment in precipitate. Optimal particle destabilization was further confirmed by evaluation of post-coagulation zeta potential.

To evaluate the effect of particle size on MPs removal by CFS, MPs removal for the three sizes were compared. Also, the turbidity curves plotted for all three sizes of MPs as a function of alum dose were compared to observe the change in turbidity reduction with increasing particle size. To assess the influence of weathering on MPs removal by CFS, two-tailed paired t-tests were conducted on counts of pristine and weathered MPs at different alum doses, as summarized in Table 3.5. Three t-tests for each size (i.e., 1, 5, and 10  $\mu\text{m}$ ) were conducted at different alum doses to determine if there were differences in (1) initial concentrations of pristine and weathered MPs, (2) particle destabilization by adsorption and

charge neutralization between pristine and weathered MPs, and (3) particle destabilization by sweep flocculation between pristine and weathered MPs. The t-tests on the initial concentrations of pristine and weathered MPs were conducted to determine whether the targeted MPs concentrations were achieved during the experiments and to assess the consistency between the prepared MPs stock suspensions. Additionally, t-tests were performed to compare destabilization of pristine and weathered MPs destabilization by (1) adsorption and charge neutralization and (2) enmeshment in precipitate followed by removal during sedimentation. These analyses were conducted to assess if particle destabilization by coagulant addition is maximized regardless of surface modifications or presence of surface functional groups. Additionally, t-tests were conducted on selected residual turbidity data for 1, 5 and 10  $\mu\text{m}$  to compare if higher turbidity reduction occurred through sweep flocculation than through adsorption and charge neutralization, as shown in Table 3.6. All statistical calculations were performed using Microsoft Excel®.

Table 3.5 Summary of count data used at selected alum doses for two-tailed paired t-test analyses for three sizes of pristine and weathered MPs and their rationale.

<b>Rationale</b>	<b>MPs size (<math>\mu\text{m}</math>)</b>	<b>Alum doses included in the analysis (mg/L)</b>
To analyze whether there is a difference in initial concentrations of pristine and weathered MPs	1	0
	5	0
	10	0
To analyze whether there is a difference in MPs destabilization—by adsorption and charge neutralization when maximized—for pristine and weathered.	1	1.46 & 1.94
	5	1.94 & 2.92
	10	1.94 & 2.92
To analyze whether there is a difference in MPs destabilization—by sweep flocculation when maximized—for pristine and weathered.	1	29.17
	5	29.17
	10	29.17

Table 3.6 Summary of turbidity data used at selected alum doses for two-tailed paired t-test analyses for three sizes of MPs and their rationale.

<b>Rationale</b>	<b>MPs size (µm)</b>	<b>Alum doses included in the analysis for adsorption &amp; charge neutralization (mg/L)</b>	<b>Alum doses included in the analysis for sweep flocculation (mg/L)</b>
To analyze whether turbidity reduction through sweep flocculation was significantly different than through adsorption and charge neutralization	1	1.46 & 1.94	29.17 & 38.89
	5	1.46, 1.94 & 2.92	19.45, 29.17 & 38.89
	10	1.46, 1.94 & 2.92	19.45, 29.17 & 38.89

## Chapter 4 Results and discussion

It is generally understood that smaller colloidal and nano-sized particles can be removed to some extent by conventional CFS and subsequent physico-chemical filtration. While the removal of MPs during conventional CFS has been reported in several studies conducted under a variety of treatment conditions, this study aimed to confirm expectations of MPs removal by conventional chemical pretreatment (i.e., coagulation, flocculation, and sedimentation) using common metal salt coagulants such as alum. The specific focus of this work was to demonstrate that fundamental mechanisms of particle destabilization are foundational to MPs removal during conventional chemical pretreatment and overcome differences in MPs surface properties due to weathering. Thus, similar removals of pristine and weathered MPs by chemical pretreatment with CFS were expected when particle destabilization was optimized.

The literature review presented in Chapter 2 indicated that removals of MPs (from 1 to 500  $\mu\text{m}$  in size) by conventional CFS at bench-scale have ranged from 0.097- to 3-log. In comparison, approximately 0.15- to 4-log removal of other colloidal particles (Table 2.2)—such as *Cryptosporidium* oocysts, *Giardia* cysts, *E. coli*, silica and kaolin—has been reported for CFS. Comparison of Tables 2.2 and 2.3 indicates that while these ranges of particle removals span several orders of magnitude, MPs removals by CFS do not appear patently different from those of other colloidal particles (including 3 to 6  $\mu\text{m}$  spherical *Cryptosporidium* oocysts) of similar size (i.e., 1 to 20  $\mu\text{m}$ ). Notably, investigations of smaller (1-10  $\mu\text{m}$ ) sized MPs by CFS have been limited largely to case studies in which foundational mechanisms of particle destabilization that are necessary for maximizing treatment performance have only been superficially addressed, if at all.

### 4.1 Synthetic raw/untreated water matrix selection

Several experiments were conducted with varying combinations of turbidity and ionic strength added to MilliQ™ water to identify the optimal raw/untreated water conditions for clearly observing particle destabilization by both relevant destabilization mechanisms: (1) adsorption and charge neutralization and (2) sweep flocculation. For example, in Figure 4.1A (0.1 M ionic strength), the initial turbidity of 45 NTU gradually decreased after 17 mg/L of alum, whereas in Figure 4.1B (0.25 M ionic strength), with an initial turbidity of 70 NTU, there was a rapid decrease in turbidity from 1.45 mg/L of alum. These figures demonstrate the impact of increasing both ionic strength and initial turbidity by approximately 50% and, in this case, illustrate the disproportionately greater impact of increased ionic strength on turbidity reduction. In Figure 4.1A, the zeta potential approached zero at an alum dose of

approximately 2 to 3 mg/L; this corresponded to a slight reduction in post-treatment turbidity. In contrast, in Figure 4.1B, the zeta potential reached zero at an alum dose of approximately 10 mg/L; however, this dose was slightly higher than the dose at which the local maximum for turbidity reduction by adsorption and charge neutralization was observed. These observations underscore that alum precipitates are colloidally unstable (regardless of pH) and difficult to predict because of the relative influences of anions present in the system and ongoing hydrolysis reactions, van der Waals attraction, hydration force, etc. (Duan et al., 2014). Thus, alum precipitates may also reconfigure and change somewhat over time, emphasizing the need to consider residence time between the point of coagulant addition and the treatment process(es) for which coagulant addition is relevant and optimized (e.g., clarification, physico-chemical filtration, etc.). While an investigation of the various factors that affect turbidity reduction by alum-based coagulation is beyond the scope of this thesis research, this work re-iterates the conclusions of Ballantyne et al. (2024), which emphasized that while achieving post-coagulation zeta potential that is within a few millivolts of zero is likely to ensure optimal particle destabilization by coagulation, zeta potential targets will be somewhat case specific. Here, as shown in Figure 4.2, the final combination of turbidity and ionic strength composing the raw/untreated water matrix was selected based on the shape of the residual (i.e., post-CFS) turbidity curve to ensure clear identification of both particle destabilization zones: (1) adsorption and charge neutralization and (2) sweep flocculation, as reflected in the characteristic curve suggested by Stumm and O'Melia (1968), which is shown in Figure 3.1C. As shown in Figure 4.2, this curve could reproducibly be generated. Additional scenarios investigated as part of synthetic raw/untreated water matrix development are presented in Appendix A.

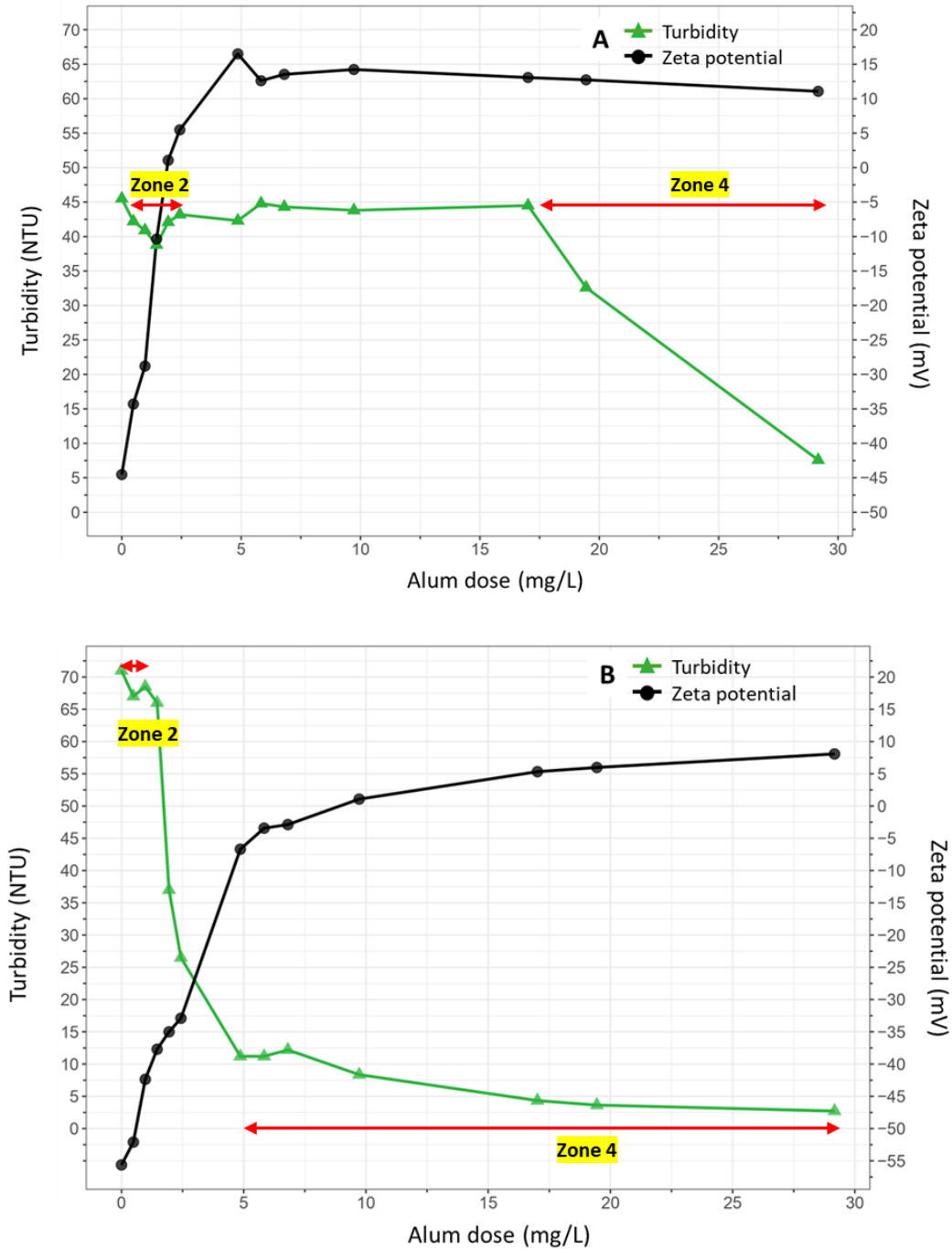


Figure 4.1 Turbidity and zeta potential after alum addition for 5  $\mu\text{m}$  MPs at pH 7 with (A) ionic strength of 0.1 M and initial turbidity of 45 NTU and (B) ionic strength of 0.25 M and initial turbidity of 71 NTU. In each of the plots, the two destabilization zones: adsorption and charge neutralization (“Zone 2” from Stumm & O’Melia, 1968) and sweep flocculation (“Zone 4” from Stumm & O’Melia, 1968)—are visible, but the turbidity reduction observed due to adsorption and charge neutralization is not substantial. Data points are connected by lines to assist with visualization.

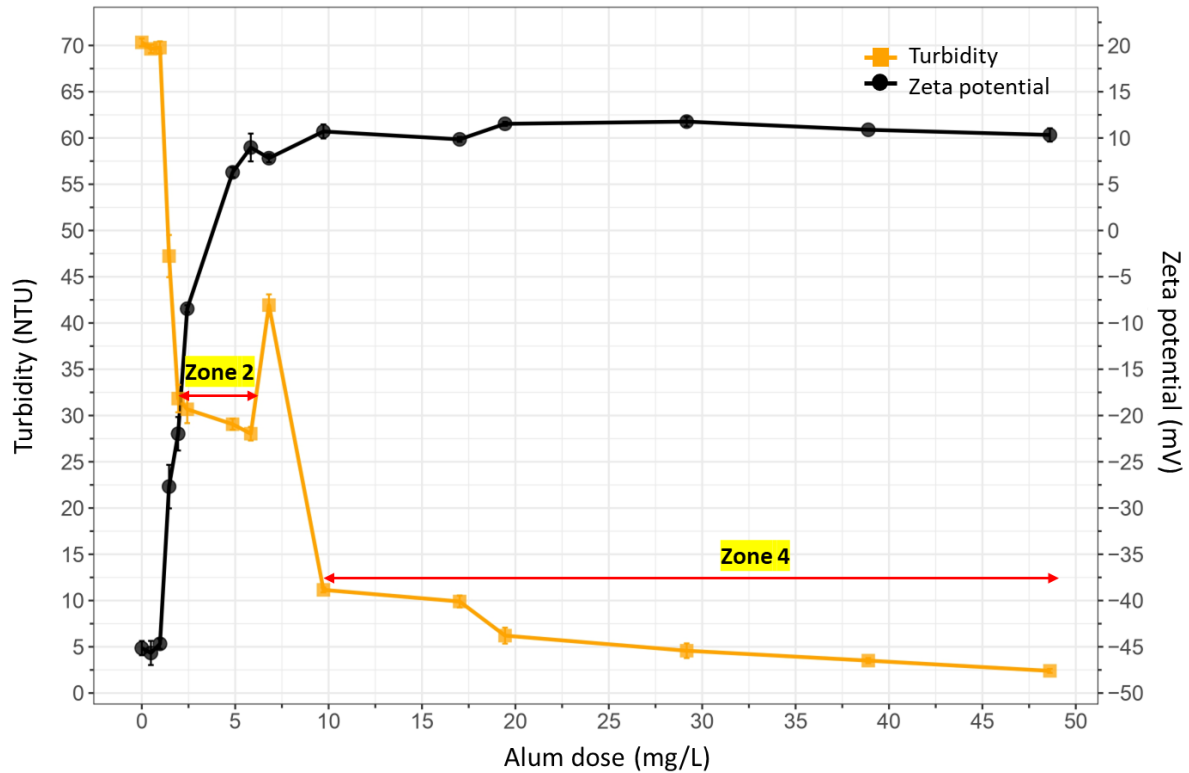


Figure 4.2 Final study matrix without MPs at an ionic strength of 0.1 M and turbidity of 70 NTU at pH 7, clearly identifying both particle destabilization zones: (adsorption and charge neutralization (“Zone 2” from Stumm & O’Melia, 1968) and sweep flocculation (“Zone 4” from Stumm & O’Melia, 1968). Data points are connected by lines for better visualization.

#### 4.2 Turbidity reduction by CFS

In Figure 4.3, the turbidity curves for experiments conducted with both pristine and weathered MPs of a particular size are presented (n = 6 per MPs size). The MPs types were added to the study matrix at the start of the jar test experiments, which were performed in triplicate for each MPs (Appendix B). Mean turbidity  $\pm$  one standard deviation is presented to provide an indication of reproducibility in generating these characteristics curves.

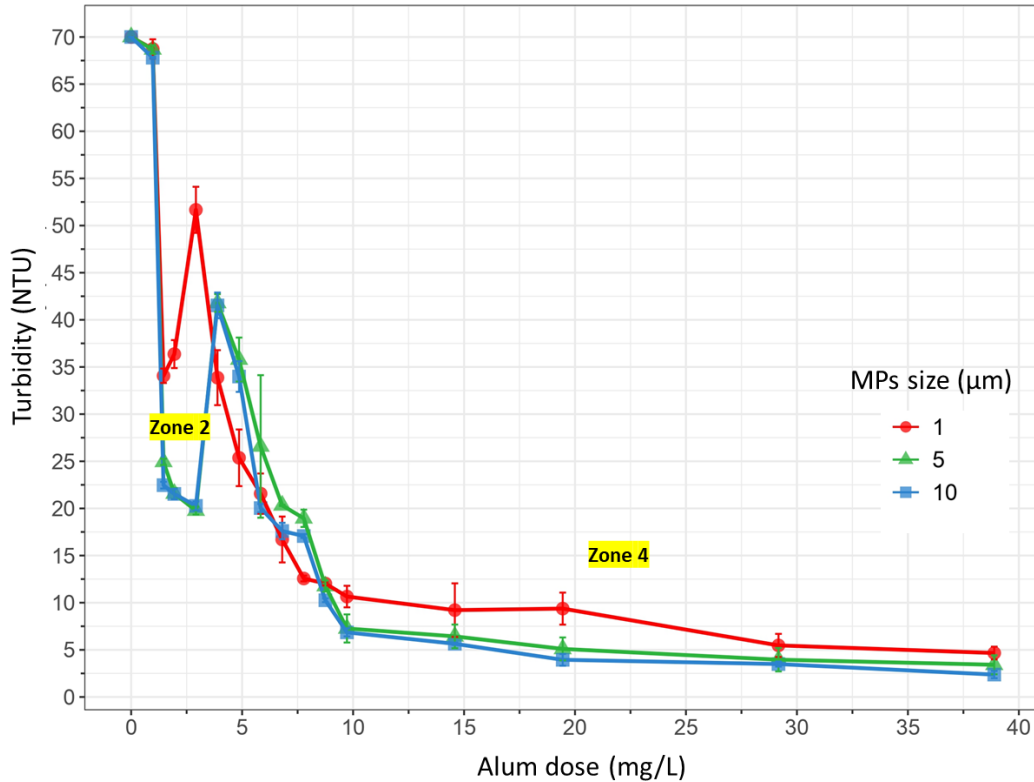


Figure 4.3 Combined residual turbidity ( $n = 6$  per MPs size) after alum addition for 1, 5 and 10  $\mu\text{m}$  pristine ( $n = 3$  for each size) and weathered ( $n = 3$  for each size) MPs suspended in the study matrix (mean  $\pm$  standard deviation). Herein, the two destabilization zones—adsorption and charge neutralization (“Zone 2” from Stumm & O’Melia, 1968) and sweep flocculation (“Zone 4” from Stumm & O’Melia, 1968)—can be clearly discerned for all three sizes of MPs. Data points are connected by lines to assist with visualization.

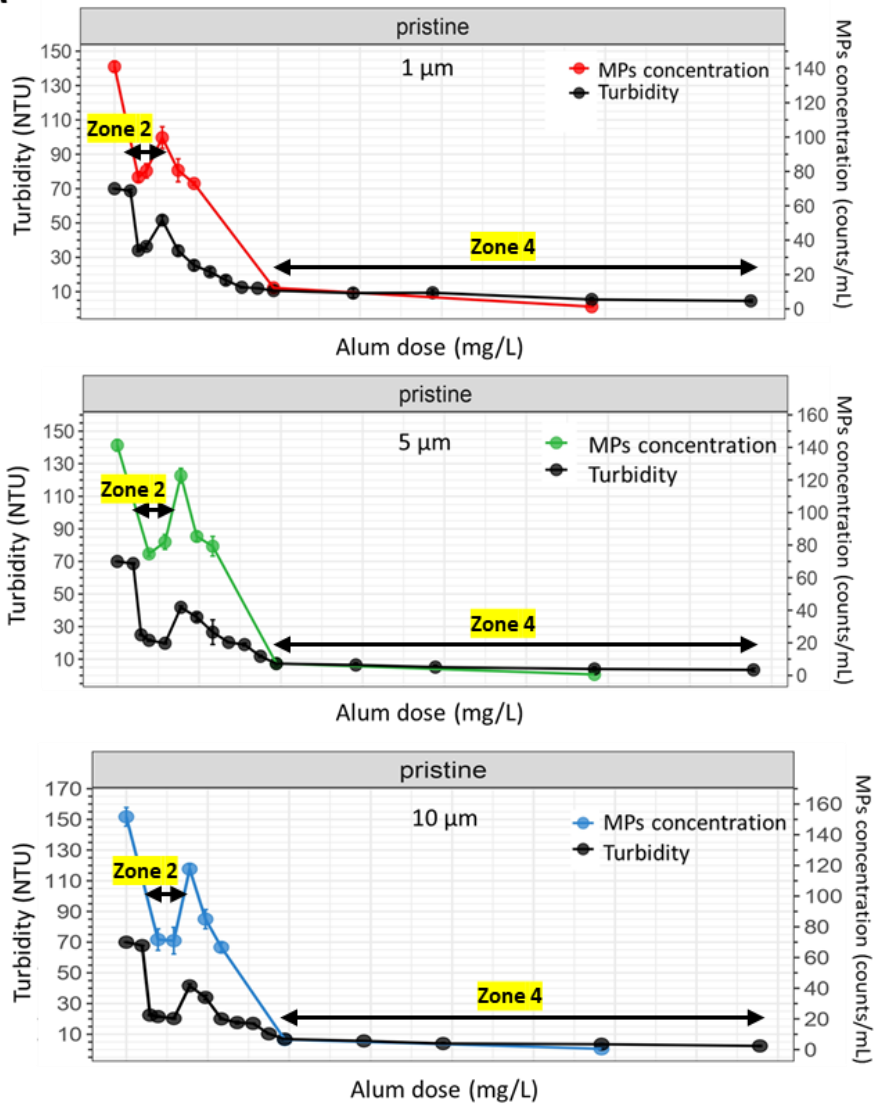
The initial turbidity for suspensions of all three MPs sizes—1  $\mu\text{m}$ , 5  $\mu\text{m}$ , and 10  $\mu\text{m}$ —was 70 NTU. A rapid decrease in turbidity was observed up to an alum dose of approximately 1.46 mg/L for 1  $\mu\text{m}$  MPs and between 1.46 and 2.92 mg/L for 5  $\mu\text{m}$  and 10  $\mu\text{m}$  MPs. As shown in Figure 4.3, this region is associated with adsorption and charge neutralization. Upon further addition of alum, turbidity increased up to 2.92 mg/L for 1  $\mu\text{m}$  MPs (51.7 NTU), and up to 3.88 mg/L for 5  $\mu\text{m}$  (41.8 NTU) and 10  $\mu\text{m}$  (41.5 NTU) MPs. Beyond 2.92 to 3.88 mg/L, turbidity decreased because of enmeshment in precipitate until an alum dose of 38.89 mg/L for 1 (4.7 NTU), 5 (3.4 NTU) and 10 (2.4 NTU)  $\mu\text{m}$  MPs. The lowest residual turbidity (i.e., greatest extent of solids reduction) as a function of MPs size was 10  $\mu\text{m} < 5 \mu\text{m} < 1 \mu\text{m}$ .

The trends in turbidity reduction observed in Figure 4.3 align with theoretical expectations related to particle size. All the flocs that formed were relatively dense, and not visibly porous. Thus, they could be

simplistically considered as discrete particles (formed by aggregation of smaller particles). Although turbidity for 1  $\mu\text{m}$  MPs began to decrease at a lower alum dose compared to 5  $\mu\text{m}$  and 10  $\mu\text{m}$  MPs, larger MPs exhibited greater turbidity reduction. This can be attributed to the formation of heavier flocs for larger particles, which experience greater gravitational forces, resulting in faster sedimentation, consistent with Stokes' law for discrete particle settling (Crittenden et al., 2012; Tadros, 2013). During the jar test experiments, particles of different sizes were tested in separate jars under identical conditions—same water matrix and coagulant dose—leading to similar precipitation behavior. Thus, it is reasonable to assume that the particles will aggregate in a similar manner, even if their surface areas differ slightly (i.e., pristine vs. weathered). While Stokes' law may not perfectly describe the system in a jar, it provides a useful approximation for understanding how larger, aggregated particles settle more quickly than smaller ones in a system with coagulants.

In Figure 4.4, changes in turbidity and variation of MPs concentrations with different concentrations of coagulant for all three MPs sizes (1  $\mu\text{m}$ , 5  $\mu\text{m}$ , and 10  $\mu\text{m}$ ) and two types are shown. The turbidity curves represent both types of MPs for all three sizes. The curves for MPs concentrations for all three sizes and two types confirm the removal of MPs through (1) adsorption and charge neutralization and (2) sweep flocculation exhibiting two substantial local minima that can be observed from the residual turbidity curves for all three sizes. Initially, the MPs concentration was high for all three sizes and types of MPs. Upon addition of alum, the MPs concentration for 1  $\mu\text{m}$  decreased at 1.46 mg/L. This was observed for 5 and 10  $\mu\text{m}$  MPs for both pristine and weathered, however, the reduction in MPs concentration due to adsorption and charge neutralization was observed at a higher dosage of 1.94 mg/L. With alum addition, MPs restabilized exhibiting increased concentrations and MPs concentrations finally decreased with further addition of alum due to enmeshment in precipitates.

A



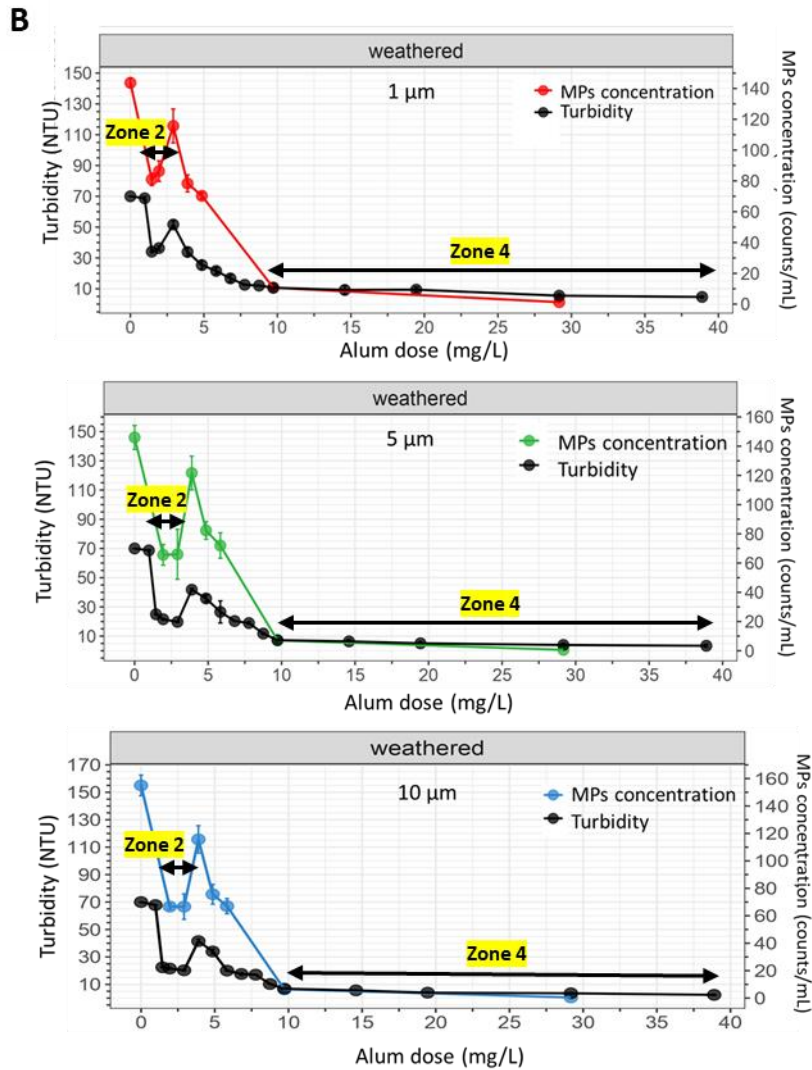


Figure 4.4 Residual turbidity and MPs concentration after alum addition for 1, 5 and 10 µm (A) pristine and (B) weathered microplastics suspended together in the study matrix at an ionic strength of 0.1 M and turbidity of 70 NTU at pH 7. Herein, the two destabilization zones— adsorption and charge neutralization (“Zone 2” from Stumm & O’Melia, 1968) and sweep flocculation (“Zone 4” from Stumm & O’Melia, 1968)—can be clearly discerned in both the curves for all three sizes of MPs for both types. Data points are connected by lines to assist with visualization.

In Figure 4.5, changes in turbidity levels and the variation of zeta potential with different concentrations of coagulant for all three MPs sizes (1 µm, 5 µm, and 10 µm) are compared. Like Figure 4.3, the turbidity curves in Figure 4.5 represent both pristine and weathered MPs of a particular size. The curves for all three MPs sizes can be divided into four zones, like the S2 curve—enabling investigation of MPs removal by CFS through adsorption and charge neutralization and enmeshment in precipitate

mechanisms—suggested by Stumm and O’Melia (1968). Zone 1 showed no significant removal of turbidity because the low alum dose was insufficient for particle destabilization. In Zone 2, sufficient alum enabled particle destabilization, predominantly with positively charged hydrolysis products adsorbing onto negatively charged MPs, neutralizing surface charge and reducing electrostatic repulsion, leading to aggregation. Zone 3 is the restabilization zone, where residual turbidity increased due to the restabilization of aggregated solids, resulting in sub-optimal turbidity reduction. In Zone 4, excess coagulant addition resulted in aluminum hydroxide precipitation; these precipitates enmeshed suspended solids/turbidity. The substantial reductions in turbidity occurred in Zones 2 and 4, regardless of MPs size. Notably, all turbidity in Zone 4 (sweep flocculation) was significantly lower than in Zone 2 (adsorption and charge neutralization) for all MPs sizes ( $1\ \mu\text{m}$ ,  $p = 4.53 \times 10^{-7}$ ,  $5\ \mu\text{m}$ ,  $p = 1.92 \times 10^{-9}$ ,  $10\ \mu\text{m}$ ,  $p = 4.7 \times 10^{-13}$ ).

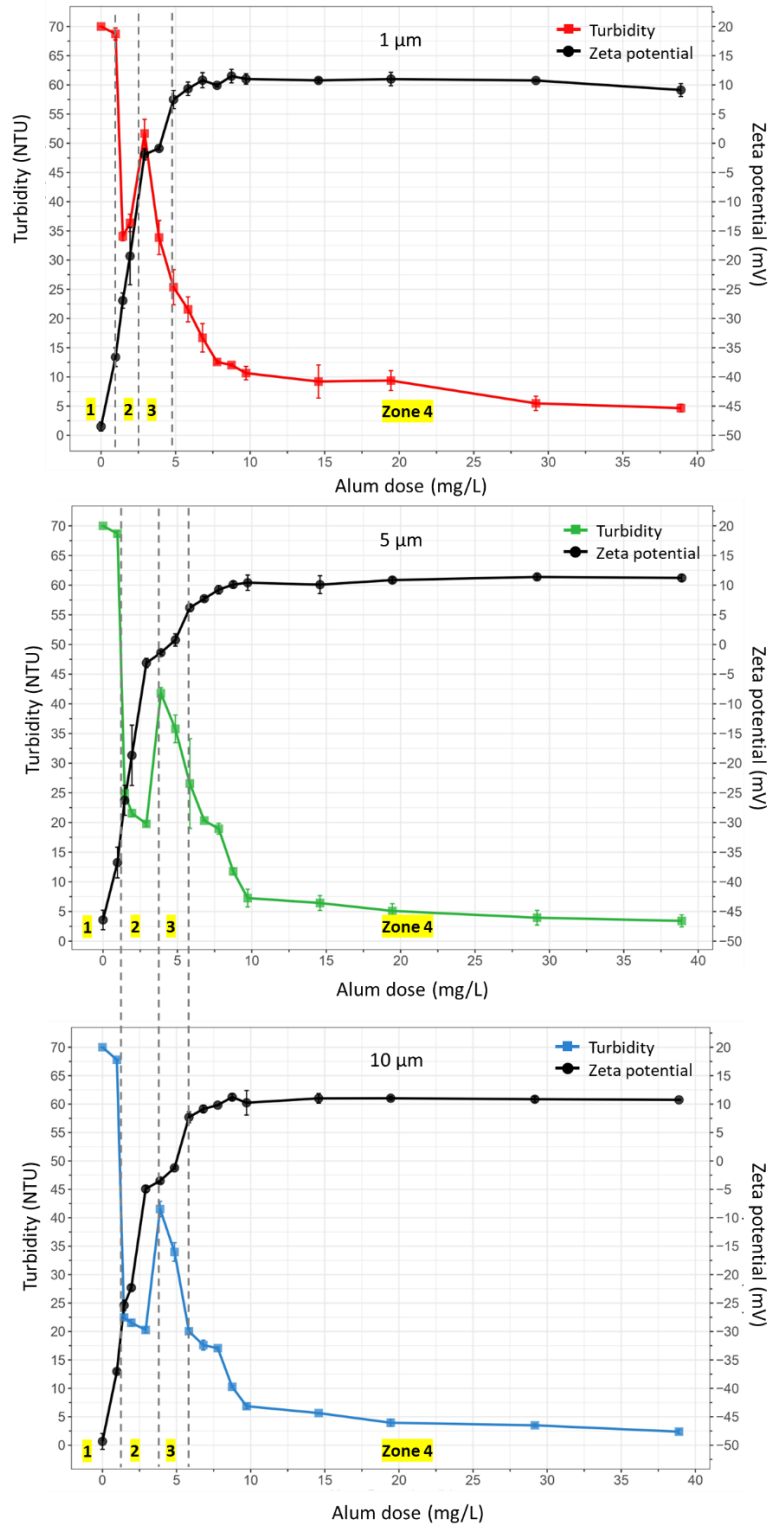


Figure 4.5 Residual turbidity and zeta potential after alum addition for 1, 5 and 10 µm pristine and weathered microplastics suspended together in the synthetic water with an ionic strength of 0.1 M and turbidity of 70 NTU at pH 7. Data points are connected by lines to assist with visualization.

Plotting the zeta potential data on the same plot as the turbidity curves demonstrates how the surface charge of the suspended solids (i.e., kaolin particles and MPs) shifted with alum addition. Initially, the zeta potential of the suspended solids was negative in all cases at approximately -50 mV. The zeta potential became less negative with alum addition and approached zero at about 5 mg/L. Upon neutralization of surface charge, the electrostatic repulsion between particles is reduced, allowing them to aggregate and eventually settle. Notably, destabilization by adsorption and charge neutralization was evident at an alum dose of 1.46 mg/L for all of the suspensions; however, those containing larger (5  $\mu\text{m}$  and 10  $\mu\text{m}$ ) were destabilized over a wider coagulant range (up to an alum dose of 2.92 mg/L). For suspensions containing 1  $\mu\text{m}$  MPs, the zeta potential was within a few millivolts of zero between generally corresponded to sweep flocculation at alum doses between 2.92 and 4.86 mg/L and generally corresponded to sweep flocculation, whereas, for 5  $\mu\text{m}$  and 10  $\mu\text{m}$  MPs, it was at alum doses between 2.92 and 6.82 mg/L. With further alum addition beyond the point of charge neutralization, the zeta potential shifted to a positive value—for all three sizes. This phenomenon, known as charge reversal, caused the restabilization of MPs, as indicated by the increase in turbidity. However, beyond an alum dose of 9.72 mg/L, the zeta potential maintained a plateau ranging between +10 mV and +12 mV. This plateau indicated that the MPs were destabilized and precipitated through sweep flocculation, as reflected in the turbidity reductions. Overall, these differences in alum dosing required to achieve optimal particle destabilization for the suspensions containing different sizes of MPs may be because smaller particles have a larger total surface area compared to larger particles on an equivalent mass basis, thereby resulting in different surface interactions as discussed above. Exploration of these differences was beyond the scope of this work. Regardless, this work underscores that when particle destabilization is maximized (i.e., zeta potential is within a few millivolts of zero) after coagulation, the potential for MPs removal by CFS is maximized after coagulation with metal salts. This is because like other particles, MPs are destabilized by (i) adsorption and charge neutralization and (ii) enmeshment in precipitate (i.e., sometimes referred to as sweep flocculation) mechanisms during coagulation with metal salts such as alum. This is analogous to what has been observed for particles like *Cryptosporidium* spp. oocysts (Bean et al., 1964; Gupta et al., 1975; Ballantyne et al., 2024), likely because in natural waters, most pristine and weathered MPs in natural waters exhibit zeta potentials in the range of -40 to -50 mV, like *Cryptosporidium* spp. oocysts and other particulate contaminants. Zeta potential targets associated with optimal particle destabilization after coagulant addition are case specific because of the relative influences of anions present in the system and ongoing hydrolysis reactions, van der Waals attraction, hydration force, etc.

### 4.3 MPs removal by bench-scale CFS

To evaluate the effects of MPs size and weathering on their removal by CFS (Objectives #2 and #3), pristine (yellow green) and weathered (bright blue) spherical MPs of 1, 5, and 10  $\mu\text{m}$  diameter were used in a bench-scale investigation of CFS with a range of alum doses. The two MPs types were evaluated concurrently to minimize potential matrix effects between batches of prepared synthetic water. The removal of 1, 5, and 10  $\mu\text{m}$  MPs, based on counting, by bench-scale CFS with various alum doses is shown in Figure 4.6.

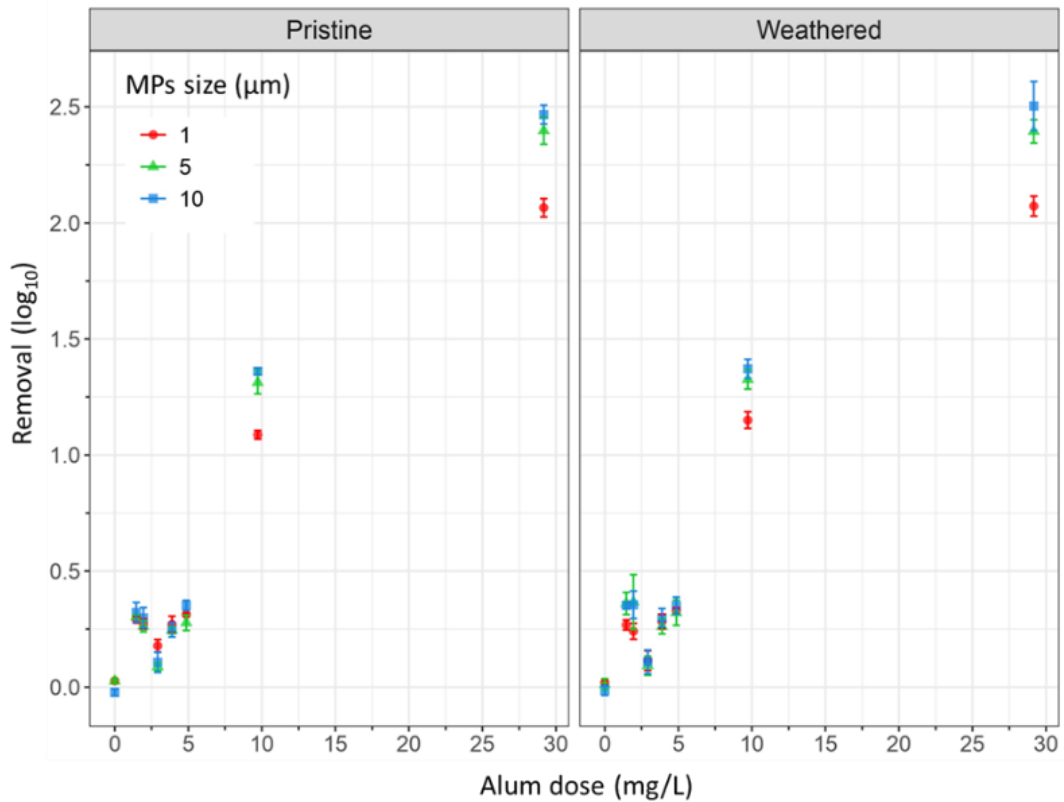


Figure 4.6 Removal of 1, 5 and 10  $\mu\text{m}$  pristine vs. weathered MPs by chemical pretreatment (i.e., CFS) at bench-scale (mean  $\pm$  standard deviation of triplicate analyses).

#### 4.3.1 Evaluating consistency in raw water MPs concentrations

Untreated water MPs concentrations must be statistically consistent to fairly compare CFS treatment performance. Paired comparison t-tests were conducted on raw count data after the MPs were added to the study matrix, prior to coagulant addition (alum dose of 0 mg/L) to assess consistency in the

MPs concentrations so that the effects of MPs size and weathering could subsequently be evaluated. The  $p$  values were 0.0153 for 1  $\mu\text{m}$ , 0.506 for 5  $\mu\text{m}$ , and 0.572 for 10  $\mu\text{m}$  MPs. Thus, statistically significant differences between pristine and weathered MPs were not observed for the 5 and 10  $\mu\text{m}$  MPs and it could be concluded that the nominal MPs concentrations were accurate and reproducible. A statistically significant difference was observed between the number of pristine and weathered 1  $\mu\text{m}$  MPs, however. The average counts for weathered MPs were only higher by 2.7 MPs—this difference is relatively small and likely inconsequential. Nevertheless, it may suggest some variability in the nominal concentration of 1  $\mu\text{m}$  MPs, potentially due to inconsistencies in the sampling strategy or analytical methods when enumerating this smaller size of MPs.

These findings highlight several critical factors to consider when assessing MPs removal during drinking water treatment. Key challenges include handling of non-detects, managing random sampling errors, accounting for analytical recovery variability, and considering the impact of operational conditions. Guidance for minimizing uncertainty in the resulting estimates of MPs concentration and risk analysis is available by adaptation from the pathogen literature and regulatory guidance (Emelko et al., 2008; Pouillot et al., 2013; Schmidt et al., 2013; Chik et al., 2018), as discussed in Section 2.5. When evaluating MPs removal effectiveness, careful attention should be given to the relevance of performance indicators, both at individual process and plant scales. Additionally, there is a need for standardized procedures for MPs sample collection and analysis to enable meaningful comparisons across different studies.

#### **4.3.2 Effect of weathering on MPs removal by CFS**

As shown in Figure 4.6, in general, approximately 0.2- to 0.5-log (36.9–68.4%) MPs removal was achieved when the MPs suspensions were destabilized by adsorption and charge neutralization (i.e., alum doses of 1.46–2.92 mg/L). Although statistically significant differences were observed between pristine and weathered 1  $\mu\text{m}$  ( $p = 0.0266$ ) and 10  $\mu\text{m}$  ( $p = 0.0264$ ) MPs, and the same difference for 5  $\mu\text{m}$  MPs was almost significant ( $p = 0.0518$ ), it is critical to note that average removals of pristine and weathered 1  $\mu\text{m}$  MPs were 0.28- and 0.27-log respectively, while they were 0.32- and 0.35-log for 10  $\mu\text{m}$  MPs and 0.30- and 0.36-log for 5  $\mu\text{m}$  MPs. Accordingly, while these differences were statistically significant in the controlled bench-scale tests, they are likely not practically relevant because the difference between them is less than 0.5-log; differences smaller than this have not been practically relevant for other particulate contaminants such as *Cryptosporidium* spp. oocysts because of inherent variability in treatment performance.

MPs removal by enmeshment in precipitate (i.e., sweep flocculation) occurred at alum doses above 9.72 mg/L, regardless of MPs weathering and size (Appendix B). At the 9.72 mg/L alum dose, removal efficiencies ranged from 1.1- to 1.4-log for pristine MPs and from 1.1- to 1.3-log for weathered MPs, regardless of MPs size. When the alum dose was further increased to 29.17 mg/L, MPs removal increased to 2.0- to 2.5-log for both pristine MPs and weathered MPs. Differences in the removal of pristine and weathered MPs by enmeshment in precipitate/sweep flocculation were not significant for 1  $\mu\text{m}$  ( $p = 0.873$ ), 5  $\mu\text{m}$  ( $p = 0.966$ ), or 10  $\mu\text{m}$  ( $p = 0.651$ ) MPs. This observation aligns with theory and practice regarding particle removal by CFS, more broadly sweep flocculation is especially effective for MPs destabilization and subsequent removal by flocculation and sedimentation. This—coupled with the widely reported zeta potentials of MPs in natural waters being similar to those of other particulate contaminants like *Cryptosporidium* spp. oocysts, suggests that weathering is unlikely to affect MPs removal by CFS when particle destabilization is optimized.

#### 4.3.3 Effect of MPs size on removal

The removal efficiency of MPs varied with particle size, with smaller MPs (1  $\mu\text{m}$ ) exhibiting lower removal rates compared to larger MPs (5  $\mu\text{m}$  and 10  $\mu\text{m}$ ). This trend was consistent for both pristine and weathered MPs. Specifically, the removals for 5  $\mu\text{m}$  and 10  $\mu\text{m}$  MPs were  $\sim 2.5$  log, respectively, while the highest observed removal of 1  $\mu\text{m}$  MPs was 2.1 log. In general, larger spherical particles (i.e., greater than 1  $\mu\text{m}$  in size), including MPs, are more readily removed by well-operated chemical pretreatment and physico-chemical filtration processes. Consequently, the removal of smaller colloidal MPs (down to approximately 1  $\mu\text{m}$  in size) should generally indicate an equal or greater extent of removal for larger MPs by these treatment processes and should be considered when evaluating treatment performance capabilities. This relationship has been demonstrated through coagulation, settling, and colloid filtration theories, as well as a rich history of documented water treatment investigations. The log removal data for both pristine and weathered 1, 5 and 10  $\mu\text{m}$  MPs in this study (2.1- to 2.5-log) fall within the range of MPs log removal reported in the literature (0.097- to 3-log) and align with the removal range (0.15- to 4-log) for colloidal particles—such as *Cryptosporidium* oocysts, *Giardia* cysts, *E. coli*, silica and kaolin—through conventional CFS at bench-scale shown in Tables 2.2 and 2.3.

Data from previous studies (as presented in Table 2.3) suggest that smaller MPs are more challenging to remove by CFS than larger ones (Links, 2015; Monis et al., 2017; Lapointe et al., 2020; Shahi et al., 2020; Li et al., 2021; Monira et al., 2021; Prokopova et al., 2021; Xue et al., 2021; Zhang et al., 2021; Zhou et al., 2021; Alioua & Lapointe, 2023; Lee et al., 2023). This can be attributed to their higher surface

area-to-volume ratio and associated greater stability in aqueous suspensions (Tang et al., 2014; Wang et al., 2020c), especially for a given concentration of coagulant. Larger MPs are also more likely to attach to flocs, increasing their likelihood of settling (Wang et al., 2020c). This observation aligns with simple settling theory (discussed in Chapter 2) for discrete particles.

While MPs affect their removal during drinking water treatment, deviations in MPs shape, porosity, and specific gravity must also be considered for case-specific risk management, as these factors can influence particle removal by CFS processes. Studies have shown that differences in removal efficiency can occur depending on the type of MPs (Lapointe et al., 2020; Zhou et al., 2021). Such variations are often attributed to differences in MPs densities, which affect their settling efficiency during coagulation. For example, Zhou et al. (2021) found that polystyrene (PS) MPs had higher removal efficiency in coagulation compared to polyethylene (PE) MPs. In the absence of a coagulant, PE had a removal rate of only 3.19% (0.01-log), while PS had a significantly higher removal rate of 50.78% (0.3-log). This difference is likely due to the higher density of PS ( $1.05 \text{ g/cm}^3$ ) compared to PE ( $0.92 \text{ g/cm}^3$ ), which makes PS more prone to settling (Zhou et al., 2021).

## Chapter 5 Conclusions and implications

### 5.1 Conclusions

In this research, MPs removal by conventional chemical pretreatment (i.e., CFS) with alum was evaluated at bench-scale to investigate if it generally aligns with the removal of other particles, including particulate contaminants such as *Cryptosporidium* oocysts (i.e., bioparticles), for which particle destabilization is essential for removal. The overall conclusions from this study are:

1. Removals ranging from 0.097- to 3-log of MPs (from 1 to 500  $\mu\text{m}$  in size) have been reported for conventional CFS at bench-scale;
2. Like other particles, MPs are destabilized by (i) adsorption and charge neutralization and (ii) enmeshment in precipitate (i.e., sometimes referred to as sweep flocculation) mechanisms during coagulation;
3. When particle destabilization is maximized, the potential for MPs removal by CFS is maximized after coagulation with metal salts and—by well-recognized theory-based extension—physico-chemical filtration;
4. Consistent with theory and practice regarding particle removal by CFS more broadly, enmeshment in precipitate is especially effective for MPs destabilization and subsequent removal by flocculation and sedimentation;
5. The efficiency of spherical colloidal MPs removal by well-operated CFS (i.e., with optimal particle destabilization during coagulation) increases with particle size and aligns with gravitational settling theory and practice;
6. Differences in pristine and weathered MPs removal by CFS can be statistically significant when particle destabilization by coagulant addition is adsorption and charge neutralization, though they are less than 0.5-log and not likely to be practically relevant;
7. Differences in pristine and weathered MPs removal by CFS are not significant when particle destabilization by coagulant addition is maximized (i.e., destabilization by enmeshment in precipitate/sweep flocculation).

## 5.2 Implications

This work has several implications for the management of public health risks attributable to MPs in drinking water supplies. Key implications stemming from this work are:

1. Reported spherical MPs particulate contaminant removals by various types and scales of water treatment at a range of operating conditions are highly variable. These observations are consistent with those that have been observed for other particulate contaminants such as the parasitic protozoa *Cryptosporidium* spp. Like for the protozoa, the MPs data reported herein underscore the need to consider (i) handling of non-detects, (ii) random sampling error, (iii) imperfect and/or variable analytical recovery, (iv) operational conditions, and (v) relevance of performance indicators when evaluating MPs removal during drinking water treatment, and relevance of individual treatment process performance to overall health risk at plant scale. Advancements in risk management for parasitic protozoa can thus inform strategies for MPs risk management when MPs in water are evaluated using count methods.

To avoid bias, (i) non-detects should be reported as zero counts per sample volume (Chik et al., 2018), (ii) MPs enumeration should include at least 10 and up to approximately 300 MPs per sample to minimize measurement errors associated with random sampling and imperfect and/or variable analytical recovery (Emelko et al., 2008; 2010; Schmidt et al., 2010; Chik et al., 2018). Dynamic operational conditions and associated potential for deteriorated treatment during those periods (Emelko, 2001; Huck et al., 2001; Huck et al., 2002; Emelko et al., 2003; Emelko et al., 2005; Ballantyne et al., 2024) also should be recognized and reflected in risk management. Risk management should further consider whether common performance indicators (e.g., turbidity) that are proposed as surrogates for treatment of other target compounds (e.g., *Cryptosporidium* spp. oocysts, MPs) should be relied upon because they may not be sensitive enough for use in all operational scenarios (e.g., a filter effluent turbidity of 0.1 NTU is not a reliable indicator for achieving at least 3-log removal by granular media filtration) (Emelko et al., 2003; Emelko & Huck, 2004; Ballantyne et al., 2024). Finally, it should be underscored that individual treatment unit performance does not necessarily reflect plant-scale risk (de Brito Cruz et al., 2023);

2. It is generally understood that smaller colloidal and nano-sized particles can be removed to some extent by conventional CFS and subsequent physico-chemical filtration—this relationship was demonstrated herein for colloidal MPs by CFS in association with specific mechanisms of particle

stabilization ubiquitously relied upon for effective water treatment. Thus, if toxicologically warranted, a regulatory framework for MPs control can be developed based on their concentration and health-based treatment targets, including strategies suggested above (#2). Coagulation for particle destabilization—not just turbidity reduction—would likely be an essential component of the treatment process in situations where there is significant potential health risk from waterborne MPs. Particle destabilization is essential to maximizing particulate contaminant (i.e., including MPs) removal by chemical pre-treatment and—by extension—physico-chemical filtration (Chowdhury et al., 2024; Ballantyne et al., 2024).

Given that the zeta potentials of most pristine and weathered MPs in natural waters are -40 to -50 mV or closer to the PZC (i.e., like *Cryptosporidium* spp. oocysts and many other particulate contaminants), a zeta potential within approximately 5 mV of the PZC after coagulation (in filter influent streams) is a reasonable initial target based on this study as well as reported evaluations with protozoa, which are especially vulnerable to insufficient coagulant addition (Ballantyne et al., 2024). This should be confirmed across a range of source waters, including all combinations of low and high turbidity and NOM to provide mechanistic and operational insights for process optimization (consistent with the particle destabilization considerations described in Ballantyne et al., 2024). As zeta potential changes based on the quality of the matrix in which particulate contaminants (including MPs) are suspended (Amirtharajah, 1988), it should not be evaluated in ultrapure or other “non-natural” matrices for reasons other than relative comparison;

3. Coagulation, settling, and colloid filtration theories and a rich history of documented water treatment investigations demonstrate that larger (i.e., greater than 1  $\mu\text{m}$  in size) spherical particles (including MPs) are generally more readily removed by well-operated chemical pretreatment and physico-chemical filtration processes. Accordingly, it follows that the removal of smaller colloidal MPs (down to approximately 1  $\mu\text{m}$  in size) should be (i) generally indicative of an equal or greater extent of larger-sized MPs removal by these treatment processes and (ii) considered when evaluating treatment performance capabilities. Deviations in MPs shape, porosity, and specific gravity should be considered for case-specific risk management because they have the potential to impact particle removal by CFS processes. Critically, health endpoints must be developed so that the sufficiency of MPs removal during drinking water treatment and associated health risks can be meaningfully evaluated and managed; and

4. Differences in the removal of pristine and weathered MPs by CFS are not significant when particle destabilization by coagulant addition is maximized (i.e., zeta potential is within a few millivolts of the PZC, enmeshment in precipitate/sweep flocculation is the main mechanism of particle destabilization), as expected. This—coupled with the widely reported zeta potentials of MPs in natural waters that are similar to those of other particulate contaminants like *Cryptosporidium* spp. oocysts, suggests that weathering does not likely affect MPs removal by CFS when particle destabilization by coagulant addition is maximized.

# Letter of copyright permission

For figure 2.2



## MEMORANDUM

To: Dana Herriman, University of Waterloo

From: Julia Dinmore

Date: August 19, 2024

Re: Copyright permission request

The Water Research Foundation is pleased to grant you permission to reprint Figure 1-4 from The Water Research Foundation's report, *Filtration Process Control for Pathogen Removal & Climate Change Adaptation* (5110).

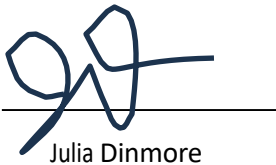
This one-time royalty-free permission is for use in Alice Gomes's forthcoming master's thesis. Please add the following source line under the tables and figures from our report:

Source: Ballantyne, et al. 2024 Reprinted with permission. © The Water Research Foundation. In

addition, the following full reference list entry should appear at the conclusion of your article:

Ballantyne, L., M. B. Emelko, W. B. Anderson, N. Ruecker, A. Anvari, E. Batista, and K. De Silva. 2024. *Filtration Process Control for Pathogen Removal & Climate Change Adaptation*. Project 5110. Denver, CO: The Water Research Foundation.

We appreciate your diligence in obtaining permission to use these copyrighted materials.



Julia Dinmore

Content Lead

8/19/24

Date

**For figure 2.3**

ELSEVIER ORDER DETAILS Oct 18, 2024

This Agreement between Alice Stephanie Gomes ("You") and Elsevier ("Elsevier") consists of your order details and the terms and conditions provided by Elsevier and Copyright Clearance Center.

Order Number 501940455

Order date Oct 18, 2024

Licensed Content Publisher Elsevier

Licensed Content Publication Advances in Colloid and Interface Science Licensed Content Title  
Coagulation by hydrolysing metal salts

Licensed Content Author Jinming Duan,John Gregory

Licensed Content Date 28 February 2003

Licensed Content Volume 100

Licensed Content Issue n/a

Licensed Content Pages 28

Start Page 475

End Page 502

Type of Use reuse in a thesis/dissertation

Portion figures/tables/illustrations Number of figures/tables/illustrations 1

Format electronic

Are you the author of this Elsevier

article? No

Will you be translating? No

Title of new work

Removal of microplastics during drinking water treatment: Linking theory to practice to advance risk management

Institution name: University of Waterloo

Expected presentation date Oct 2024

Order reference number 20996674

Figure 5. Deposition of metal hydroxide species

Portions

The Requesting Person / Organization to Appear on the License

Requestor Location

on oppositely-charged particles, showing charge neutralisation and charge reversal. (After Dentel w36x.)

Alice Stephanie Gomes Alice Gomes

Waterloo, ON N2L 3G1 Canada

Attn: Alice Gomes

Publisher Tax ID GB 494 6272 12

Billing Type Invoice

Billing Address

Alice Gomes

Waterloo, ON N2L 3G1 Canada

Attn: Alice Gomes

Total 0.00 USD

**For Figure 2.5**

JOHN WILEY AND SONS LICENSE  
TERMS AND CONDITIONS

Aug 13, 2024

---

This Agreement between Alice Stephanie Gomes ("You") and John Wiley and Sons ("John Wiley and Sons") consists of your license details and the terms and conditions provided by John Wiley and Sons and Copyright Clearance Center.

License Number 5847360977975

License date Aug 13, 2024

Licensed Content Publisher John Wiley and  
Sons Licensed Content Publication Wiley  
Books

Licensed Content Title MWH's Water Treatment: Principles and Design, 3rd  
Edition

Licensed Content Author David W. Hand George Tchobanoglous John C. Crittenden  
Kerry J. Howe R. Rhodes Trussell

Licensed Content Date Jun 1,  
2012 Licensed Content Pages 1

Type of use Dissertation/Thesis

Requestor type University/Academic

Format Electronic

Portion Figure/table

N Number of figures/tables 1

Will you be translating? No

Title of new work

R  
e  
m                      oval of microplastics during drinking water treatment:  
Linking theory to practice to advance risk  
management

Institution name                      University of Waterloo  
Expected presentation date        Sep 2024  
Order reference number            20996674

Portio  
ns                      Figure 9-11 on page 564, Solubility diagram for (a) Al(III) and (b)  
Fe(III) at 25° C. and (b) iron. (Adapted from Amirtharajah and  
Mills, 1982)

The Requesting Person /  
Organization to Appear on the  
License                      Alice Stephanie Gomes

Requestor  
Location                      Alice Gomes  
  
Waterloo, ON N2L 3G1  
Canada  
Attn: Alice Gomes

Publisher Tax ID  
  
EU826007151

Total  
  
0.00 CA

**For Figure 2.7**

JOHN WILEY AND SONS LICENSE TERMS AND CONDITIONS

Aug 13, 2024

This Agreement between Alice Stephanie Gomes ("You") and John Wiley and Sons ("John Wiley and Sons") consists of your license details and the terms and conditions provided by John Wiley and Sons and Copyright Clearance Center.

License Number 5847370944788

License date Aug 13, 2024 Licensed Content Publisher John Wiley and Sons Licensed Content Publication Journal AWWA

Licensed Content Title Stoichiometry of Coagulation Licensed Content Author Charles R. O'Melia, Werner Stumm Licensed Content Date May 1, 1968

Licensed Content Volume 60

Licensed Content Issue 5

Licensed Content Pages 26

Type of use Dissertation/Thesis

Requestor type University/Academic

Format Print and electronic

Portion Figure/table

Number of figures/tables 1

Will you be translating? No

Title of new work

Removal of Microplastics during Drinking Water Treatment: Linking theory in practice to inform Risk Management

Institution name University of Waterloo Expected presentation date Sep 2024

Order reference number 20996674

Portions      Figure 4. Schematic coagulation curves

The Requesting Person / Organization to Appear on the License

Alice Stephanie Gomes

Requestor Location

Alice Gomes

Waterloo, ON N2L 3G1 Canada

Attn: Alice Gomes

Publisher Tax IDEU826007151

Total    0.00 CAD

## References

- Abbaszadegan, M., Manteiga, R., Bell, K., & LeChevallier, M. (1997). Enhanced coagulation for removal of microbial contaminants. In Proceedings of the *American Water Works Association Water Quality Technology Conference*, Denver, CO, November 1997.
- Abu-Orf, M., Tchobanoglous, G., & Stensel, H. D. (2013). *Wastewater engineering: Treatment and resource recovery*. McGraw-Hill Education.
- Ahmad, M., Chen, J., Khan, M. T., Yu, Q., Phairuang, W., Furuuchi, M., Ali, S. W., Nawab, A., & Panyametheekul, S. (2023). Sources, analysis, and health implications of atmospheric microplastics. *Emerging Contaminants*, 9(3), 100233.  
<https://doi.org/10.1016/j.emcon.2023.100233>
- Alessio, P., Dunne, T., & Morell, K. (2021). Post-wildfire generation of debris-flow slurry by rill erosion on colluvial hillslopes. *Journal of Geophysical Research: Earth Surface*, 126 (11), e2021JF006108.  
<https://doi.org/10.1029/2021JF006108>
- Alioua, W., & Lapointe, M. (2023). Fiber-based super-bridging agents enable efficient contaminant removal via settling and screening: Impact on microplastics, textile fibers, and turbidity. *Environmental Science & Technology*, 57(15), 6528-6538.  
<https://doi.org/10.1016/j.jece.2023.110195>
- Allen, S., Allen, D., Phoenix, V.R., Le Roux, G., Durántez Jiménez, P., Simonneau, A., & Galop, D. (2019). Atmospheric transport and deposition of microplastics in a remote mountain catchment. *Nature Geoscience*, 12(5), 339–344. <https://doi.org/10.1038/s41561-019-0335-5>.
- Amburgey, J.E., Amirtharajah, A., York, M.T., Brouckaert, B.M., Spivey, N.C., & Arrowood, M.J. (2005). Comparison of conventional and biological filter performance for *Cryptosporidium* and microsphere removal. *Journal of American Water Works Association*, 97, 77-91.
- Amirtharajah, A. (1988). Some theoretical and conceptual views of filtration. *Journal of American Water Works Association*, 80(12), 36-46.
- Amirtharajah, A., & Mills, K. M. (1982). Rapid-mix design for mechanisms of alum coagulation. *Journal of American Water Works Association*, 74(4), 210-216. <https://doi.org/10.1002/j.1551-8833.1982.tb04890.x>

- Amirtharajah, A., & O'Melia, C. R. (1990). Coagulation processes: Destabilization, mixing, and flocculation. In J. O. Leckie (Ed.), *Water quality and treatment: A handbook of community water supplies* (4th ed., pp. 269–365). McGraw-Hill.
- Anderson, P.J., Warrack, S., Langen, V., Challis, J.K., Hanson, M.L., & Rennie, M.D. (2017). Microplastic contamination in Lake Winnipeg, Canada. *Environmental Pollution*, 225, 223-231. <https://doi.org/10.1016/j.envpol.2017.02.072>.
- Assavasilavasukul, P., Lau, B. L., Harrington, G. W., Hoffman, R. M., & Borchardt, M. A. (2008). Effect of pathogen concentrations on removal of *Cryptosporidium* and *Giardia* by conventional drinking water treatment. *Water Research*, 2678-2690. <https://doi.org/10.1016/j.watres.2008.01.021>
- Bache, D. H., Johnson, C., Papavasiliopoulos, E., Rasool, E., & McGilligan, F. J. (1999). Sweep coagulation: structures, mechanisms and practice. *Journal of Water Supply: Research and Technology–Aqua*, 48(5), 201-210. <https://doi.org/10.2166/aqua.1999.0022>
- Bakir, A., Rowland, S. J., & Thompson, R. C. (2014). Enhanced desorption of persistent organic pollutants from microplastics under simulated physiological conditions. *Environmental Pollution*, 185, 16-23. <https://doi.org/10.1016/j.envpol.2013.10.007>
- Ballantyne, L., M.B. Emelko, W.B. Anderson, and N.J. Ruecker, 2024. Filtration Process Control for Pathogen Removal & Climate Change Adaptation. *Water Research Foundation (WRF) Tailored Collaboration Project 5110*, Denver, CO. <https://www.waterrf.org/research/projects/filtration-process-control-pathogen-removal-and-climate-change-adaptation>
- Barboza, L. G. A., Vethaak, A. D., Lavorante, B., Lundebye, A. K., & Guilhermino, L. (2018). Marine microplastic debris: An emerging issue for food security, food safety and human health. *Marine Pollution Bulletin*, 133, 336–348. <https://doi.org/10.1016/j.marpolbul.2018.05.047>
- Batch, L. F., Schulz, C. R., & Linden, K. G. (2004). Evaluating water quality effects on UV disinfection of MS2 coliphage. *Journal of American Water Works Association*, 96(7), 75-87.
- Baudin, I., & Laine, J. M. (1998). Assessment and optimization of clarification process for *Cryptosporidium* removal. In Proceedings of the American Water Works Association Water Quality Technology Conference. Denver, CO: American Water Works Association.

- Bauer-Civiello, A., Critchell, K., Hoogenboom, M., & Hamann, M. (2019). Input of plastic debris in an urban tropical river system. *Marine Pollution Bulletin*, *144*, 235-242. <https://doi.org/10.1016/j.marpolbul.2019.04.070>.
- Bean, E., Campbell, S., Anspach, F. R., Ockershausen, R. W., & Peterman, C. J. (1964). Zeta potential measurements in the control of coagulation chemical doses. *Journal of American Water Works Association*, *56*(2), 214-227. <https://doi.org/10.1002/j.1551-8833.1964.tb01202.x>
- Beckett, R., & Le, N. P. (1990). The role of organic matter and ionic composition in determining the surface charge of suspended particles in natural waters. *Colloids and Surfaces*, *44*, 35-49. [https://doi.org/10.1016/0166-6622\(90\)80185-7](https://doi.org/10.1016/0166-6622(90)80185-7)
- Bergmann, M., Mützel, S., Primpke, S., Tekman, M. B., Trachsel, J., & Gerdt, G. (2019). White and wonderful? Microplastics prevail in snow from the Alps to the Arctic. *Environmental Science & Technology*, *51*, 11000-11010. <https://doi.org/10.1021/acs.est.7b03331>
- Bina, B., Mehdinejad, M. H., Nikaeen, M., & Movahedian Attar, H. (2009). Effectiveness of chitosan as natural coagulant aid in treating turbid water. *Iranian Journal of Environmental Health Science and Engineering*, *6*, 247-252.
- Blackburn, E. A., Dickson-Anderson, S. E., Anderson, W. B., & Emelko, M. B. (2023). Biological filtration is resilient to wildfire ash-associated organic carbon threats to drinking water treatment. *ACS Environment Science & Technology, Water*, *3*(3), 639-649. <https://doi.org/10.1021/acsestwater.2c00209>
- Blackburn, E. A., Emelko, M. B., Dickson-Anderson, S., & Stone, M. (2021). Advancing on the promises of techno-ecological nature-based solutions: A framework for green technology in water supply and treatment. *Blue-Green Systems*, *3*(1), 81-94. <https://doi.org/10.2166/bgs.2021.008>
- Bouwmeester, H., Hollman, P. C. H., & Peters, R. J. B. (2015). Potential health impact of environmentally released micro- and nanoplastics in the human food production chain: Experiences from nanotoxicology. *Environmental Science & Technology*, *49*(15), 8932-8947. <https://doi.org/10.1021/acs.est.5b01090>
- Bratby, J. (1980). Coagulation and flocculation - with an emphasis on water and wastewater treatment. Uplands: Croydon, England. [http://refhub.elsevier.com/S0048-9697\(22\)06196-4/rf202209270655521604](http://refhub.elsevier.com/S0048-9697(22)06196-4/rf202209270655521604)

- Brown, T. J., & Emelko, M. (2009). Chitosan and metal salt coagulant impacts on *Cryptosporidium* and microsphere removal by filtration. *Water Research*, 43, 331-338.  
<https://doi.org/10.1016/j.watres.2008.10.035>
- Browne, M. A., Crump, P., Niven, S. J., Teuten, E., Tonkin, A., Galloway, T., & Thompson, R. (2011). Accumulation of microplastic on shorelines worldwide: Sources and sinks. *Environmental Science & Technology*, 45(21), 9175-9179. <https://doi.org/10.1021/es201811s>
- Cai, H., Wang, Y., Wu, K., & Guo, W. (2020). Enhanced hydrophilic and electrophilic properties of polyvinyl chloride (PVC) biofilm carrier. *Polymers (Basel)*, 12(6), 1240.  
<https://doi.org/10.3390/POLYM12061240>.
- California State Water Resources Control Board. (2020). *Microplastics*.  
[https://www.waterboards.ca.gov/drinking\\_water/certlic/drinkingwater/microplastics.html](https://www.waterboards.ca.gov/drinking_water/certlic/drinkingwater/microplastics.html)
- Campanale, C., Massarelli, C., Savino, I., Locaputo, V., & Uricchio, V. F. (2020). A detailed review study on potential effects of microplastics and additives of concern on human health. *International Journal of Environmental Research and Public Health*, 17(4), 1212.  
<https://doi.org/10.3390/ijerph17041212>
- Casagrande, N., Verones, F., Sobral, P., & Martinho, G. (2024). Physical properties of microplastics affecting the aquatic biota: A review. *Environmental Advances*, 100566.  
<https://doi.org/10.1016/j.envadv.2024.100566>
- Cesa, F. S., Turra, A., & Baruque-Ramos, J. (2017). Synthetic fibers as microplastics in the marine environment: a review from textile perspective with a focus on domestic washings. *Science of the Total Environment*, 598, 1116-1129. <https://doi.org/10.1016/j.scitotenv.2017.04.172>
- Chang, M., Sun, P., Zhang, L., Liu, Y., Chen, L., Ren, H., & Wu, B. (2024). Changes in characteristics and risk of freshwater microplastics under global warming. *Water Research*, 121960.  
<https://doi.org/10.1016/j.watres.2024.121960>
- Chen, Z., Zhao, W., Xing, R., Xie, S., Yang, X., Cui, P., Lü, J., Liao, H., Yu, Z., Wang, S., & Zhou, S. (2020). Enhanced in situ biodegradation of microplastics in sewage sludge using hyperthermophilic composting technology. *Journal of Hazardous Materials*, 384, 121271.  
<https://doi.org/10.1016/j.jhazmat.2019.121271>

- Chik, A. H. S., Schmidt, P. J., & Emelko, M. B. (2018). Learning something from nothing: the critical importance of rethinking microbial non-detects. *Frontiers in Microbiology*, 9, 2304. <https://doi.org/10.3389/fmicb.2018.02304>
- Chowdhury, O. S. (2021). Evaluation of Potential Health Risks from Microplastics in Drinking Water. MASc thesis. Waterloo: University of Waterloo. <http://hdl.handle.net/10012/16941>
- Chowdhury, O. S., Schmidt, P. J., Anderson, W. B., & Emelko, M. B. (2024). Advancing evaluation of microplastics thresholds to inform water treatment needs and risks. *Environment & Health*. <https://doi.org/10.1021/envhealth.3c00174>
- Chuang, S. H., Chang, T. C., Ouyang, C. F., & Leu, J. M. (2007). Colloidal silica removal in coagulation processes for wastewater reuse in a high-tech industrial park. *Water Science and Technology: a journal of the International Association on Water Pollution Research*, 55(1-2), 187-195. <https://doi.org/10.2166/wst.2007.054>
- Crittenden, J. C., Trussell, R. R., Hand, D. W., Howe, K. J., & Tchobanoglous, G. (2012). *MWH's Water Treatment Principles and Design*. New Jersey: John Wiley & Sons. <https://doi.org/10.1002/9781118131473>
- Dai, X., & Hozalski, R. M. (2003). Evaluation of microspheres as surrogates for *Cryptosporidium parvum* oocysts in filtration experiments. *Environmental Science & Technology*, 37(5), 1037-1042. <https://doi.org/10.1021/es025521w>
- Darby, J. L., & Lawler, D. F. (1990). Ripening in depth filtration: Effect of particle size on removal and head loss. *Environmental Science & Technology*, 24(7), 1069-1079. <https://doi.org/10.1021/es00077a018>
- de Brito Cruz, D., Brown, T. J., Jin, C., Kundert, K. L., Ruecker, N. J., Ballantyne, L., Schmidt, P. J., Anderson, W.B., & Emelko, M. B. (2023). Filter operation effects on plant-scale microbial risk: Opportunities for enhanced treatment performance. *Journal of American Water Works Association Water Science*, 5(5), e1357. <https://doi.org/10.1002/aws2.1357>
- de Sá, L. C., Oliveira, M., Ribeiro, F., Rocha, T. L., & Futter, M. N. (2018). Studies of the effects of microplastics on aquatic organisms: What do we know and where should we focus our efforts in the future? *Science of the Total Environment*, 645, 1029-1039. <https://doi.org/10.1016/j.scitotenv.2018.07.207>

- Deng, Y., Zhang, Y., Lemos, B., & Ren, H. (2017). Tissue accumulation of microplastics in mice and biomarker responses suggest widespread health risks of exposure. *Scientific Reports*, 7(1), 46687. <https://doi.org/10.1038/srep46687>
- Di, M., & Wang, J. (2018). Microplastics in surface waters and sediments of the three gorges reservoir, China. *Science of the Total Environment*, 616-617, 1620-1627. <https://doi.org/10.1016/j.scitotenv.2017.10.150>
- Dong, Z., Qiu, Y., Zhang, W., Yang, Z., & Wei, L. (2018). Size-dependent transport and retention of micron-sized plastic spheres in natural sand saturated with seawater. *Water Research*, 143, 518-526. <https://doi.org/10.1016/j.watres.2018.07.007>
- Dris, R., Gasperi, J., Rocher, V., Saad, M., Renault, N., & Tassin, B. (2015). Microplastic contamination in an urban area: A case study in Greater Paris. *Environmental Chemistry*, 12(5). <https://doi.org/10.1071/EN14167>
- Duan, J. (1997). Influence of dissolved silica on flocculation of clay suspensions with hydrolysing metal salts. Doctoral dissertation, University College London, University of London, United Kingdom.
- Duan, J., & Gregory, J. (2003). Coagulation by hydrolysing metal salts. *Advances in Colloid and Interface Science*, 100–102, 475-502. [https://doi.org/10.1016/s0001-8686\(02\)00067-2](https://doi.org/10.1016/s0001-8686(02)00067-2)
- Duan, J., Wang, J., Guo, T., & Gregory, J. (2014). Zeta potentials and sizes of aluminum salt precipitates—effect of anions and organics and implications for coagulation mechanisms. *Journal of Water Process Engineering*, 4, 224-232. <https://doi.org/10.1016/j.jwpe.2014.10.008>
- Dugan, N. R., Fox, K. R., Owens, J. H., & Miltner, R. J. (2001). Controlling *Cryptosporidium* oocysts using conventional treatment. *Journal of American Water Works Association*, 93(12), 64-76. <https://doi.org/10.1002/j.1551-8833.2001.tb09356.x>
- Edzwald, J. K. (1993). Coagulation in drinking water treatment: particles, organics and coagulants. *Water Science & Technology*, 27(11), 21-35. <https://doi.org/10.2166/wst.1993.0261>
- Elimelech, M., Gregory, J., Jia, X., & Williams, R. (1995). *Particle deposition & aggregation: Measurement, modelling and simulation*. Butterworth-Heinemann Ltd. <https://doi.org/10.1016/B978-0-7506-7024-1.X5000-6>

- Emelko MB, Schmidt PJ, Borchardt MA. (2019). Confirming the need for virus disinfection in municipal subsurface drinking water supplies. *Water Research*, 157, 356-364.  
<https://doi.org/10.1016/j.watres.2019.03.057>
- Emelko, M. B. (2001). Removal of *Cryptosporidium parvum* by granular media filtration. Waterloo: University of Waterloo. Doctoral thesis. <http://hdl.handle.net/10012/614>
- Emelko, M. B. (2003). Removal of viable and inactivated *Cryptosporidium* by dual- and tri-media filtration. *Water Research*, 37(12), 2998-3008. [https://doi.org/10.1016/S0043-1354\(03\)00113-1](https://doi.org/10.1016/S0043-1354(03)00113-1)
- Emelko, M. B., & Huck, P. M. (2004). Microspheres as surrogates for *Cryptosporidium* filtration. *Journal of American Water Works Association*, 96(3), 94-105. <https://doi.org/10.1002/j.1551-8833.2004.tb10577.x>
- Emelko, M. B., Huck, P. M., & Douglas, I. P. (2003). *Cryptosporidium* and microsphere removal during late in-cycle filtration. *Journal of American Water Works Association*, 95(5), 173–182.  
<https://doi.org/10.1002/j.1551-8833.2003.tb10371.x>
- Emelko, M. B., Huck, P. M., Coffey, B. M. (2005). A review of *Cryptosporidium* removal by granular media filtration. *Journal of American Water Works Association*, 97(12), 101–115.
- Emelko, M. B., Schmidt, P. J., & Reilly, P. M. (2010). Particle and microorganism enumeration data: enabling quantitative rigor and judicious interpretation. *Environmental Science & Technology*, 44(5), 1720-1727. <https://doi.org/10.1021/es902382a>
- Emelko, M. B., Schmidt, P. J., & Roberson, J. A. (2008). Quantification of uncertainty in microbial data—reporting and regulatory implications. *Journal of American Water Works Association*, 100(3), 94-104. <https://doi.org/10.1002/j.1551-8833.2008.tb09584.x>
- Emelko, M. B., Silins, U., Bladon, K. D., & Stone, M. (2011). Implications of land disturbance on drinking water treatability in a changing climate: Demonstrating the need for “source water supply and protection” strategies. *Water Research*, 45(2), 461-472.  
<https://doi.org/10.1016/j.watres.2010.08.051>
- Emelko, M. B., Stone, M., Silins, U., Allin, D., Collins, A. L., Williams, C. H., Martens, A. M., & Bladon, K. D. (2016). Sediment-phosphorus dynamics can shift aquatic ecology and cause downstream legacy effects after wildfire in large river systems. *Global Change Biology*, 22(3), 1168-1184.  
<https://doi.org/10.1111/gcb.13073>

- Emelko, M., & Sham, C. H. (2014). Wildfire impacts on water supplies and the potential for mitigation: Workshop Report. *Water Research Foundation (WRF), Web Report #4529*.  
<https://coilink.org/20.500.12592/n93hfw>
- Emelko, M.B., Schmidt, P.J., & Borchardt, M.A. (2019). Confirming the need for virus disinfection in municipal subsurface drinking water supplies. *Water Research*, 157, 356-364.  
<https://doi.org/10.1016/j.watres.2019.03.057>
- Emmerton, C.A., Cooke, C.A., Hustins, S., Silins, U., Emelko, M.B., Lewis, T., Kruk, M.K., Taube, N., Zhu, D., Jackson, B. and Stone, M. (2020). Severe western Canadian wildfire affects water quality even at large basin scales. *Water Research*, 183, 116071. <https://doi.org/10.1016/j.watres.2020.116071>
- Environment Canada. (1999). *Canadian Environmental Protection Act, 1999*. Government of Canada.  
<https://laws.justice.gc.ca/eng/acts/C-15.31/FullText.html>
- Environment Canada. (2015). *Microbeads – A Science Summary July 2015* (pp. 1-34). Government of Canada. <https://www.canada.ca/en/environment-climate-change/services/evaluating-existing-substances/microbeads-science-summary.html>
- Fahrenfeld, N. L., Arbuckle-Keil, G., Naderi Beni, N., & Bartelt-Hunt, S. L. (2019). Source tracking microplastics in the freshwater environment. *Trends in Analytical Chemistry*, 112, 248-254.  
<https://doi.org/10.1016/j.trac.2018.11.030>
- Fang, Q., Niu, S., & Yu, J. (2021). Characterising microplastic pollution in sediments from urban water systems using the diversity index. *Journal of Cleaner Production*, 318, 128537.  
<https://doi.org/10.1016/j.jclepro.2021.128537>
- Feder, P. I., Ma, Z. J., Bull, R. J., Teuschler, L. K., & Rice, G. (2009). Evaluating sufficient similarity for drinking-water disinfection by-product (DBP) mixtures with bootstrap hypothesis test procedures. *Journal of Toxicology and Environmental Health, Part A*, 72(7), 494-504.  
<https://doi.org/10.1080/15287390802608981>
- Feldman, D. (2002). Polymer weathering: Photo-oxidation. *Journal of Polymers and the Environment*, 10(4), 163-173. <https://doi.org/10.1023/A:1021148205366>
- Fox, K. R., Dugan, N., Miltner, R., Lytle, D. A., Williams, D., Parrett, C., Feld, C., Owens, J., Rice, E. W., & Johnson, C. H. (1998). Comparative removal of *Cryptosporidium* and surrogates in a low flow

- pilot plant system. In *Proceedings of the American Water Works Association Water Quality Technology Conference*, San Diego, CA, November 1998.
- Free, C. M., Jensen, O. P., Mason, S. A., Eriksen, M., Williamson, N. J., & Boldgiv, B. (2014). High levels of microplastic pollution in a large, remote, mountain lake. *Marine Pollution Bulletin*, *85*, 156-163. <https://doi.org/10.1016/j.marpolbul.2014.06.001>
- Gewert, B., Plassmann, M. M., & MacLeod, M. (2015). Pathways for degradation of plastic polymers floating in the marine environment. *Environmental Science: Processes & Impacts*, *17*(9), 1513-1521. <https://doi.org/10.1039/C5EM00207A>
- Government of Alberta. (2012) Standards and guidelines for municipal waterworks, wastewater and storm drainage systems. *Environment and Sustainable Resource Development*.
- Government of Canada. (2022). *Metals of concern*. <https://www.rcaanc-cirnac.gc.ca/eng/1663270886550/1663270938204>
- Green, D. S., Kregting, L., Boots, B., Blockley, D. J., Brickle, P., da Costa, M., & Crowley, Q. (2018). A comparison of sampling methods for seawater microplastics and a first report of the microplastic litter in coastal waters of Ascension and Falkland Islands. *Marine Pollution Bulletin*, *137*, 695-701. <https://doi.org/10.1016/j.marpolbul.2018.11.004>
- Gregory, J. (1973). Rate of flocculation of latex particles by cationic polymers. *Journal of Colloid and Interface Science*, *42* (2), 448-456. [https://doi.org/10.1016/0021-9797\(73\)90311-1](https://doi.org/10.1016/0021-9797(73)90311-1)
- Gregory, J. (1976). The effect of cationic polymers on the colloidal stability of latex particles. *Journal of Colloid and Interface Science*, *55*, 35-44. [https://doi.org/10.1016/0021-9797\(76\)90006-0](https://doi.org/10.1016/0021-9797(76)90006-0)
- Gronewold, A. D., Borsuk, M. E., Wolpert, R. L., & Reckhow, K. H. (2008). An assessment of fecal indicator bacteria-based water quality standards. *Environmental Science & Technology*, *42*, 13, 4676-4682. <https://doi.org/10.1021/es703144k>
- Guo, X., & Wang, J. (2019). The chemical behaviors of microplastics in marine environment: A review. *Marine pollution bulletin*, *142*, 1-14. <https://doi.org/10.1016/j.marpolbul.2019.03.019>
- Gupta, V. S., Bhattacharjya, S. K., & Dutta, B. K. (1975). Zeta-potential control for alum coagulation. *Journal of American Water Works Association*, *67*(1), 21-23. <https://doi.org/10.1002/j.1551-8833.1975.tb02145.x> <https://www.jstor.org/stable/41267739>

- Gustine, R. N., Hanan, E. J., Robichaud, P. R., & Elliot, W. J. (2022). From burned slopes to streams: how wildfire affects nitrogen cycling and retention in forests and fire-prone watersheds. *Biogeochemistry*, 157(1), 51-68. <https://doi.org/10.1007/s10533-021-00861-0>
- Haas, C. N., Crockett, C. S., Rose, J. B., Gerba, C. P., & Fazil, A. M. (1996). Assessing the risk posed by oocysts in drinking water. *Journal of American Water Works Association*, 88(9), 131. <https://proxy.lib.uwaterloo.ca/login?url=https://www.proquest.com/scholarly-journals/assessing-risk-posed-oocysts-drinking-water/docview/221533104/se-2>
- Habibian, M. T., & O'Melia, C. R. (1975). Particles, polymers, and performance in filtration. *Journal of the Environmental Engineering Division*, 101(4), 567-583. <https://doi.org/10.1061/JEEGAV.0000376>
- Hach Company, Hach Method 10133 - Determination of Turbidity by Laser Nephelometry, 2005.
- Han, N., Zhao, Q., Ao, H., Hu, H., & Wu, C. (2022). Horizontal transport of macro- and microplastics on soil surface by rainfall induced surface runoff as affected by vegetations. *Science of the Total Environment*, 831, 154989. <https://doi.org/10.1016/j.scitotenv.2022.154989>
- Haque, F., & Fan, C. (2023). Fate of microplastics under the influence of climate change. *iScience*. <https://doi.org/10.1016/j.isci.2023.107649>
- Harrington, G. W., Xagorarakis, I., Assavasilavasukul, P., & Standridge, J. H. (2003). Effect of filtration conditions on removal of emerging waterborne pathogens. *Journal of American Water Works Association*, 95(12), 95-104. <https://doi.org/10.1002/j.1551-8833.2003.tb10514.x>
- Hashimoto, A., Hirata, T., & Kunikane, S. (2001). Occurrence of *Cryptosporidium* oocysts and *Giardia* cysts in a conventional water purification plant. *Water, Science & Technology*, 43(12), 89-92. <https://doi.org/10.2166/wst.2001.0717>
- He, D., Luo, Y., Lu, S., Liu, M., Song, Y., & Lei, L. (2018). Microplastics in soils: Analytical methods, pollution characteristics and ecological risks. *Trends in Analytical Chemistry*, 109, 163-172. <https://doi.org/10.1016/j.trac.2018.10.006>
- He, L., Ji, L., Sun, X., Chen, S., & Kuang, S. (2022). Investigation of mini-hydrocyclone performance in removing small-size microplastics. *Particuology*, 71, 1-10. <https://doi.org/10.1016/j.partic.2022.01.011>
- Health Canada. (2012). Guidelines for Canadian Drinking Water Quality Summary Table Prepared by the Federal-Provincial-Territorial

- Committee on Drinking Water of the Federal-Provincial-Territorial Committee on Health and the Environment March 2006. *Environments* 1-16.
- Health Canada (2016). *Enteric Protozoa in Drinking Water: Giardia and Cryptosporidium – Document for Public Consultation*. Federal-Provincial-Territorial Committee on Drinking Water, Health Canada. Ottawa, Ontario. <https://www.canada.ca/en/health-canada/programs/enteric-protozoa-drinking-water/consultation-document.html>
- Health Canada. (2019). Guidelines for Canadian drinking water quality: Guideline technical document – Enteric protozoa: *Giardia* and *Cryptosporidium*. Water and Air Quality Bureau, Healthy Environments and Consumer Safety Branch, Health Canada, Ottawa, Ontario. (Catalogue No. H144-13/10-2018EPDF). <https://www.canada.ca/content/dam/hc-sc/documents/services/environmental-workplace-health/reports-publications/water-quality/enteric-protozoa-giardia-cryptosporidium/pub1-eng.pdf>
- Health Canada. (2022). *Guidance on waterborne pathogens in drinking water*. <https://www.canada.ca/en/health-canada/services/environmental-workplace-health/reports-publications/water-quality/guidance-waterborne-pathogens-drinking-water.html>
- Health Canada. (2024). *Guidelines for Canadian drinking water quality summary table*. Retrieved from [https://www.canada.ca/content/dam/hc-sc/migration/hc-sc/ewh-semt/alt\\_formats/pdf/pubs/water-eau/sum\\_guide-res\\_recom/summary-tables-eng-2024-02.pdf](https://www.canada.ca/content/dam/hc-sc/migration/hc-sc/ewh-semt/alt_formats/pdf/pubs/water-eau/sum_guide-res_recom/summary-tables-eng-2024-02.pdf)
- Health Canada. (2024). *Guidelines for Canadian drinking water quality summary table*. Retrieved from [https://www.canada.ca/content/dam/hc-sc/migration/hc-sc/ewh-semt/alt\\_formats/pdf/pubs/water-eau/sum\\_guide-res\\_recom/summary-tables-eng-2024-02.pdf](https://www.canada.ca/content/dam/hc-sc/migration/hc-sc/ewh-semt/alt_formats/pdf/pubs/water-eau/sum_guide-res_recom/summary-tables-eng-2024-02.pdf)
- Hidalgo-Ruz, V., Gutow, L., Thompson, R. C., & Thiel, M. (2012). Microplastics in the marine environment: a review of the methods used for identification and quantification. *Environmental Science & Technology*, 46(6), 3060-3075. <https://doi.org/10.1021/es2031505>
- Hijnen, W. A. M., & Medema, G. J. (2010). *Elimination of micro-organisms by drinking water treatment processes: A review*. IWA Publishing. <https://doi.org/10.2166/9781780401584>

- Holmes, L. A., Turner, A., & Thompson, R. C. (2012). Adsorption of trace metals to plastic resin pellets in the marine environment. *Environmental Pollution*, *160*, 42-48.  
<https://doi.org/10.1016/j.envpol.2011.08.052>
- Hou, J., Xu, X., Lan, L., Miao, L., Xu, Y., You, G., & Liu, Z. (2020). Transport behavior of micro polyethylene particles in saturated quartz sand: Impacts of input concentration and physicochemical factors. *Environmental Pollution*, *263*, 114499. <https://doi.org/10.1016/j.envpol.2020.114499>
- Huck, P. M., Coffey, B. M., Emelko, M. B., & O'Melia, C. R. (2000). The importance of coagulation for the removal of *Cryptosporidium* and surrogates by filtration. In H. H. Hahn, E. Hoffmann, & H. Ødegaard (Eds.), *Chemical Water and Wastewater Treatment VI* (pp. 159-171). Springer.  
[https://doi.org/10.1007/978-3-642-59791-6\\_18](https://doi.org/10.1007/978-3-642-59791-6_18)
- Huck, P. M., Coffey, B. M., Emelko, M. B., Maurizio, D. D., Slawson, R. M., Anderson, W. B., Oever, J. V., Douglas, A. P., & O'Melia, C. R. (2002). Effects of filter operation on *Cryptosporidium* removal microbial pathogens. *Journal of American Water Works Association*, *94*(6), 97-111.
- Huck, P. M., Emelko, M. B., Coffey, B. M., Maurizio, D. D., & O'Melia, C. R. (2001). Filter operation effects on pathogen passage. *American Water Works Association Research Foundation*, Denver, CO, USA.
- Imhof, H. K., Laforsch, C., Wiesheu, A. C., Schmid, J., Anger, P. M., Niessner, R., & Ivleva, N. P. (2016). Pigments and plastic in limnetic ecosystems: A qualitative and quantitative study on microparticles of different size classes. *Water Research*, *98*, 64-74.  
<https://doi.org/10.1016/j.watres.2016.03.015>
- Ingram, A. G., Hoskins, J. H., Sovik, J. H., Maringer, R. E., & Holden, F. C. (1968). Study of microplastic properties and dimensional stability of materials. Technical Report AFMLTR-67-232, Part II. United States Air Force Materials Laboratory.  
<https://ntrl.ntis.gov/NTRL/dashboard/searchResults/titleDetail/AD838802.xhtml>
- Iñiguez, M. E., Conesa, J. A., & Fullana, A. (2018). Recyclability of four types of plastics exposed to UV irradiation in a marine environment. *Waste Management*, *79*, 339-345.  
<https://doi.org/10.1016/j.wasman.2018.08.006>
- ISO 13099-1. (2012). *Colloidal systems — Methods for zeta-potential determination — Part 1: Electroacoustic and electrokinetic phenomena*. International Organization for Standardization.  
<https://www.iso.org/standard/52807.html>

- Jiang, H., Luo, D., Wang, L., Zhang, Y., Wang, H., & Wang, C. (2023). A review of disposable facemasks during the COVID-19 pandemic: a focus on microplastics release. *Chemosphere*, *312*, 137178. <https://doi.org/10.1016/j.chemosphere.2022.137178>
- Jiang, H., Zhu, W., Ding, J., Zou, H., Zhang, S., & Razanajatovo, R. M. (2018). Interactive effects of polystyrene microplastics and roxithromycin on bioaccumulation and biochemical status in the freshwater fish red tilapia (*Oreochromis niloticus*). *Science of the Total Environment*, *648*, 1431-1439. <https://doi.org/10.1016/j.scitotenv.2018.08.266>
- Jiang, J.-Q. (2001). Development of coagulation theory and pre-polymerized coagulants for water treatment. *Separation and Purification Reviews*, *30*(1), 127-141. <https://doi.org/10.1081/SPM-100102986>
- Jin, C., Glawdel, T., Ren, C. L., & Emelko, M. B. (2015a). Non-linear, non-monotonic effect of nano-scale roughness on particle deposition in absence of an energy barrier: Experiments and modeling. *Scientific Reports*, *5*(1), 17747. <https://doi.org/10.1038/srep17747>
- Jin, C., Normani, S. D., & Emelko, M. B. (2015b). Surface roughness impacts on granular media filtration at favorable deposition conditions: experiments and modeling. *Environmental Science & Technology*, *49*(13), 7879-7888. <https://doi.org/10.1021/acs.est.5b01998>
- Jin, C., Ren, C. L., & Emelko, M. B. (2016). Concurrent modeling of hydrodynamics and interaction forces improves particle deposition predictions. *Environmental Science & Technology*, *50*(8), 4401-4412. <https://doi.org/10.1021/acs.est.6b00218>
- Jin, C., Zhao, W., Normani, S. D., Zhao, P., & Emelko, M. B. (2017). Synergies of media surface roughness and ionic strength on particle deposition during filtration. *Water research*, *114*, 286-295. <https://doi.org/10.1016/j.watres.2017.02.010>
- Katare, Y., Singh, P., Sankhla, M. S., Singhal, M., Jadhav, E. B., Parihar, K., Nikalje, B. T., Trpathi, A., & Bhardwaj, L. (2021). Microplastics in aquatic environments: sources, ecotoxicity, detection & remediation. *Biointerface Research in Applied Chemistry*, *12*, 3407-3428. <https://doi.org/10.33263/BRIAC123.34073428>
- Kelley, M. B., Warriar, P. K., Brokaw, J. K., Barrett, K. L., & Komisar, S. J. (1995). A study of two U.S. Army installation drinking water sources and treatment systems for the removal of *Giardia* and *Cryptosporidium*. In *Proceedings of the American Water Works Association Water Quality Technology Conference*. Denver, CO: American Water Works Association.

- Khan, M. T., Ahmad, M., Hossain, M. F., Nawab, A., Ahmad, I., Ahmad, K., & Panyametheekul, S. (2023). Microplastic removal by coagulation: A review of optimizing the reaction conditions and mechanisms. <https://doi.org/10.20517/wecn.2023.39>
- Khan, M. T., Cheng, Y. L., Hafeez, S., Tsang, Y. F., Yang, J., & Nawab, A. (2020). Microplastics in wastewater. In T. Rocha-Santos, M. Costa, & C. Mouneyrac (Eds.), *Handbook of Microplastics in the Environment*, 1-33. [https://doi.org/10.1007/978-3-030-10618-8\\_39-1](https://doi.org/10.1007/978-3-030-10618-8_39-1)
- Kim, S., Bowen, R. A., & Zare, R. N. (2015). Transforming plastic surfaces with electrophilic backbones from hydrophobic to hydrophilic. *ACS Applied Materials & Interfaces*, 7(4), 1925-1931. <https://doi.org/10.1021/am507606r>
- Kolska, Z., Makajova, Z., Kolarova, K., Kasalkova, N., Trostova, S., Reznickova, A., Siegel, J., & Svorcik, V. (2013). Electrokinetic potential and other surface properties of polymer foils and their modifications. *Polymer Science*, 4, 203-228. <https://doi.org/10.5772/46144>
- Kooi, M., Besseling, E., Kroeze, C., Van Wezel, A. P., & Koelmans, A. A. (2018). Modeling the fate and transport of plastic debris in freshwaters: review and guidance. *Freshwater microplastics: Emerging environmental contaminants?*, 125-152. [https://doi.org/10.1007/978-3-319-61615-5\\_14](https://doi.org/10.1007/978-3-319-61615-5_14)
- Lameiras, F. S., de Souza, A. L., de Melo, V. A. R., Nunes, E. H. M., & Braga, I. D. (2008). Measurement of the zeta potential of planar surfaces with a rotating disk. *Materials Research*, 11(2), 217-19. <https://doi.org/10.1590/S1516-14392008000200018>
- Lapointe, M., Farner, J. M., Hernandez, L. M., & Tufenkji, N. (2020). Understanding and improving microplastic removal during water treatment: Impact of coagulation and flocculation. *Environmental Science & Technology*, 54(14), 8719-8727. <https://doi.org/10.1021/acs.est.0c00712>
- Lartiges, B. S., Bottero, J. Y., Derrendinger, L. S., Humbert, B., Tekely, P., & Suty, H. (1997). Flocculation of colloidal silica with hydrolyzed aluminum: An <sup>27</sup>Al solid state NMR investigation. *Langmuir*, 13, 147-152. <https://doi.org/10.1021/la951029x>
- Latour, I., Miranda, R., & Blanco, A. (2013). Silica removal from newsprint mill effluents with aluminum salts. *Chemical Engineering Journal*, 230, 522-531. <https://doi.org/10.1016/j.cej.2013.06.039>

- LeChevallier, M. W., Norton, W. D., & Lee, R. G. (1991). *Giardia* and *Cryptosporidium* spp. in filtered drinking water supplies. *Applied & Environmental Microbiology*, 57(9), 2617-2621.  
<https://doi.org/10.1128/aem.57.9.2610-2616.1991>
- LeChevallier, M.W. and W.D. Norton. (1992). Examining Relationships Between Particle Counts and *Giardia*, *Cryptosporidium*, and Turbidity. *Journal of American Water Works Association*, 84(12), 54-60. <https://doi.org/10.1002/j.1551-8833.1992.tb05902.x>
- Lee, J., Wang, J., & Oh, Y., & Jeong, S. (2023). Highly efficient microplastics removal from water using in-situ ferrate coagulation: Performance evaluation by micro-Fourier transformed infrared spectroscopy and coagulation mechanism. *Chemical Engineering Journal*, 451, 138556.  
<https://doi.org/10.1016/j.cej.2022.138556>
- Lehner, R., Weder, C., Petri-Fink, A., & Rothen-Rutishauser, B. (2019). Emergence of nanoplastic in the environment and possible impact on human health. *Environmental Science & Technology*, 53(4), 1748-1765. <https://doi.org/10.1021/acs.est.8b05512>
- Leslie, H. A. (2014). Review of microplastics in cosmetics. *IVM Institute for Environmental Studies*, 476, 1-33. <https://hdl.handle.net/1871.1/3266b09c-95e6-499b-aa40-0607152580ce>
- Leslie, H. A., Brandsma, S. H., van Velzen, M. J. M., & Vethaak, A. D. (2017). Microplastics en route: Field measurements in the Dutch river delta and Amsterdam canals, wastewater treatment plants, North Sea sediments and biota. *Environment International*, 101, 133-142.  
<https://doi.org/10.1016/j.envint.2017.01.018>
- Letterman, R.D. and Vanderbrook, S.G. (1983). Effect of solution chemistry on coagulation with hydrolyzed Al (III), significance of sulfate ion and pH. *Water Research*, 17, 195-204.  
[https://doi.org/10.1016/0043-1354\(83\)90100-8](https://doi.org/10.1016/0043-1354(83)90100-8)
- Li, C., Busquets, R., Moruzzi, R. B., & Campos, L. C. (2021). Preliminary study on low-density polystyrene microplastics bead removal from drinking water by coagulation flocculation and sedimentation. *Journal of Water Process Engineering*, 44, 102346. <https://doi.org/10.1016/j.jwpe.2021.102346>
- Links, A. G. (2015). *Utilization of fluorescent microspheres as a surrogate for Cryptosporidium removal in conventional drinking water treatment* (Master's thesis, Arizona State University). Arizona State University Digital Repository. <https://hdl.handle.net/2286/R.I.36394>

- Liu, F., Olesen, K. B., Borregaard, A. R., & Vollertsen, J. (2019b). Microplastics in urban and highway stormwater retention ponds. *Science of the Total Environment*, 671, 992-1000.  
<https://doi.org/10.1016/j.scitotenv.2019.03.416>
- Liu, G., & Liu, S. (2019a). Advances in applications of waterborne pathogen surrogates. *Environmental Science & Technology*, 53(20), 11655-11667. <https://doi.org/10.1021/acs.est.9b02698>
- Where is Liu et al. (2019b)?
- Liu, P., Qian, L., Wang, H., Zhan, X., Lu, K., Gu, C., Gao, S. (2019c). New insights into the aging behavior of microplastics accelerated by advanced oxidation processes. *Environmental Science & Technology*, 53 (7), 3579-3588. <https://doi.org/10.1021/acs.est.9b00493>.
- Liu, P., Zhan, X., Wu, X., Li, J., Wang, H., & Gao, S. (2020). Effect of weathering on environmental behavior of microplastics: Properties, sorption and potential risks. *Chemosphere*, 242, 125193.  
<https://doi.org/10.1016/j.chemosphere.2019.125193>
- Lowry, G. V., Hill, R. J., Harper, S., Rawle, A. F., Hendren, C. O., Klaessig, F., Nobbmann, U., Sayre, P., & Rumble, J.(2016). Guidance to improve the scientific value of zeta potential measurements in nano EHS. *Environmental Science Nano*, 3, 953–965. <https://doi.org/10.1039/c6en00136j>
- Lu, P., & Amburgey, J. E. (2016). A pilot-scale study of *Cryptosporidium*-sized microsphere removals from swimming pools via sand filtration. *Journal of Water and Health*, 14(1), 109-120.  
<https://doi.org/10.2166/wh.2015.047>
- Lu, S., Liu, L., Yang, Q., Demissie, H., Jiao, R., An, G., & Wang, D. (2021). Removal characteristics and mechanism of microplastics and tetracycline composite pollutants by coagulation process. *Science of the Total Environment*, 786, 147508.  
<http://dx.doi.org/10.1016/j.scitotenv.2021.147508>
- Lu, S., Zhu, K., Song, W., Song, G., Chen, D., Hayat, T., Alharbi, N. S., Chen, C., & Sun, Y. (2018). Impact of water chemistry on surface charge and aggregation of polystyrene microspheres suspensions. *Science of the Total Environment*, 630, 951-959. <https://doi.org/10.1016/j.scitotenv.2018.02.296>
- Lu, Y., Li, M. C., Lee, J., Liu, C., & Mei, C. (2023). Microplastic remediation technologies in water and wastewater treatment processes: Current status and future perspectives. *Science of the Total Environment*, 868, 161618. <https://doi.org/10.1016/j.scitotenv.2023.161618>

- Mahler, G. J., Esch, M. B., Tako, E., Southard, T. L., Archer, S. D., Glahn, R. P., & Shuler, M. L. (2012). Oral exposure to polystyrene nanoparticles affects iron absorption. *Nature Nanotechnology*, 7, 264-271. <https://doi.org/10.1038/nnano.2012.3>
- Malmqvist, B., & Rundle, S. (2002). Threats to the running water ecosystems of the world. *Environmental Conservation*, 29(2), 134-153. <https://doi.org/10.1017/S0376892902000097>
- Maltauro, R., Stone, M., Collins, A. L., Krishnappan, B. G., & Silins, U. (2023). The effect of shear-dependent flocculation on the multimodality of effective particle size distributions in a gravel-bed river during high flows. *Journal of Soils and Sediments*, 23(10), 3589-3601. <https://doi.org/10.1007/s11368-023-03455-5>
- Martens, A. M., Silins, U., Proctor, H. C., Williams, C. H., Wagner, M. J., Emelko, M. B., & Stone, M. (2019). Long-term impact of severe wildfire and post-wildfire salvage logging on macroinvertebrate assemblage structure in Alberta's Rocky Mountains. *International Journal of Wildland Fire*, 28(10), 738-749. <https://doi.org/10.1071/WF18177>
- Matijevic, E. (1976). The role of chemical complexing in the formation and stability of colloidal dispersions. *Proceedings of the International Conference on colloids and surfaces*, 1, 397-412. Academic Press, New York. <https://doi.org/10.1016/B978-0-12-404501-9.50035-3>
- Matos, T., Martins, M. S., Henriques, R., & Goncalves, L. M. (2024). A review of methods and instruments to monitor turbidity and suspended sediment concentration. *Journal of Water Process Engineering*, 64, 105624. <https://doi.org/10.1016/j.jwpe.2024.105624>
- Mattsson, K., Hansson, L. A., & Cedervall, T. (2015). Nano-plastics in the aquatic environment. *Environmental Science: Processes & Impacts*, 17(10), 1712-1721. <https://doi.org/10.1039/C5EM00227C>
- Mei, W., Chen, G., Bao, J., Song, M., Li, Y., & Luo, C. (2020). Interactions between microplastics and organic compounds in aquatic environments: A mini review. *Science of the Total Environment*, 736, 139472. <https://doi.org/10.1016/j.scitotenv.2020.139472>
- Miller, M. E., Hamann, M., & Kroon, F. J. (2020). Bioaccumulation and biomagnification of microplastics in marine organisms: A review and meta-analysis of current data. *PLoS one*, 15(10), e0240792. <https://doi.org/10.1371/journal.pone.0240792>

- Mintenig, S. M., Löder, M. G. J., Primpke, S., & Gerdt, G. (2019). Low numbers of microplastics detected in drinking water from groundwater sources. *Science of the Total Environment*, 648, 631-635. <https://doi.org/10.1016/j.scitotenv.2018.08.178>
- Mishra, R. K. (2023). Fresh water availability and its global challenge. *British Journal of Multidisciplinary and Advanced Studies*, 4(3), 1-78. <https://doi.org/10.37745/bjmas.2022.0208>
- Monira, S., Bhuiyan, M. A., Haque, N., & Pramanik, B. K. (2021). Assess the performance of chemical coagulation process for microplastics removal from stormwater. *Process Safety and Environmental Protection*, 155, 11-16. <https://doi.org/10.1016/j.psep.2021.09.002>
- Monis, P., Lau, M., Harris, M., Cook, D., & Drikas, M. (2017). Risk-based management of drinking water safety in Australia: Implementation of health-based targets to determine water treatment requirements and identification of pathogen surrogates for validation of conventional filtration. *Food and Waterborne Parasitology*, 8-9, 64-74. <https://doi.org/10.1016/j.fawpar.2017.08.002>
- Moran, D. C., Moran, M. C., Cushing, R. S., & Lawler, D. F. (1993). Particle behavior in deep-bed filtration: Part 1—Ripening and breakthrough. *Journal of American Water Works Association*, 85(12), 69-81. <https://doi.org/10.1002/j.1551-8833.1993.tb06120.x>
- Munyaneza, J., Jia, Q., Qaraah, F. A., Hossain, M. F., Wu, C., Zhen, H., & Xiu, G. (2022). A review of atmospheric microplastics pollution: In-depth sighting of sources, analytical methods, physiognomies, transport and risks. *Science of the Total Environment*, 822, 153339. <https://doi.org/10.1016/j.scitotenv.2022.153339>
- Nahrstedt, A., & Gimbel, R. (1996). A statistical method for determining the reliability of the analytical results in the detection of *Cryptosporidium* and *Giardia* in water. *Aqua- Journal of Water Supply: Research and Technology*, 45(3), 101-111.
- Nasrin, T., Sharma, A. K., & Muttill, N. (2017). Impact of short duration intense rainfall events on sanitary sewer network performance. *Water*, 9(3), 225. <https://doi.org/10.3390/w9030225>
- Nieminski, E.C. and J.E. Ongerth. 1995. Removing *Giardia* and *Cryptosporidium* by Conventional Treatment and Direct Filtration. *Journal of American Water Works Association*, 87(9), 96-106. <https://doi.org/10.1002/j.1551-8833.1995.tb06426.x>

- Oilier, L. L., Miltner, R. J., & Summers, R. S. (1997). Microbial and particulate control under conventional and enhanced coagulation. In *Proceedings of the American Water Works Association Water Quality Technology Conference*, Denver, CO, November 1997.
- Oliveira, M., Ribeiro, A., Hylland, K., & Guilhermino, L. (2013). Single and combined effects of microplastics and pyrene on juveniles (0+ group) of the common goby *Pomatoschistus microps* (Teleostei, Gobiidae). *Ecological Indicators*, 34, 641-647.  
<https://doi.org/10.1016/j.ecolind.2013.06.019>
- Ongerth, J. E., & Pecoraro, J. P. (1996). Electrophoretic mobility of *Cryptosporidium* oocysts and *Giardia* cysts. *Journal of Environmental Engineering*, 122(3), 228-231.  
[https://doi.org/10.1061/\(asce\)0733-9372\(1996\)122:3\(228\)](https://doi.org/10.1061/(asce)0733-9372(1996)122:3(228))
- Ontario Regulation (O. Reg.) 170/03. (2003). *Drinking water systems*.  
<https://www.ontario.ca/laws/regulation/030170>
- Oßmann, B. E., Sarau, G., Holtmannspötter, H., Pischetsrieder, M., Christiansen, S. H., & Dicke, W. (2018). Small-sized microplastics and pigmented particles in bottled mineral water. *Water Research*, 141, 307-316. <https://doi.org/10.1016/j.watres.2018.05.027>
- Packham, R. F. (1965). Some studies of the coagulation of dispersed clays with hydrolyzing salts. *Journal of Colloid Science*, 20, 81-92. [https://doi.org/10.1016/0095-8522\(65\)90094-2](https://doi.org/10.1016/0095-8522(65)90094-2)
- Pandian, A. M. K., Rajamehala, M., Singh, M. V. P., Sarojini, G., & Rajamohan, N. (2022). Potential risks and approaches to reduce the toxicity of disinfection by-product—A review. *Science of the Total Environment*, 822, 153323. <https://doi.org/10.1016/j.scitotenv.2022.153323>
- Papineau, I., Tufenkji, N., & Barbeau, B. (2013). Impact of kaolinite clay particles on the filtration of *Cryptosporidium*-sized microspheres. *Water Science and Technology: Water Supply*, 13(6), 1583-1592. <https://doi.org/10.2166/ws.2013.173>
- Parashar, N., & Hait, S. (2022). Occurrence and removal of microplastics in a hybrid growth sewage treatment plant from Bihar, India: A preliminary study. *Journal of Cleaner Production*, 376, 134295. <https://doi.org/10.1016/j.jclepro.2022.134295>
- Parashar, N., & Hait, S. (2023). Plastic rain-atmospheric microplastics deposition in urban and peri-urban areas of Patna City, Bihar, India: Distribution, characteristics, transport, and source analysis. *Journal of Hazardous Materials*, 131883. <https://doi.org/10.1016/j.jhazmat.2023.131883>

- Passantino, L., Malley, J., Knudson, M., Ward, R., & Kim, J. (2004). Effect of low turbidity and algae on UV disinfection performance. *Journal of American Water Works Association*, 96(6), 128-137. <https://doi.org/10.1002/j.1551-8833.2004.tb10786.x>
- Patania, N.L., J.G. Jacangelo, L. Cummings, A. Wilczak. K. Riley, and J. Oppenheimer. (1995). *Optimization of Filtration for Cyst Removal*. Denver, CO.: AWWARF and AWWA.
- Pernitsky, D. J., & Edzwald, J. K. (2006). Selection of alum and polyaluminum coagulants: principles and applications. *Journal of Water Supply: Research and Technology-AQUA*, 55(2), 121-141. <https://doi.org/10.2166/aqua.2006.062>
- Petersen, H. H., Petersen, T. B., Enemark, H. L., Olsen, A., & Dalgaard, A. (2016). Removal of *Cryptosporidium parvum* oocysts in low-quality water using *Moringa oleifera* seed extract as a coagulant. *Food and Waterborne Parasitology*, 3, 1-8. <https://doi.org/10.1016/j.fawpar.2016.03.002>
- Pitt, J. A., Trevisan, R., Massarsky, A., Kozal, J. S., Levin, E. D., & Di Giulio, R. T. (2018). Maternal transfer of nanoplastics to offspring in zebrafish (*Danio rerio*): A case study with nanopolystyrene. *Science of the Total Environment*, 643, 324-334. <https://doi.org/10.1016/j.scitotenv.2018.06.186>
- Pivokonsky, M., Cermakova, L., Novotna, K., Peer, P., Cajthaml, T., & Janda, V. (2018). Occurrence of microplastics in raw and treated drinking water. *Science of the Total Environment*, 643, 1644-1651. <https://doi.org/10.1016/j.scitotenv.2018.08.102>
- Plummer, J. D., Edzwald, J. K., & Kelley, M. B. (1995). Removing *Cryptosporidium* by dissolved-air flotation. *Journal of American Water Works Association*, 87(9), 85-95.
- Postel, S. L. (2000). Entering an era of water scarcity: the challenges ahead. *Ecological applications*, 10(4), 941-948. [https://doi.org/10.1890/1051-0761\(2000\)010\[0941:EAEOVS\]2.0.CO;2](https://doi.org/10.1890/1051-0761(2000)010[0941:EAEOVS]2.0.CO;2)
- Prata, J. C., Silva, C. J., Serpa, D., Soares, A. M., Gravato, C., & Silva, A. L. P. (2023). Mechanisms influencing the impact of microplastics on freshwater benthic invertebrates: uptake dynamics and adverse effects on *Chironomus riparius*. *Science of The Total Environment*, 859, 160426. <https://doi.org/10.1016/j.scitotenv.2022.160426>
- Prokopova, M., Novotna, K., Pivokonska, L., Cermakova, L., Cajthaml, T., & Pivokonsky, M. (2021). Coagulation of polyvinyl chloride microplastics by ferric and aluminium sulphate: Optimisation of reaction conditions and removal mechanisms. *Journal of Environmental Chemical Engineering*, 9(6), 106465. <https://doi.org/10.1016/j.jece.2021.106465>

- Rafiee, M., Dargahi, L., Eslami, A., Beirami, E., Jahangiri-Rad, M., Sabour, S., & Amereh, F. (2018). Neurobehavioral assessment of rats exposed to pristine polystyrene nanoplastics upon oral exposure. *Chemosphere*, *193*, 745-753. <https://doi.org/10.1016/j.chemosphere.2017.11.076>
- Regli, S., Rose, J. B., Haas, C. N., & Gerba, C. P. (1991). Modeling the risk from *Giardia* and viruses in drinking water. *Journal of American Water Works Association*, *83*(11), 76-84
- Rice, E. W., Fox, K. R., Miltner, R. J., Lytle, D. A., & Johnson, C. H. (1996). Evaluating plant performance with endospores. *Journal of American Water Works Association*, *88*(9), 122.
- Sait, S. T. L., Sørensen, L., Kubowicz, S., Vike-Jonas, K., Gonzalez, S. V., Asimakopoulos, A. G., & Booth, A. M. (2021). Microplastic fibres from synthetic textiles: Environmental degradation and additive chemical content. *Environmental Pollution*, *268*, 115745. <https://doi.org/10.1016/j.envpol.2020.115745>
- Sanchez, J. G., Tsuchii, A., & Tokiwa, Y. (2000). Degradation of polycaprolactone at 50° C by a thermotolerant *Aspergillus* sp. *Biotechnology Letters*, *22*, 849-853. <https://doi.org/10.1023/A:1005603112688>
- Santos, I. R., Friedrich, A. C., & Ivar do Sul, J. A. (2009). Marine debris contamination along undeveloped tropical beaches from northeast Brazil. *Environmental Monitoring and Assessment*, *148*, 455-462. <https://doi.org/10.1007/s10661-008-0175-z>
- Saxena, K., Brighu, U., & Choudhary, A. (2018). Parameters affecting enhanced coagulation: A review. *Environmental Technology Reviews*, *7*(1), 156–176. <https://doi.org/10.1080/21622515.2018.1478456>
- Schirinzi, G.F., Pérez-Pomeda, I., Sanchís, J., Rossini, C., Farré, M., & Barceló, D. (2017). Cytotoxic effects of commonly used nanomaterials and microplastics on cerebral and epithelial human cells. *Environmental Research*, *159*, 579-587. <https://doi.org/10.1016/j.envres.2017.08.043>
- Schmidt, P. J., & Emelko, M. B. (2011). QMRA and decision-making: are we handling measurement errors associated with pathogen concentration data correctly? *Water Research*, *45*(2), 427-438. <https://doi.org/10.1016/j.watres.2010.08.042>
- Schmidt, P. J., Anderson, W. B., & Emelko, M. B. (2020). Describing water treatment process performance: Why average log-reduction can be a misleading statistic. *Water Research*, *176*, 115702. <https://doi.org/10.1016/j.watres.2020.115702>

- Schmidt, P. J., Emelko, M. B., & Reilly, P. M. (2010). Quantification of analytical recovery in particle and microorganism enumeration methods. *Environmental Science & Technology*, 44(5), 1705-1712. <https://doi.org/10.1021/es902237f>
- Seddon, N., Daniels, E., Davis, R., Chausson, A., Harris, R., Hou-Jones, X., Huq, S., Kapos, V., Mace, G. M., Rizvi, A. R., Reid, H., Roe, D., Turner, B. & Wicander, S. (2020). Global recognition of the importance of nature-based solutions to the impacts of climate change. *Global Sustainability*, 3, e15. <https://doi.org/10.1017/sus.2020.8>
- Shah, A. A., Hasan, F., Hameed, A., & Ahmed, S. (2008). Biological degradation of plastics: A comprehensive review. *Biotechnology Advances*, 26(3), 246-265. <https://doi.org/10.1016/j.biotechadv.2007.12.005>
- Shahi, N. K., Maeng, M., Kim, D., & Dockko, S. (2020). Removal behavior of microplastics using alum coagulant and its enhancement using polyamine-coated sand. *Process Safety and Environmental Protection*, 141, 9-17. <http://dx.doi.org/10.1016/j.psep.2020.05.020>
- Sharp, E. L., Jarvis, P., Parsons, S. A., & Jefferson, B. (2006). Impact of fractional character on the coagulation of NOM. *Colloids and Surfaces A: Physicochemical and Engineering Aspects*, 286(1-3), 104-111. <https://doi.org/10.1016/j.colsurfa.2006.03.009>
- Shen, M., Ye, S., Zeng, G., Zhang, Y., Xing, L., Tang, W., Wen, X., & Liu, S. (2020). Can microplastics pose a threat to ocean carbon sequestration? *Marine Pollution Bulletin*, 150, 110712. <https://doi.org/10.1016/j.marpolbul.2019.110712>
- Shruti, V.C., Pérez-Guevara, F., Elizalde-Martínez, I., & Kuttralam-Muniasamy, G. (2021). Current trends and analytical methods for evaluation of microplastics in stormwater. *Trends in Environmental Analytical Chemistry*, 30, e00123. <https://doi.org/10.1016/j.teac.2021.e00123>
- Silins U., Bladon K. D., Kelly E. N., Esch E., Spence J. R., Stone M., Emelko M. B., Boon S., Wagner M. J., Williams C. H. S., & Tichkowsky I. (2014). Five-year legacy of wildfire and salvage logging impacts on nutrient runoff and aquatic plant, invertebrate, and fish productivity. *Ecohydrology*, 7(6), 1508-1523. <https://doi.org/10.1002/eco.1474>
- Silins, U., Stone, M., Emelko, M. B., & Bladon, K. D. (2009). Sediment production following severe wildfire and post-fire salvage logging in the Rocky Mountain headwaters of the Oldman River Basin, Alberta. *Catena*, 79(3), 189-197. <https://doi.org/10.1016/j.catena.2009.04.001>

- Sillanpää, M. (2014). NOM removal by coagulation. *Natural organic matter in water: characterization and treatment methods*, 55. IWA Publishing.
- Singh, B., & Sharma, N. (2008). Mechanistic implications of plastic degradation. *Polymer Degradation and Stability*, 93(3), 561-584. <https://doi.org/10.1016/j.polymdegradstab.2007.11.008>
- Sivan, A., Szanto, M., & Pavlov, V. (2006). Biofilm development of the polyethylene-degrading bacterium *Rhodococcus ruber*. *Applied Microbiology and Biotechnology*, 72(2), 346-352. <https://doi.org/10.1007/s00253-005-0259-4>
- Skaf, D.W., Punzi, V.L., Rolle, J.T., & Kleinberg, K.A. (2020). Removal of micron-sized microplastic particles from simulated drinking water via alum coagulation. *Chemical Engineering Journal*, 386, 123807. <https://doi.org/10.1016/j.cej.2019.123807>
- Smith, M., Love, D. C., Rochman, C. M., & Neff, R. A. (2018). Microplastics in seafood and the implications for human health. *Current Environmental Health Reports*, 5(3), 375-386. <https://doi.org/10.1007/s40572-018-0206-z>
- Stone, M., Emelko, M. B., Droppo, I. G., & Silins, U. (2011). Biostabilization and erodibility of cohesive sediment deposits in wildfire-affected streams. *Water Research*, 45(2), 521–534. <https://doi.org/10.1016/j.watres.2010.09.016>
- Stone, M., Krishnappan, B. G., Silins, U., Emelko, M. B., Williams, C. H., Collins, A. L., & Spencer, S. A. (2021). A new framework for modelling fine sediment transport in rivers includes flocculation to inform reservoir management in wildfire impacted watersheds. *Water*, 13(17), 2319. <https://doi.org/10.3390/w13172319>
- Stumm, W. (1992). *Chemistry of the solid-water interface: Processes at the mineral-water and particle-water interface in natural systems*. A Wiley-Interscience Publication, John Wiley & Sons, Inc.
- Stumm, W., & Morgan, J. J. (1996). *Aquatic chemistry*. John Wiley & Sons, Inc.
- Stumm, W., & O'Melia, C. R. (1968). Stoichiometry of coagulation. *Journal of American Water Works Association*, 60(5), 514-539. <https://doi.org/10.1002/j.1551-8833.1968.tb03579.x>
- Su, L., Xue, Y., Li, L., Yang, D., Kolandhasamy, P., Li, D., & Shi, H. (2016). Microplastics in Taihu Lake, China. *Environmental Pollution*, 216, 711-719. <https://doi.org/10.1016/j.envpol.2016.06.036>
- Sulukan, E., Baran, A., Şenol, O., Yildirim, S., Mavi, A., Ceyhun, H. A., Toraman, E., & Ceyhun, S. B. (2022). The synergic toxicity of temperature increases and nanopolystyrene on zebrafish brain implies

- that global warming may worsen the current risk based on plastic debris. *Science of The Total Environment*, 808, 152092. <https://doi.org/10.1016/j.scitotenv.2021.152092>
- Sun, J., Dai, X., Wang, Q., Van Loosdrecht, M. C., & Ni, B. J. (2019). Microplastics in wastewater treatment plants: Detection, occurrence and removal. *Water Research*, 152, 21-37. <https://doi.org/10.1016/j.watres.2018.12.050>
- Tadros, T. F. (2013). *Encyclopedia of colloid and interface science*. <https://doi.org/10.1007/978-3-642-20665-8>
- Tang, W. W., Zeng, G. M., Gong, J. L., Liang, J., Xu, P., Zhang, C., & Huang, B. B. (2014). Impact of humic/fulvic acid on the removal of heavy metals from aqueous solutions using nanomaterials: A review. *Science of the Total Environment*, 468, 1014–1027. <https://doi.org/10.1016/j.scitotenv.2013.09.044>
- Tang, W., Li, H., Fei, L., Wei, B., Zhou, T., & Zhang, H. (2022). The removal of microplastics from water by coagulation: A comprehensive review. *Science of the Total Environment*. <https://doi.org/10.1016/j.scitotenv.2022.158224>
- Tchobanoglous, G., Stensel, H. D., Tsuchihashi, R., & Burton, F. L. (2014). *Wastewater engineering: Treatment and resource recovery* (5th ed.). McGraw-Hill Education.
- Teunis, P. F. M., Rutjes, S. A., Westrell, T., & de Roda Husman, A. M. (2009). Characterization of drinking water treatment for virus risk assessment. *Water Research*, 43(2), 395-404.
- Teuten, E., Rowland, S., Galloway, T., & Thompson, R. (2007). Potential for plastics to transport hydrophobic contaminants. *Environmental Science & Technology*, 41, 7759–7764. <https://doi.org/10.1021/es071737s>
- Thompson, R. C., Olsen, Y., Mitchell, R. P., et al. (2004). Lost at sea: Where is all the plastic? *Science*, 304, 838. <https://doi.org/10.1126/science.1094559>
- Thubagere, A., & Reinhard, B. M. (2010). Nanoparticle-induced apoptosis propagates through hydrogen peroxide-mediated bystander killing: Insights from a human intestinal epithelium in vitro model. *American Chemistry Society Nano*, 4(7), 3611–3622. <https://doi.org/10.1021/nn100389a>
- Tian, L., Chen, Q., Jiang, W., Wang, L., Xie, H., Kalogerakis, N., Ma, Y., & Ji, R. (2019). A carbon-14 radiotracer-based study on the phototransformation of polystyrene nanoplastics in water versus in air. *Environmental Science: Nano*, 6(9), 2907–2917. <https://doi.org/10.1039/C9EN00662A>

- Tokiwa, Y., Calabia, B. P., Ugwu, C. U., and Aiba, S. 2009. Biodegradability of plastics. *International Journal of Molecular Sciences*, 10(9),3722–3742. <https://doi.org/10.3390/ijms10093722>
- Triebkorn, R., Braunbeck, T., Grummt, T., Hanslik, L., Huppertsberg, S., Jekel, M., Knepper, T.P., Kraus, S., Müller, Y.K., Pittroff, M., Ruhl, A.S., Schmiege, H., Schür, C., Strobel, C., Wagner, M., Zumbülte, N., & Köhler, H.-R. (2019). Relevance of nano- and microplastics for freshwater ecosystems: A critical review. *Trends in Analytical Chemistry*, 110, 375-392. <https://doi.org/10.1016/j.trac.2018.11.023>
- Turgay, E., Steinum, T. M., Colquhoun, D., & Karatas, S. (2019). Environmental biofilm communities associated with early-stage common dentex (*Dentex dentex*) culture. *Journal of Applied Microbiology*, 126(4), 1032–1043. <https://doi.org/10.1111/jam.14205>
- UNEP, NOAA. (2011). *The Honolulu Strategy*. United Nations. <https://doi.org/10.1002/jgrd.50152>
- UNEP. (2019). *World pledges to protect polluted, degraded planet as it adopts blueprint for more sustainable, resilient Earth*. <https://www.unep.org/news-and-stories/press-release/world-pledges-protect-polluted-degraded-planet-it-adopts-blueprint>
- UNEP. (2022). Preparation of an international legally binding instrument on plastic pollution, including in the marine environment. Retrieved from <https://wedocs.unep.org/bitstream/handle/20.500.11822/40831/K2221533%20-%20%20UNEP-PPINC.1-7%20-%20AMENDED%20ADVANCE%20-%2014.10.2022.pdf>
- U.S. Environmental Protection Agency. (1974). *National interim primary drinking water regulations* (EPA 570/9-76-003). <https://nepis.epa.gov/Exe/ZyPURL.cgi?Dockey=2000J6TU.TXT>
- U.S. Environmental Protection Agency. (1989). National Primary Drinking Water Regulations: Filtration and Disinfection; Turbidity; *Giardia lamblia*, Viruses, *Legionella*, and Heterotrophic Bacteria. *Federal Register*, 54(124), 27486-27541.
- U.S. Environmental Protection Agency. (1998). Interim enhanced surface water treatment rule (EPA 815-F-98-009). *Federal Register*, 63(241), 69477–69521. [https://www.epa.gov/sites/default/files/2015-11/documents/ieswtr\\_fs\\_finalrule.pdf](https://www.epa.gov/sites/default/files/2015-11/documents/ieswtr_fs_finalrule.pdf)
- U.S. Environmental Protection Agency. (1999). *Disinfection profiling and benchmarking guidance manual* (EPA 815-R-99-013). Office of Water.

- U. S. Environmental Protection Agency. (2002). National primary drinking water regulations: Long term 1 enhanced surface water treatment rule (LT1SWTR); final rule. Federal Register, 67(9), 1812–1844. <https://www.govinfo.gov/content/pkg/FR-2002-01-14/pdf/02-409.pdf>
- U.S. Environmental Protection Agency. (2006). National primary drinking water regulations: Long term 2 enhanced surface water treatment rule (LT2ESWTR); final rule. Federal Register, 71(3), 654–786. <https://www.govinfo.gov/content/pkg/FR-2006-01-05/pdf/06-4.pdf>
- U.S. Environmental Protection Agency. (2018). *Drinking Water Standards and Health Advisories Tables*.
- U.S. Environmental Protection Agency. (2024). *National primary drinking water regulations: Turbidity*. <https://www.epa.gov/dwreginfo/national-primary-drinking-water-regulations-turbidity>
- Waller, C.L., Griffiths, H.J., Waluda, C.M., Thorpe, S.E., Loaiza, I., Moreno, B., Pacherrres, C.O., & Hughes, K.A. (2017). Microplastics in the Antarctic marine system: An emerging area of research. *Science of the Total Environment*, 598, 220–227. <https://doi.org/10.1016/j.scitotenv.2017.03.283>
- Wang, C., O'Connor, D., Wang, L., Wu, W.M., Luo, J., & Hou, D. (2022). Microplastics in urban runoff: Global occurrence and fate. *Water Research*, 119129. <https://doi.org/10.1016/j.watres.2022.119129>
- Wang, D., Kundert, K. L., & Emelko, M. B. (2020b). Optimisation and improvement of in-line filtration performance in water treatment for a typical low turbidity source water. *Environmental Technology*. <https://doi.org/10.1080/09593330.2018.1493147>
- Wang, F., Zhang, M., Sha, W., Wang, Y., Hao, H., Dou, Y., Li, Y. (2020a). Sorption behavior and mechanisms of organic contaminants to nano and microplastics. *Molecules* 25. <https://doi.org/10.3390/molecules25081827>
- Wang, Y., Narain, R., Liu, Y., Zeng, H., Seaman, J., Ulrich, A., & Zhang, H. (2017). Filtration of glycoprotein-modified carbonylated Polystyrene Microspheres as *Cryptosporidium* Oocysts Surrogates: Effects of Flow Rate, Alum, and Humic Acid. *Journal of Environmental Engineering*. <https://doi.org/10.7939/r3-vwen-b322>
- Wang, Z., Lin, T., & Chen, W. (2020c). Occurrence and removal of microplastics in an advanced drinking water treatment plant (ADWTP). *Science of the Total Environment*, 700. <https://doi.org/10.1016/j.scitotenv.2019.134520>

- Wang, Z., Sedighi, M., & Lea-Langton, M. (2020c). Filtration of microplastic spheres by biochar: Removal efficiency and immobilisation mechanisms. *Water Research*, *184*, 116165. <https://doi.org/10.1016/j.watres.2020.116165>
- Watt, C., Emelko, M. B., Silins, U., Collins, A. L., & Stone, M. (2021). Anthropogenic and climate-exacerbated landscape disturbances converge to alter phosphorus bioavailability in an oligotrophic river. *Water*, *13*(22), 3151. <https://doi.org/10.3390/w13223151>
- Welden, N. A., & Lusher, A. L. (2017). Impacts of changing ocean circulation on the distribution of marine microplastic litter. *Integrated environmental assessment and management*, *13*(3), 483-487. <https://doi.org/10.1002/ieam.1911>
- West, T., Daniel, P., Meyerhofer, P., DeGraca, A., Leonard, S., & Gerba, C. (1994). Evaluation of *Cryptosporidium* removal through high-rate filtration. In *Proceedings American Water Works Association Annual Conference*. Denver, CO.: AWWA.
- Williams, C. H., Silins, U., Spencer, S. A., Wagner, M. J., Stone, M., & Emelko, M. B. (2019). Net precipitation in burned and unburned subalpine forest stands after wildfire in the northern Rocky Mountains. *International Journal of Wildland Fire*, *28*(10), 750-760. <https://doi.org/10.1071/WF18181>
- Wright, S. L., & Kelly, F. J. (2017). Plastic and human health: A micro issue? *Environmental Science & Technology*, *51*(12), 6634-6647. <https://doi.org/10.1021/acs.est.7b00423>
- Wu, J., Zhang, Y., & Tang, Y. (2022). Fragmentation of microplastics in the drinking water treatment process - a case study in Yangtze River region, China. *Science of the Total Environment*, *806*, 150545. <https://doi.org/10.1016/j.scitotenv.2021.150545>
- Xagorarakis, I. (2001). Coagulation and sedimentation of *Cryptosporidium parvum*. Doctoral dissertation, The University of Wisconsin-Madison.
- Xue, J., Peldszus, S., Van Dyke, M. I., & Huck, P. M. (2021). Removal of polystyrene microplastic spheres by alum-based coagulation-flocculation-sedimentation (CFS) treatment of surface waters. *Chemical Engineering Journal*, *422*, 130023. <http://dx.doi.org/10.1016/j.cej.2021.130023>
- Yamatake, A., Angeloni, D. M., Dickson, S. E., Emelko, M. B., Yasuoka, K., & Chang, J. S. (2006). Characteristics of pulsed arc electrohydraulic discharge for eccentric electrode cylindrical

- reactor using phosphate-buffered saline water. *Japanese Journal of Applied Physics*, 45(10S), 8298-8303. [www.doi.org/10.1143/JJAP.45.8298](http://www.doi.org/10.1143/JJAP.45.8298)
- Yoon, J. S., Germaine, J. T., & Culligan, P. J. (2006). Visualization of particle behavior within a porous medium: Mechanisms for particle filtration and retardation during downward transport. *Water Resources Research*, 42(6). <https://doi.org/10.1029/2004WR003660>
- Zeghioud, H., Nguyen-Tri, P., Khezami, L., Amrane, A., & Assadi, A. A. (2020). Review on discharge plasma for water treatment: Mechanism, reactor geometries, active species and combined processes. *Journal of Water Process Engineering*, 38, 101664. <https://doi.org/10.1016/j.jwpe.2020.101664>
- Zhang, H., Seaman, J., Wang, Y., Zeng, H., Narain, R., Ulrich, A., & Liu, Y. (2017). Filtration of glycoprotein modified carboxylated polystyrene microspheres as *Cryptosporidium* oocysts surrogates: Effects of flow rate, alum, and humic acid. *Journal of Environmental Engineering*, 143(1), 1-9. [https://doi.org/10.1061/\(ASCE\)EE.1943-7870.0001201](https://doi.org/10.1061/(ASCE)EE.1943-7870.0001201)
- Zhang, Y., Wang, X., Li, Y., et al. (2022). Improving nanoplastic removal by coagulation: Impact mechanism of particle size and water chemical conditions. *Journal of Hazardous Materials*, 425, 127962. <https://doi.org/10.1016/j.jhazmat.2021.127962>
- Zhang, Y., Zhou, G., Yue, J., Xing, X., Yang, Z., Wang, X., & Zhang, J. (2021). Enhanced removal of polyethylene terephthalate microplastics through polyaluminum chloride coagulation with three typical coagulant aids. *Science of the Total Environment*, 800, 149589. <https://doi.org/10.1016/j.scitotenv.2021.149589>
- Zheng, Y., Yanful, E. K., & Bassi, A. S. (2005). A review of plastic waste biodegradation. *Critical Reviews in Biotechnology*, 25(3), 243-250. <https://doi.org/10.1080/07388550500346359>
- Zhou, G., Wang, Q., Li, J., Li, Q., Xu, H., Ye, Q., & Zhang, J. (2021). Removal of polystyrene and polyethylene microplastics using PAC and FeCl<sub>3</sub> coagulation: Performance and mechanism. *Science of the Total Environment*, 752, 141837. <https://doi.org/10.1016/j.scitotenv.2020.141837>
- Zhou, L., Wang, R., Liu, Y., Zhang, Y., Zhou, J., Qu, G., Tang, S., & Wang, T. (2022). Plasma-induced conversion of polystyrene nanoplastics in water: Intermediates release, toxicity, and disinfection byproducts formation. *Chemical Engineering Journal*, 433, 134543. <https://doi.org/10.1016/j.cej.2022.134543>

Zhu, Z., Schmidt, P. J., Parker, W. J., & Emelko, M. B. (2024). Framework to Quantify Uncertainty in Microplastic Concentrations in Wastewaters and Sludges Incorporating Analytical Recovery Information into Data Analysis. *Analytical Chemistry*, 96(16), 6245-6254.

<https://doi.org/10.1021/acs.analchem.3c05484>

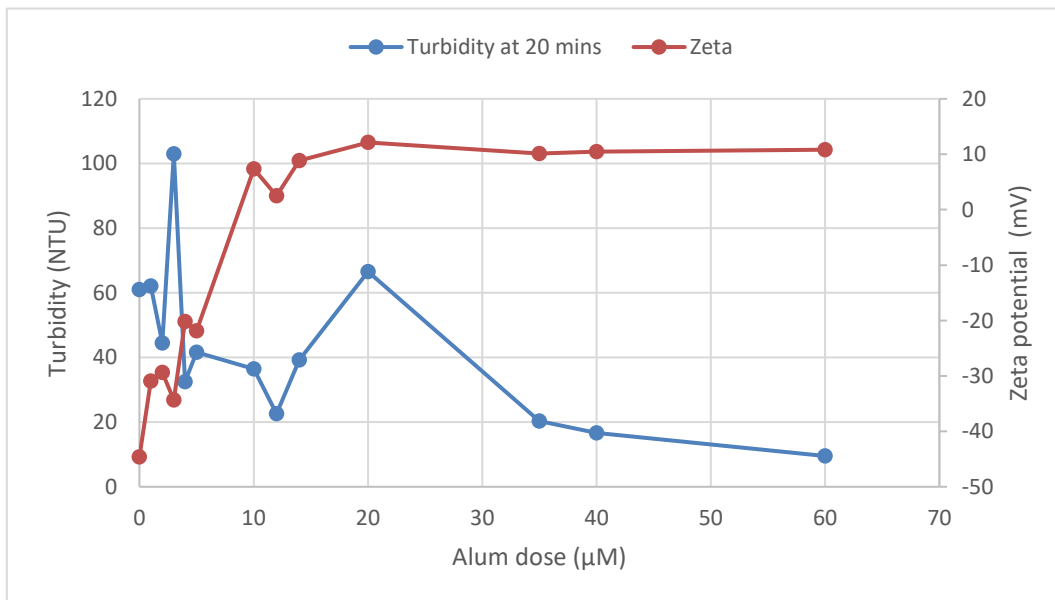
## Appendix A:

### Test runs for the jar test conditions

Jar test results from first trial (29<sup>th</sup> September):

Initial Turbidity: 61 NTU; 0.1 N of Na<sub>2</sub>CO<sub>3</sub>

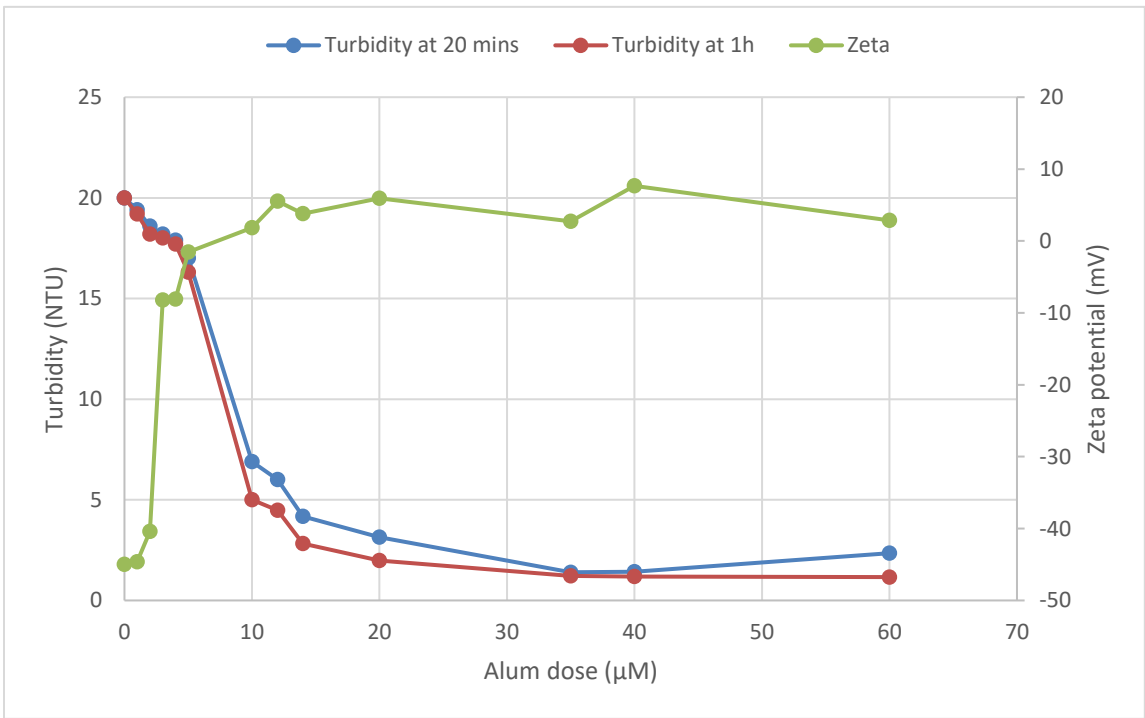
Jar no.	Alum dose (μM)	Turbidity (NTU)	Zeta potential (mV)	pH	Volume of NaOH added (μL)
Control	0	61	-44.62	7.03	0
Jar 1	1	62.1	-30.90	7.03	0
Jar 2	2	44.5	-29.37	6.98	0
Jar 3	3	103	-34.33	7	0
Jar 4	4	32.5	-20.20	6.96	0
Jar 5	5	41.6	-21.87	6.97	0
Jar 6	10	36.5	7.35	7.03	250
Jar 7	12	22.6	2.51	7.06	350
Jar 8	14	39.2	8.88	7.07	450
Jar 9	20	66.6	12.13	7.03	630
Jar 10	35	20.3	10.13	7.06	1330
Jar 11	40	16.7	10.50	7.06	1530
Jar 12	60	9.52	10.83	7	2335



Jar test results from first trial with new turbidity (27<sup>th</sup> October):

Initial Turbidity: 20 NTU; 0.5N of Na<sub>2</sub>CO<sub>3</sub>

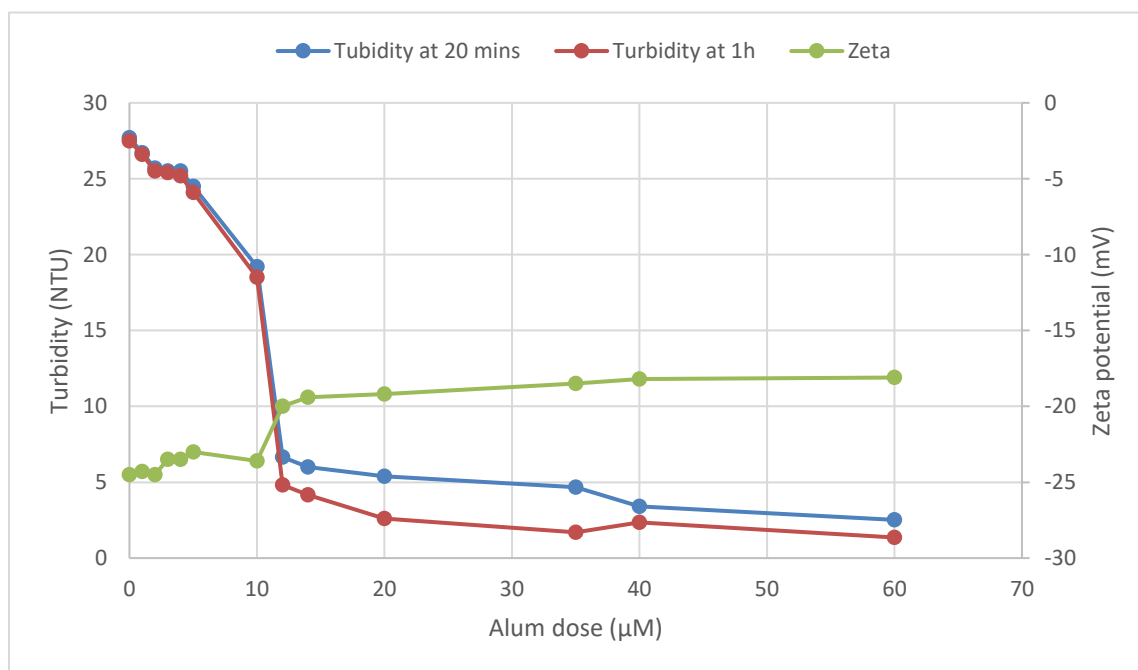
Jar no.	Alum dose (μM)	Turbidity at 20 mins (NTU)	Turbidity at 1 h (NTU)	Zeta potential (mV)	pH
Control	0	20.0	20.0	-45.0	7.00
Jar 1	1	19.4	19.2	-44.6	6.98
Jar 2	2	18.6	18.2	-40.4	7.00
Jar 3	3	18.2	18.0	-8.22	6.97
Jar 4	4	17.9	17.7	-8.10	6.96
Jar 5	5	17.0	16.3	-1.56	6.97
Jar 6	10	6.89	5.00	1.82	7.01
Jar 7	12	6.00	4.47	5.54	6.96
Jar 8	14	4.18	2.82	3.82	7.04
Jar 9	20	3.15	1.98	5.93	7.00
Jar 10	35	1.40	1.22	2.71	6.98
Jar 11	40	1.42	1.18	7.67	7.02
Jar 12	60	2.35	1.16	2.86	6.98



Jar test results from first trial with new turbidity with microplastics of 4.5  $\mu\text{m}$  (30<sup>th</sup> October):

Initial Turbidity: 27.7 NTU; 0.5N of  $\text{Na}_2\text{CO}_3$

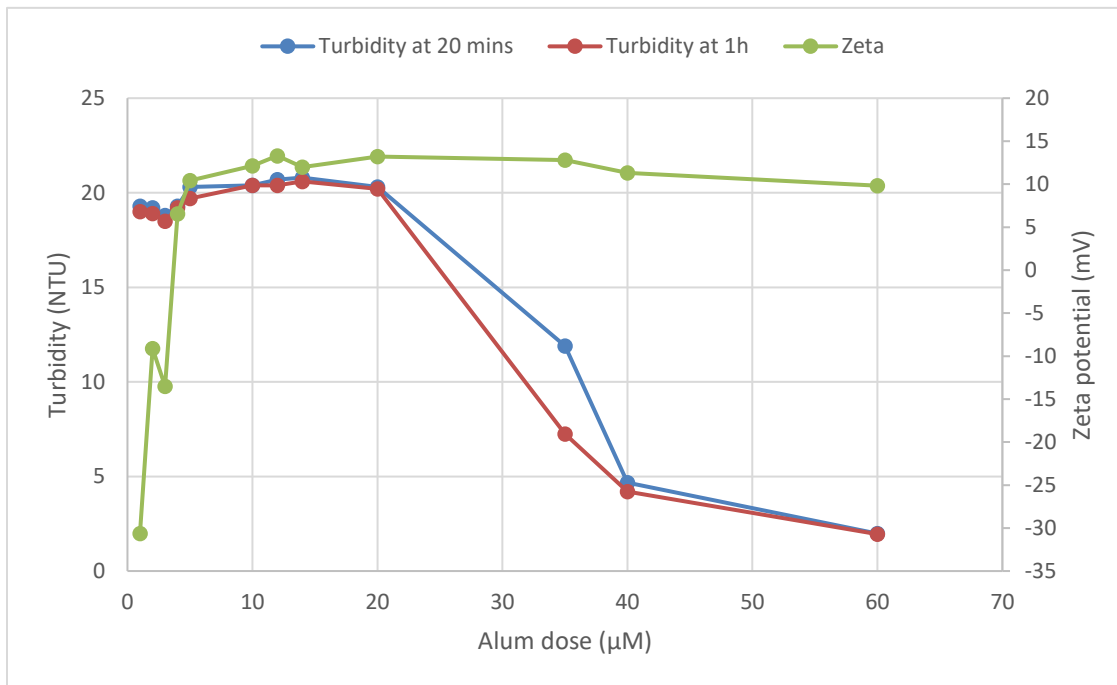
Jar no.	Alum dose ( $\mu\text{M}$ )	Turbidity at 20 mins (NTU)	Turbidity at 1 h (NTU)	Zeta potential (mV)	pH
Control	0.00	27.7	27.5	-24.5	7.03
Jar 1	1.00	26.7	26.6	-24.3	6.99
Jar 2	2.00	25.7	25.5	-24.5	7.03
Jar 3	3.00	25.5	25.4	-23.5	7.04
Jar 4	4.00	25.5	25.2	-23.5	7.00
Jar 5	5.00	24.5	24.1	-23.0	6.99
Jar 6	10.0	19.2	18.5	-23.6	7.00
Jar 7	12.0	6.66	4.83	-20.0	7.04
Jar 8	14.0	6.00	4.16	-19.4	7.04
Jar 9	20.0	5.39	2.61	-19.2	7.00
Jar 10	35.0	4.68	1.69	-18.5	6.98
Jar 11	40.0	3.41	2.36	-18.2	6.97
Jar 12	60.0	2.52	1.36	-18.1	7.02



Jar test results from first trial with new turbidity and 0.1N of Na<sub>2</sub>CO<sub>3</sub> (6<sup>th</sup> November):

Initial Turbidity: 20 NTU; 0.1N of Na<sub>2</sub>CO<sub>3</sub>

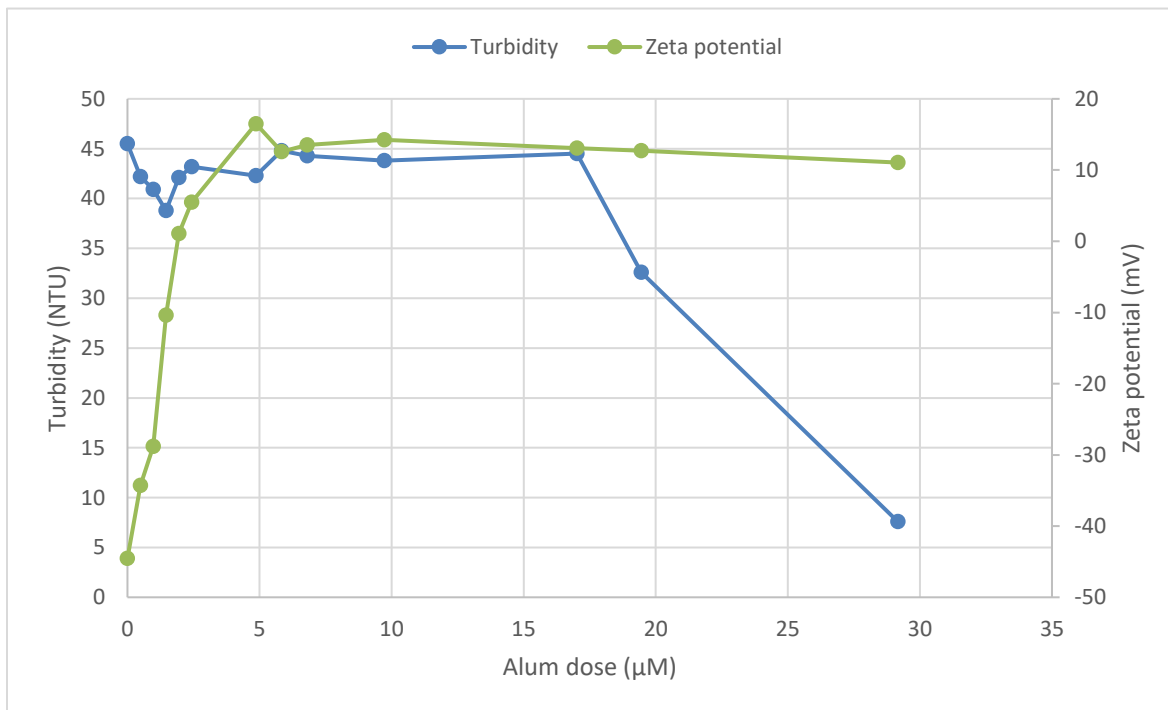
Jar no.	Alum dose (μM)	Turbidity at 20 mins (NTU)	Turbidity at 1 h (NTU)	Zeta potential (mV)	pH
Jar 1	1.00	19.3	19.0	-30.6	6.98
Jar 2	2.00	19.2	18.9	-9.11	7.00
Jar 3	3.00	18.8	18.5	-13.5	6.97
Jar 4	4.00	19.3	19.2	6.56	6.98
Jar 5	5.00	20.3	19.7	10.4	7.02
Jar 6	10.0	20.4	20.4	12.1	6.98
Jar 7	12.0	20.7	20.4	13.3	7.02
Jar 8	14.0	20.8	20.6	12.0	6.98
Jar 9	20.0	20.3	20.2	13.2	7.00
Jar 10	35.0	11.9	7.24	12.8	6.98
Jar 11	40.0	4.67	4.20	11.3	7.02
Jar 12	60.0	1.98	1.95	9.83	6.98



Jar test results from first trial with new turbidity and 0.1N of Na<sub>2</sub>CO<sub>3</sub> (7<sup>th</sup> November):

Initial Turbidity: 45.5 NTU; 0.1N of Na<sub>2</sub>CO<sub>3</sub>

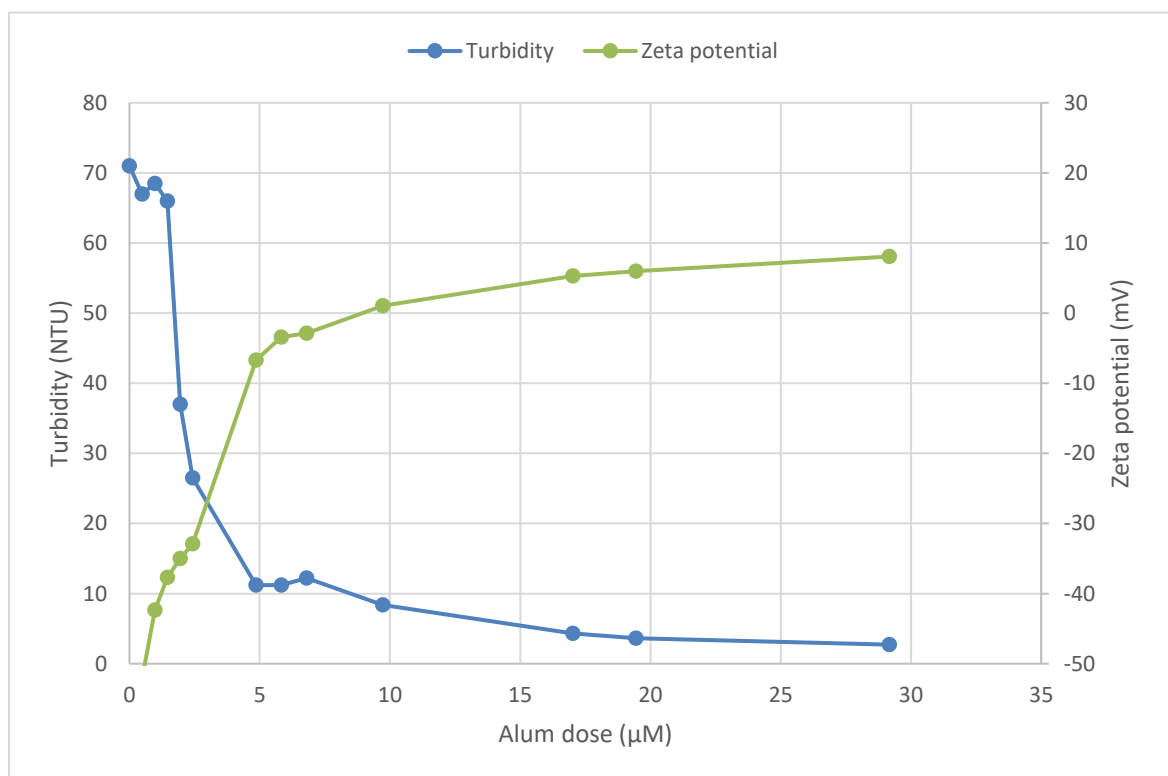
Jar no.	Alum dose (μM)	Turbidity at 20 mins (NTU)	Turbidity at 1 h (NTU)	Zeta potential (mV)	pH
Control	0.00	45.5	45.3	-44.5	7.05
Jar 1	1.00	42.2	41.9	-34.3	6.98
Jar 2	2.00	40.9	39.8	-28.8	6.95
Jar 3	3.00	38.8	38.2	-10.4	6.96
Jar 4	4.00	42.1	41.4	1.07	6.95
Jar 5	5.00	43.2	42.7	5.48	6.96
Jar 6	10.0	42.3	41.6	16.5	7.01
Jar 7	12.0	44.8	42.5	12.6	7.07
Jar 8	14.0	44.3	43.4	13.5	7.03
Jar 9	20.0	43.8	43.5	14.2	7.04
Jar 10	35.0	44.5	42.3	13.1	7.07
Jar 11	40.0	32.6	26.5	12.7	7.06
Jar 12	60.0	7.58	6.93	11.1	7.05



Jar test results with new turbidity (9<sup>th</sup> November):

Initial Turbidity: 70 NTU; 0.5N of Na<sub>2</sub>CO<sub>3</sub>

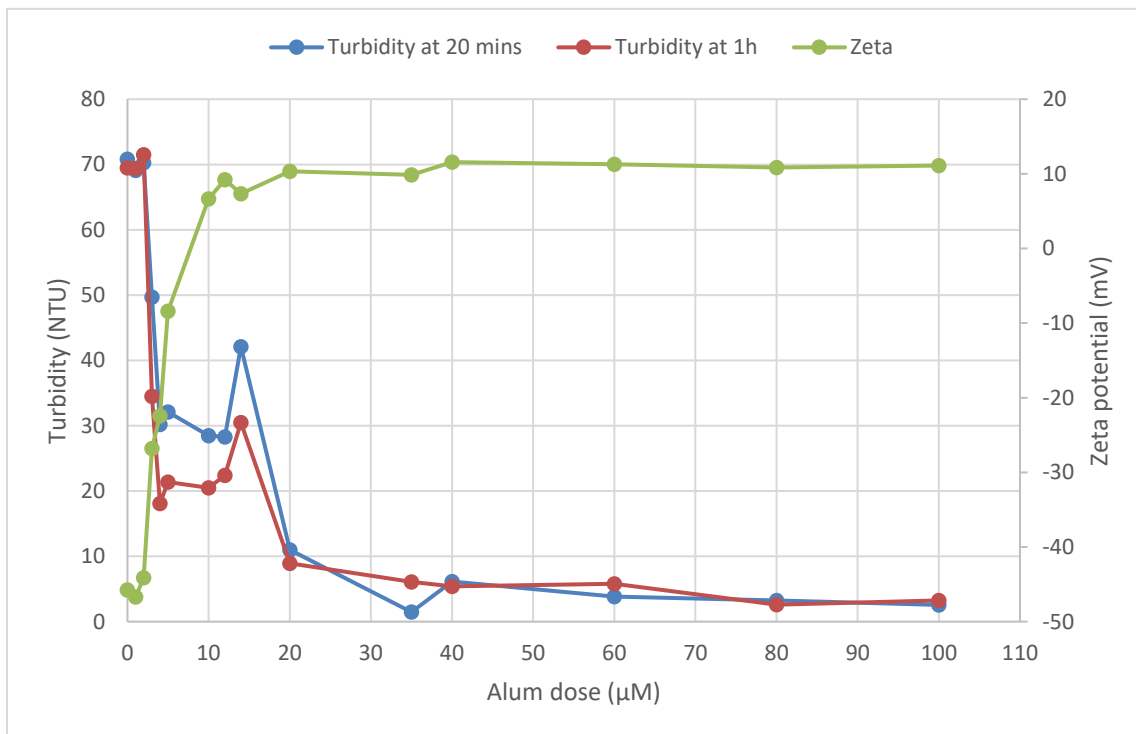
Jar no.	Alum dose (μM)	Turbidity at 20 mins (NTU)	Turbidity at 1 h (NTU)	pH	Zeta Potential (mV)
Control	0.00	71.0	69.9	7.02	-55.6
Jar 1	1.00	67.0	66.9	7.05	-52.1
Jar 2	2.00	68.5	67.8	6.97	-42.37
Jar 3	3.00	66.0	64.4	7.02	-37.7
Jar 4	4.00	37.0	26.9	7.00	-35.0
Jar 5	5.00	26.5	8.72	7.04	-32.9
Jar 6	10.0	11.2	8.63	7.02	-6.69
Jar 7	12.0	11.2	8.56	7.02	-3.43
Jar 8	14.0	12.2	7.27	6.95	-2.87
Jar 9	20.0	8.36	6.53	6.98	1.08
Jar 10	35.0	4.34	5.13	7.02	5.33
Jar 11	40.0	3.64	3.32	7.01	5.98
Jar 12	60.0	2.72	1.87	6.99	8.08



Jar test results with new turbidity (10<sup>th</sup> November):

Initial Turbidity: 70 NTU; 0.2N of Na<sub>2</sub>CO<sub>3</sub>

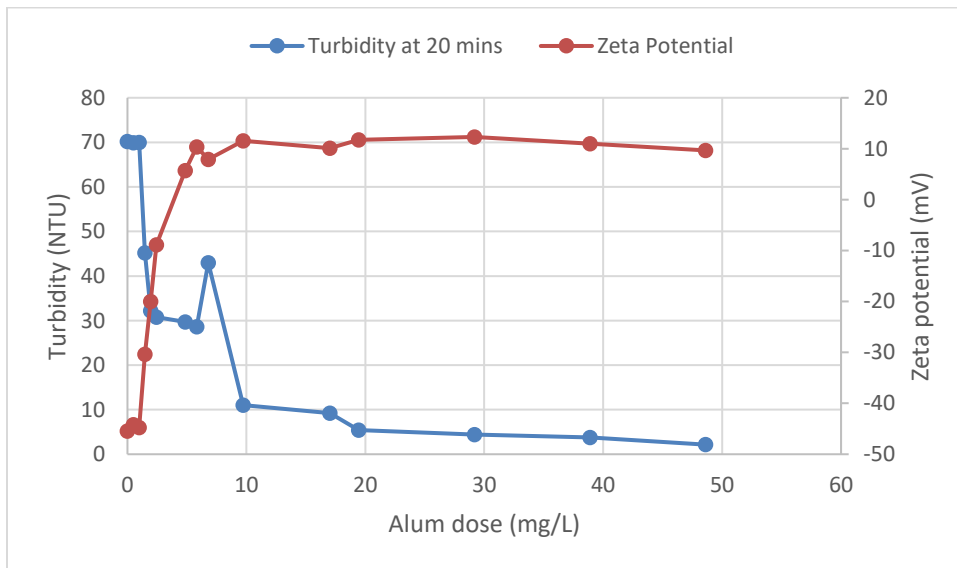
Jar no.	Alum dose (μM)	Turbidity at 20 mins (NTU)	Turbidity at 1 h (NTU)	Zeta potential (mV)	pH
Control	0.00	70.8	69.5	-45.7	7.02
Jar 1	1.00	69.1	69.4	-46.7	7.01
Jar 2	2.00	70.3	71.5	-44.1	7.06
Jar 3	3.00	49.7	34.5	-26.8	7.00
Jar 4	4.00	30.2	18.1	-22.4	7.00
Jar 5	5.00	32.1	21.4	-8.41	7.01
Jar 6	10.0	28.5	20.5	6.66	6.99
Jar 7	12.0	28.3	22.4	9.23	7.04
Jar 8	14.0	42.1	30.5	7.33	7.06
Jar 9	20.0	11.0	8.94	10.3	7.05
Jar 10	35.0	1.47	6.10	9.86	7.02
Jar 11	40.0	6.12	5.40	11.6	7.00
Jar 12	60.0	3.86	5.79	11.3	7.01
Jar 13	80.0	3.23	2.60	10.9	7.01
Jar 14	100	2.54	3.27	11.1	7.01



Jar test results with new turbidity (13<sup>th</sup> November):

Initial Turbidity: 70 NTU; 0.2N of Na<sub>2</sub>CO<sub>3</sub>

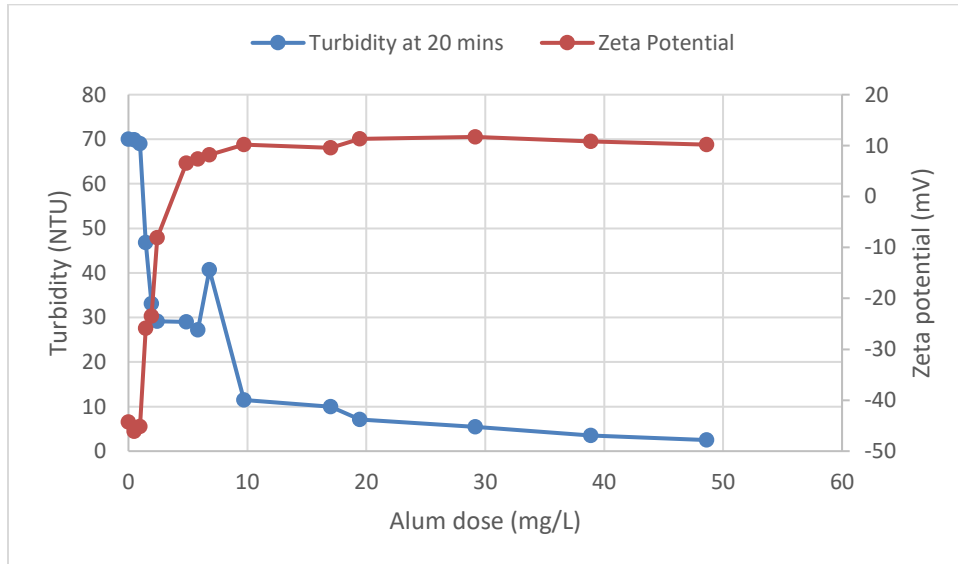
Jar no.	Alum dose (mg/L)	Turbidity at 20 mins (NTU)	Zeta potential (mV)
Jar 0	0.00	70.2	-45.4
Jar 1	1.00	69.9	-44.2
Jar 2	2.00	70.0	-44.8
Jar 3	3.00	45.2	-30.4
Jar 4	4.00	32.2	-19.9
Jar 5	5.00	30.8	-8.86
Jar 6	10.0	29.7	5.68
Jar 7	12.0	28.6	10.3
Jar 8	14.0	43.0	7.94
Jar 9	20.0	11.0	11.6
Jar 10	35.0	9.21	10.1
Jar 11	40.0	5.39	11.7
Jar 12	60.0	4.44	12.3
Jar 13	80.0	3.78	10.9
Jar 14	100	2.16	9.68



Jar test results with new turbidity (14<sup>th</sup> November):

Initial Turbidity: 70 NTU; 0.2N of Na<sub>2</sub>CO<sub>3</sub>

Jar no.	Alum dose (mg/L)	Turbidity at 20 mins (NTU)	Zeta potential (mV)
Jar 0	0.00	70.0	-44.3
Jar 1	1.00	69.9	-46.1
Jar 2	2.00	69.0	-45.2
Jar 3	3.00	46.8	-25.9
Jar 4	4.00	33.1	-23.5
Jar 5	5.00	29.1	-8.11
Jar 6	10.0	28.9	6.52
Jar 7	12.0	27.2	7.36
Jar 8	14.0	40.7	8.19
Jar 9	20.0	11.5	10.2
Jar 10	35.0	9.98	9.58
Jar 11	40.0	7.11	11.3
Jar 12	60.0	5.43	11.7
Jar 13	80.0	3.51	10.8
Jar 14	100	2.49	10.2



## Appendix B Detailed jar test data

Table A1 Count and log removal data for all combinations of microplastic type (2) and sizes (3).

MPs size ( $\mu\text{m}$ )	Date	Alum dose ( $\mu\text{M}$ )	Alum dose (mg/L)	Particle dose (particles/mL)	Volume of the effluent (mL)	Turbidity (NTU)	Effluent count (Carboxylated BB polybeads)	Effluent count (Plain YG polybead)	BB removal ( $\log_{10}$ )	YG removal ( $\log_{10}$ )
1	27-Nov-23	0	0	150	1	70.0	143	141	0.0187	0.0269
1	27-Nov-23	3	1.46	150	1	33.4	77	74	0.268	0.291
1	27-Nov-23	4	1.94	150	1	38.0	92	79	0.240	0.271
1	27-Nov-23	6	2.92	150	1	53.8	123	96	0.113	0.178
1	27-Nov-23	8	3.89	150	1	35.6	82	88	0.282	0.269
1	27-Nov-23	10	4.86	150	1	28.3	68	72	0.329	0.313
1	27-Nov-23	20	9.72	150	10	9.35	108	117	1.15	1.09
1	27-Nov-23	60	29.17	150	100	4.06	116	140	2.07	2.06
1	28-Nov-23	0 (Control)	0	150	1	70.0	147	144	0.009	0.0182

MPs size (µm)	Date	Alum dose (µM)	Alum dose (mg/L)	Particle dose (particles/mL)	Volume of the effluent (mL)	Turbidity (NTU)	Effluent count (Carboxylated BB polybeads)	Effluent count (Plain YG polybead)	BB Log removal (log <sub>10</sub> (Influent/Effluent))	YG Log removal (log <sub>10</sub> (Influent/Effluent))
1	28-Nov-23	3	1.46	150	1	34.9	85	79	0.247	0.278
1	28-Nov-23	4	1.94	150	1	35.1	79	77	0.278	0.290
1	28-Nov-23	6	2.92	150	1	49.0	103	96	0.163	0.194
1	28-Nov-23	8	3.89	150	1	35.5	81	79	0.268	0.278
1	28-Nov-23	10	4.86	150	1	25.5	72	74	0.319	0.307
1	28-Nov-23	20	9.72	150	10	11.1	97	124	1.189	1.08
1	28-Nov-23	60	29.17	150	100	6.15	141	131	2.027	2.06
1	29-Nov-23	0 (Control)	0	150	1	70.0	141	138	0.027	0.0360
1	29-Nov-23	3	1.46	150	1	33.9	81	77	0.268	0.291
1	29-Nov-23	4	1.94	150	1	36.0	88	85	0.232	0.247

MPs size (µm)	Date	Alum dose (µM)	Alum dose (mg/L)	Particle dose (particles/mL)	Volume of the effluent (mL)	Turbidity (NTU)	Effluent count (Carboxylated BB polybeads)	Effluent count (Plain YG polybead)	BB Log removal (log <sub>10</sub> (Influent/Effluent))	YG Log removal (log <sub>10</sub> (Influent/Effluent))
1	29-Nov-23	6	2.92	150	1	52.2	121	107	0.093	0.147
1	29-Nov-23	8	3.89	150	1	30.5	72	75	0.319	0.301
1	29-Nov-23	10	4.86	150	1	22.3	71	73	0.325	0.313
1	29-Nov-23	20	9.72	150	10	11.5	114	127	1.12	1.07
1	29-Nov-23	60	29.17	150	100	6.20	125	117	2.079	2.11
5	12-Jan-24	0 (Control)	0	150	1	70.0	139	145	0.033	0.0150
5	12-Jan-24	4	1.94	150	1	24.9	58	75	0.413	0.301
5	12-Jan-24	6	2.92	150	1	21.9	48	83	0.495	0.257
5	12-Jan-24	8	3.89	150	1	19.3	110	123	0.135	0.0860
5	12-Jan-24	10	4.86	150	1	40.8	76	87	0.295	0.237

MPs size ( $\mu\text{m}$ )	Date	Alum dose ( $\mu\text{M}$ )	Alum dose (mg/L)	Particle dose (particles/mL)	Volume of the effluent (mL)	Turbidity (NTU)	Effluent count (Carboxylated BB polybeads)	Effluent count (Plain YG polybead)	BB Log removal ( $\log_{10}(\text{Influent}/\text{Effluent})$ )	YG Log removal ( $\log_{10}(\text{Influent}/\text{Effluent})$ )
5	12-Jan-24	12	5.83	150	1	38.1	62	73	0.384	0.313
5	12-Jan-24	20	9.72	150	10	6.44	68	67	1.34	1.35
5	12-Jan-24	60	29.17	150	100	2.74	66	52	2.36	2.46
5	18-Jan-24	0 (Control)	0	150	1	70.0	144	138	0.018	0.036
5	18-Jan-24	4	1.94	150	1	24.7	72	76	0.319	0.295
5	18-Jan-24	6	2.92	150	1	21.9	68	77	0.344	0.290
5	18-Jan-24	8	3.89	150	1	20.1	122	118	0.0901	0.104
5	18-Jan-24	10	4.86	150	1	42.0	83	87	0.257	0.237
5	18-Jan-24	12	5.83	150	1	35.8	78	80	0.284	0.273
5	18-Jan-24	20	9.72	150	10	8.99	66	70	1.36	1.33

MPs size ( $\mu\text{m}$ )	Date	Alum dose ( $\mu\text{M}$ )	Alum dose (mg/L)	Particle dose (particles/mL)	Volume of the effluent (mL)	Turbidity (NTU)	Effluent count (Carboxylated BB polybeads)	Effluent count (Plain YG polybead)	BB Log removal ( $\log_{10}(\text{Influent}/\text{Effluent})$ )	YG Log removal ( $\log_{10}(\text{Influent}/\text{Effluent})$ )
5	18-Jan-24	60	29.17	150	100	5.22	53	61	2.45	2.39
5	19-Jan-24	0 (Control)	0	150	1	70.0	155	141	-0.0140	0.0270
5	19-Jan-24	4	1.94	150	1	25.3	67	73	0.350	0.313
5	19-Jan-24	6	2.92	150	1	20.9	82	86	0.262	0.242
5	19-Jan-24	8	3.89	150	1	19.9	133	127	0.0520	0.0720
5	19-Jan-24	10	4.86	150	1	42.6	88	82	0.232	0.262
5	19-Jan-24	12	5.83	150	1	33.4	76	85	0.295	0.247
5	19-Jan-24	20	9.72	150	10	6.37	79	83	1.28	1.257
5	19-Jan-24	60	29.17	150	100	3.90	63	68	2.38	2.34
10	12-Dec-24	0 (Control)	0	150	1	70.0	162	157	-0.0334	-0.0198

MPs size ( $\mu\text{m}$ )	Date	Alum dose ( $\mu\text{M}$ )	Alum dose (mg/L)	Particle dose (particles/mL)	Volume of the effluent (mL)	Turbidity (NTU)	Effluent count (Carboxylated BB polybeads)	Effluent count (Plain YG polybead)	BB Log removal ( $\log_{10}(\text{Influent}/\text{Effluent})$ )	YG Log removal ( $\log_{10}(\text{Influent}/\text{Effluent})$ )
10	12-Dec-24	4	1.94	150	1	21.8	65	71	0.363	0.325
10	12-Dec-24	6	2.92	150	1	20.8	59	65	0.405	0.363
10	12-Dec-24	8	3.89	150	1	40.0	112	119	0.127	0.101
10	12-Dec-24	10	4.86	150	1	32.7	72	83	0.319	0.257
10	12-Dec-24	12	5.83	150	1	20.3	61	69	0.391	0.337
10	12-Dec-24	20	9.72	150	10	7.20	59	63	1.41	1.38
10	12-Dec-24	60	29.17	150	100	3.50	43	55	2.54	2.436
10	13-Dec-24	0 (Control)	0	150	1	70.0	156	145	-0.0170	0.0147
10	13-Dec-24	4	1.94	150	1	21.9	66	65	0.357	0.363
10	13-Dec-24	6	2.92	150	1	20.1	64	67	0.370	0.350

MPs size ( $\mu\text{m}$ )	Date	Alum dose ( $\mu\text{M}$ )	Alum dose (mg/L)	Particle dose (particles/mL)	Volume of the effluent (mL)	Turbidity (NTU)	Effluent count (Carboxylated BB polybeads)	Effluent count (Plain YG polybead)	BB Log removal ( $\log_{10}(\text{Influent}/\text{Effluent})$ )	YG Log removal ( $\log_{10}(\text{Influent}/\text{Effluent})$ )
10	13-Dec-24	8	3.89	150	1	42.0	108	114	0.143	0.119
10	13-Dec-24	10	4.86	150	1	35.8	71	80	0.325	0.273
10	13-Dec-24	12	5.83	150	1	20.3	68	63	0.344	0.377
10	13-Dec-24	20	9.72	150	10	6.99	62	67	1.38	1.35
10	13-Dec-24	60	29.17	150	100	3.22	39	46	2.59	2.51
10	15-Dec-24	0 (Control)	0	150	1	70.0	147	153	0.00877	-0.00860
10	15-Dec-24	4	1.94	150	1	20.9	69	79	0.337	0.278
10	15-Dec-24	6	2.92	150	1	19.9	77	81	0.290	0.268
10	15-Dec-24	8	3.89	150	1	42.6	127	120	0.0723	0.0969
10	15-Dec-24	10	4.86	150	1	33.4	84	92	0.252	0.212

MPs size ( $\mu\text{m}$ )	Date	Alum dose ( $\mu\text{M}$ )	Alum dose (mg/L)	Particle dose (particles/mL)	Volume of the effluent (mL)	Turbidity (NTU)	Effluent count (Carboxylated BB polybeads)	Effluent count (Plain YG polybead)	BB Log removal ( $\log_{10}(\text{Influent}/\text{Effluent})$ )	YG Log removal ( $\log_{10}(\text{Influent}/\text{Effluent})$ )
10	15-Dec-24	12	5.83	150	1	19.5	72	68	0.319	0.344
10	15-Dec-24	20	9.72	150	10	6.37	71	66	1.32	1.36
10	15-Dec-24	60	29.1	150	100	3.76	62	53	2.38	2.45

Table A2 Data for average and standard deviation of turbidity and zeta potential results.

MPs size ( $\mu\text{m}$ )	Alum dose (mg/L)	Turbidity 1 (NTU)	Turbidity 2 (NTU)	Turbidity 3 (NTU)	Zeta potential 1 (mV)	Zeta potential 2 (mV)	Zeta potential 3 (mV)	Turbidity average	Zeta potential average	Standard deviation of turbidity	Standard deviation of zeta potential
1	0.000	70.0	70.0	70.0	-47.6	-49.1	-48.8	70.0	-48.5	0.00	0.788
1	0.972	69.9	68.3	68.0	-34.9	-38.0	-36.9	68.7	-36.6	1.02	1.61
1	1.46	33.4	34.9	33.9	-28.3	-26.7	-25.8	34.1	-26.9	0.764	1.30
1	1.95	38.0	35.1	36.0	-13.7	-22.5	-21.8	36.4	-19.3	1.48	4.90
1	2.92	53.8	49.0	52.2	-0.818	-2.27	-2.61	51.7	-1.90	2.44	0.950
1	3.89	35.6	35.5	30.5	-0.517	-1.02	-1.09	33.9	-0.875	2.92	0.313
1	4.86	28.3	25.5	22.3	5.71	8.57	8.18	25.4	7.49	3.00	1.55
1	5.83	20.7	24.0	20.0	8.01	10.0	10.0	21.6	9.33	2.14	1.15
1	6.81	13.9	18.3	17.9	9.31	11.6	11.5	16.7	10.8	2.43	1.29
1	7.78	12.9	12.5	12.3	10.2	9.75	9.80	12.6	9.93	0.306	0.266

Note : Turbidity 1 is replicate 1; Turbidity 2 is replicate 2; Turbidity 3 is replicate 3; Zeta potential 1 is replicate 1; Zeta potential 2 is replicate 2; Zeta potential 3 is replicate 3.

MPs size (µm)	Alum dose (mg/L)	Turbidity 1 (NTU)	Turbidity 2 (NTU)	Turbidity 3 (NTU)	Zeta potential 1 (mV)	Zeta potential 2 (mV)	Zeta potential 3 (mV)	Turbidity average	Zeta potential average	Standard deviation of turbidity	Standard deviation of zeta potential
1	8.75	11.8	12.1	12.2	10.2	12.1	12.2	12.0	11.5	0.208	1.16
1	9.72	9.35	11.1	11.5	9.99	11.5	11.5	10.7	11.0	1.14	0.891
1	14.6	5.93	10.9	10.8	10.3	11.0	11.0	9.21	10.8	2.84	0.404
1	19.4	7.42	10.2	10.5	12.3	10.3	10.3	9.37	11.0	1.70	1.16
1	29.2	4.06	6.15	6.20	10.9	10.8	10.5	5.47	10.8	1.22	0.195
1	38.9	3.92	4.85	5.22	10.4	8.54	8.43	4.66	9.12	0.670	1.11
5	0.00	70.0	70.0	70.0	-47.2	-47.5	-44.5	70.0	-46.4	0.00	1.64
5	0.972	68.7	69.1	68.2	-39.5	-36.5	-34.3	68.7	-36.8	0.461	2.59
5	1.46	24.9	24.7	25.3	-26.2	-23.7	-28.8	24.9	-26.3	0.332	2.53
5	1.95	21.9	21.9	20.9	-23.5	-13.4	-19.1	21.6	-18.7	0.583	5.09
5	2.92	19.3	20.1	19.9	-3.81	-3.26	-2.27	19.8	-3.11	0.416	0.782
5	3.89	40.8	42.0	42.6	-1.40	-1.02	-1.74	41.8	-1.38	0.938	0.363
5	4.86	38.1	35.8	33.4	-0.380	1.61	1.07	35.8	0.764	2.33	1.03
5	5.83	35.3	22.1	22.4	6.44	6.64	5.48	26.6	6.19	7.56	0.621
5	6.81	20.4	20.3	20.4	8.08	7.76	7.33	20.3	7.72	0.0690	0.377
5	7.78	17.9	19.4	19.5	9.93	8.53	9.23	19.0	9.23	0.917	0.700
5	8.75	11.1	12.2	12.0	10.5	9.53	10.3	11.8	10.1	0.582	0.509
5	9.72	6.44	8.99	6.40	9.04	11.6	10.6	7.27	10.4	1.49	1.29
5	14.6	5.30	7.78	6.20	8.54	10.2	11.5	6.43	10.1	1.26	1.50
5	19.4	3.88	6.31	5.10	10.6	11.4	10.6	5.10	10.9	1.22	0.472
5	29.2	2.74	5.22	3.90	10.9	11.8	11.4	3.95	11.4	1.24	0.450
5	38.9	2.28	4.21	3.80	10.6	11.6	11.4	3.42	11.2	1.01	0.523
10	0.00	70.0	70.0	70.0	-50.4	-49.8	-47.8	70.0	-49.3	0.00	1.40

Note : Turbidity 1 is replicate 1; Turbidity 2 is replicate 2; Turbidity 3 is replicate 3; Zeta potential 1 is replicate 1; Zeta potential 2 is replicate 2; Zeta potential 3 is replicate 3.

MPs size (µm)	Alum dose (mg/L)	Turbidity 1 (NTU)	Turbidity 2 (NTU)	Turbidity 3 (NTU)	Zeta potential 1 (mV)	Zeta potential 2 (mV)	Zeta potential 3 (mV)	Turbidity average	Zeta potential average	Standard deviation of turbidity	Standard deviation of zeta potential
10	0.972	67.9	67.7	67.8	-37.0	-37.3	-36.8	67.8	-37.0	0.0950	0.252
10	1.46	22.6	22.7	22.1	-25.5	-26.2	-24.4	22.5	-25.4	0.355	0.918
10	1.95	21.8	21.9	20.9	-22.6	-22.5	-21.8	21.5	-22.3	0.554	0.461
10	2.92	20.8	20.1	19.9	-5.57	-4.74	-4.47	20.3	-4.93	0.473	0.571
10	3.89	40.0	42.0	42.6	-3.01	-3.73	-3.75	41.5	-3.49	1.36	0.420
10	4.86	32.7	35.8	33.4	-1.14	-1.08	-1.44	34.0	-1.22	1.63	0.195
10	5.83	20.3	20.3	19.5	7.64	6.76	8.67	20.0	7.69	0.439	0.954
10	6.81	18.6	17.2	17.0	8.43	9.53	9.47	17.6	9.15	0.872	0.618
10	7.78	17.3	17.0	16.9	9.84	9.84	9.77	17.1	9.82	0.204	0.042
10	8.75	10.1	10.2	10.5	11.0	10.9	11.9	10.3	11.2	0.197	0.558
10	9.72	7.20	6.99	6.37	12.3	8.00	10.4	6.85	10.2	0.432	2.16
10	14.6	5.60	5.78	5.55	11.5	11.5	10.0	5.64	11.0	0.121	0.847
10	19.4	4.30	4.31	3.22	11.0	10.7	11.4	3.94	11.0	0.626	0.348
10	29.2	3.50	3.22	3.76	10.3	10.9	11.3	3.49	10.9	0.270	0.506
10	38.9	2.10	2.21	2.81	10.7	10.9	10.7	2.37	10.8	0.382	0.106

Note : Turbidity 1 is replicate 1; Turbidity 2 is replicate 2; Turbidity 3 is replicate 3; Zeta potential 1 is replicate 1; Zeta potential 2 is replicate 2; Zeta potential 3 is replicate 3.

Table A3 Data used for two tailed paired T-test analyses

Size (µm)	Alum dose (mg/L)	Effluent count (Weathered BB Carboxylate)			Average	Log removal	10 <sup>^</sup> (-LR)	1 - 10 <sup>^</sup> (-LR)	% removal	Effluent count (Pristine YG Polybead)			Average	Log removal	10 <sup>^</sup> (-LR)	1 - 10 <sup>^</sup> (-LR)	% removal
1	0.00	143	147	141	144	0.0187	0.958	0.0422	4.22	141	144	138	141	0.0269	0.940	0.0600	6.00
	1.46	77	85	81	81.0	0.268	0.540	0.460	46.0	74	79	77	76.7	0.291	0.511	0.489	48.9
	1.94	92	79	88	86.3	0.240	0.576	0.424	42.4	79	77	85	80.3	0.271	0.536	0.464	46.4
	2.92	123	103	121	116	0.113	0.771	0.229	22.9	96	96	107	99.7	0.178	0.664	0.336	33.6
	3.89	82	81	72	78.3	0.282	0.522	0.478	47.8	88	79	75	80.7	0.269	0.538	0.462	46.2
	4.86	68	72	71	70.3	0.329	0.469	0.531	53.1	72	74	73	73.0	0.313	0.487	0.513	51.3
	9.72	108	97	114	106	1.15	0.0709	0.929	92.9	117	124	127	123	1.09	0.0818	0.918	91.8
	29.2	116	141	125	127	2.07	0.00849	0.992	99.2	140	131	117	129	2.06	0.008622	0.991	99.1
5	0.00	139	144	155	146	0.0117	0.973	0.0267	2.67	145	138	141	141	0.0258	0.942	0.0578	5.8
	1.94	58	72	67	65.7	0.359	0.438	0.562	56.2	75	76	73	75	0.303	0.498	0.502	50.2
	2.92	48	68	82	66.0	0.357	0.440	0.560	56.0	83	77	86	82.0	0.262	0.547	0.453	45.3
	3.89	110	122	133	122	0.0909	0.811	0.189	18.9	123	118	127	123	0.0874	0.818	0.182	18.2
	4.86	76	83	88	82.3	0.261	0.549	0.451	45.1	87	87	82	85.3	0.245	0.569	0.431	43.1
	5.83	62	78	76	72.0	0.319	0.480	0.520	52.0	73	80	85	79.3	0.277	0.529	0.471	47.1
	9.72	68	66	79	71.0	1.32	0.0473	0.953	95.3	67	70	83	73.3	1.31	0.0489	0.951	95.1
	29.2	66	53	63	60.7	2.39	0.00404	0.996	99.6	52	61	68	60.3	2.40	0.004022	0.996	99.6
10	0.00	162	156	147	155	-0.0142	1.03	-0.0333	-3.33	157	145	153	151.7	-0.0048	1.011	-0.011	-1.1
	1.94	65	66	69	66.7	0.352	0.444	0.556	55.6	71	65	79	71.7	0.321	0.478	0.522	52.2
	2.92	59	64	77	66.7	0.352	0.444	0.556	55.6	65	67	81	71.0	0.325	0.473	0.527	52.7
	3.89	112	108	127	115.67	0.113	0.771	0.229	22.9	119	114	120	117.7	0.105	0.784	0.216	21.6
	4.86	72	71	84	75.7	0.297	0.504	0.496	49.6	83	80	92	85.0	0.247	0.567	0.433	43.3
	5.83	61	68	72	67.0	0.350	0.447	0.553	55.3	69	63	68	66.7	0.352	0.444	0.556	55.6
	9.72	59	62	71	64.0	1.37	0.0427	0.957	95.7	63	67	66	65.3	1.36	0.0436	0.956	95.6
	29.2	43	39	62	48.0	2.49	0.00320	0.997	99.7	55	46	53	51.3	2.47	0.003422	0.997	99.7

Table A4 Statistical Analysis of pristine and weathered MPs

t-Test: Paired Two Sample for Means of counts at zero dose for 1  $\mu\text{m}$

	<i>Variable 1</i>	<i>Variable 2</i>
Mean	143.6666667	141
Variance	9.333333333	9
Observations	3	3
Pearson Correlation	0.981980506	
Hypothesized Mean Difference	0	
df	2	
t Stat	8	
P(T<=t) one-tail	0.007634036	
t Critical one-tail	2.91998558	
P(T<=t) two-tail	0.015268072	
t Critical two-tail	4.30265273	

t-Test: Paired Two Sample for Means of counts at zero dose for 5  $\mu\text{m}$

	<i>Variable 1</i>	<i>Variable 2</i>
Mean	146	141.3333333
Variance	67	12.33333333
Observations	3	3
Pearson Correlation	-0.38266	
Hypothesized Mean Difference	0	
df	2	
t Stat	0.802955	
P(T<=t) one-tail	0.253129	
t Critical one-tail	2.919986	
P(T<=t) two-tail	0.506258	
t Critical two-tail	4.302653	

t-Test: Paired Two Sample for Means of counts at zero dose for 10  $\mu\text{m}$

	<i>Variable 1</i>	<i>Variable 2</i>
Mean	155	151.6666667
Variance	57	37.33333333
Observations	3	3
Pearson Correlation	0.216777	
Hypothesized Mean Difference	0	
df	2	
t Stat	0.66965	
P(T<=t) one-tail	0.28602	
t Critical one-tail	2.919986	
P(T<=t) two-tail	0.57204	
t Critical two-tail	4.302653	

t-Test: Paired Two Sample for Means of counts at charge neutralization doses for 1  $\mu\text{m}$

	<i>Variable 1</i>	<i>Variable 2</i>
Mean	83.66666667	78.5
Variance	32.66666667	13.5
Observations	6	6
Pearson Correlation	0.704761905	
Hypothesized Mean Difference	0	
df	5	
t Stat	3.10934206	
P(T<=t) one-tail	0.013285287	
t Critical one-tail	2.015048373	
P(T<=t) two-tail	0.026570575	
t Critical two-tail	2.570581836	

t-Test: Paired Two Sample for Means of counts at charge neutralization doses for 5  $\mu\text{m}$

	<i>Variable 1</i>	<i>Variable 2</i>
Mean	65.83333	78.333333
Variance	136.9667	25.466667
Observations	6	6
Pearson Correlation	0.146743	
Hypothesized Mean Difference	0	
df	5	
t Stat	-2.541862	
P(T<=t) one-tail	0.025888	
t Critical one-tail	2.015048	
P(T<=t) two-tail	0.051776	
t Critical two-tail	2.570582	

t-Test: Paired Two Sample for Means of counts at charge neutralization doses for 10  $\mu\text{m}$

	<i>Variable 1</i>	<i>Variable 2</i>
Mean	66.66667	71.333333
Variance	36.26667	50.266667
Observations	6	6
Pearson Correlation	0.855649	
Hypothesized Mean Difference	0	
df	5	
t Stat	-3.114959	
P(T<=t) one-tail	0.013201	
t Critical one-tail	2.015048	
P(T<=t) two-tail	0.026402	
t Critical two-tail	2.570582	

t-Test: Paired Two Sample for Means of counts at sweep flocculation doses for 1  $\mu\text{m}$

	<i>Variable</i>	
	<i>1</i>	<i>Variable 2</i>
Mean	127.3333	129.3333333
Variance	160.3333	134.3333333
Observations	3	3
	-	
Pearson Correlation	0.236215	
Hypothesized Mean Difference	0	
df	2	
	-	
t Stat	0.181568	
P(T<=t) one-tail	0.436329	
t Critical one-tail	2.919986	
P(T<=t) two-tail	0.872657	
t Critical two-tail	4.302653	

t-Test: Paired Two Sample for Means of counts at sweep flocculation doses for 5  $\mu\text{m}$

	<i>Variable 1</i>	<i>Variable 2</i>
Mean	60.66667	60.3333333
Variance	46.33333	64.3333333
Observations	3	3
Pearson Correlation	-0.290006	
Hypothesized Mean Difference	0	
df	2	
t Stat	0.048393	
P(T<=t) one-tail	0.4829	
t Critical one-tail	2.919986	
P(T<=t) two-tail	0.965801	
t Critical two-tail	4.302653	

t-Test: Paired Two Sample for Means of counts at sweep flocculation doses for 10  $\mu\text{m}$

	<i>Variable 1</i>	<i>Variable 2</i>
Mean	48	51.33333333
Variance	151	22.33333333
Observations	3	3
Pearson Correlation	0.456332	
Hypothesized Mean Difference	0	
df	2	
t Stat	-0.526316	
P(T<=t) one-tail	0.325605	
t Critical one-tail	2.919986	
P(T<=t) two-tail	0.65121	
t Critical two-tail	4.302653	

t-Test: Paired Two Sample for Means of residual turbidity at particle destabilization zones for 1  $\mu\text{m}$

	<i>Variable 1</i>	<i>Variable 2</i>
Mean	35.21666667	5.066666667
Variance	2.701666667	0.971346667
Observations	6	6
Pearson Correlation	-0.376882846	
Hypothesized Mean Difference	0	
df	5	
t Stat	33.38315736	
P(T<=t) one-tail	2.2671E-07	
t Critical one-tail	2.015048373	
P(T<=t) two-tail	0.000000453	
t Critical two-tail	2.570581836	

t-Test: Paired Two Sample for Means of residual turbidity at particle destabilization zones for 5  $\mu\text{m}$

	<i>Variable 1</i>	<i>Variable 2</i>
Mean	22.09222	4.155556
Variance	5.318969	1.561103
Observations	9	9
Pearson Correlation	0.613458	
Hypothesized Mean Difference	0	
df	8	
t Stat	29.42316	
P(T<=t) one-tail	9.64E-10	
t Critical one-tail	1.859548	
P(T<=t) two-tail	1.93E-09	
t Critical two-tail	2.306004	

t-Test: Paired Two Sample for Means of residual turbidity at particle destabilization zones for 10  $\mu\text{m}$

	<i>Variable 1</i>	<i>Variable 2</i>
Mean	21.42222222	3.27
Variance	1.076269444	0.643075
Observations	9	9
Pearson Correlation	0.777956973	
Hypothesized Mean Difference	0	
df	8	
t Stat	83.54063111	
P(T<=t) one-tail	2.3508E-13	
t Critical one-tail	1.859548038	
P(T<=t) two-tail	4.70159E-13	
t Critical two-tail	2.306004135	